

Monte Carlo Simulations of Occupational Radiation Exposure During X-ray Guided Interventional Cardiology Procedures

Jon S. Dyrkolbotn



Master thesis in medical physics and technology

University of Bergen

2021/March

Acknowledgements

First, I would like to thank all my supervisors, Kristian S. Ytre-Hauge (PhD), Kirsten Bolstad, Cedric Davidsen (MD) and Vegard Tuseth (MD, PhD). Thank you for not giving up on me; this master thesis would not be possible without you!

Kristian, you have introduced and taught me many new and interesting subjects, from radiation therapy to FLUKA simulations, and for that, I am grateful. Thank you for all your help with FLUKA, the coding and, in general, comprehension of physics during this project. This master thesis caught my eye the moment I saw it, and I am glad you presented it to me.

Kirsten, thank you for being the bridge between the physics and the medicine, and for your help in learning and understanding both the medical and physical aspect of this study. All your feedback and help with the writing have been invaluable to me.

To Cedric and Vegard, I appreciate all your input along the way. Your hands-on experience with interventional cardiology has not only been vital to your patients, but also this project. Our different academical backgrounds have been crucial in challenging my own assumptions and ways of thinking, which helped to further my understanding of physics. Thanks for staying at the lab after hours, Cedric, to help my work and for our discussions there.

To all staff at the cardiac catheterization lab at Haukeland University Hospital, thank you! You have allowed me access to your equipment, treatment rooms and to observe procedures. This has not only been necessary for this project, but also a great inspiration. I hope this and subsequently work results in a safer work environment for you all, perhaps even without the need for worn lead protection.

Thank you, Lars Fredrik Fjære, for your help with crucial parts of this study, from help with my scripts to bug-fixing in FLUKA. And thanks to Helge Pettersen for processing the CT-scan used in this project and your useful input during meetings.

Last, but not least, I would like to thank my friends and family. These times have not always been easy, and your moral support has been crucial. Your experience with physics, writing, coding, and medicine may vary, but my appreciation for your input and support does not!

Abstract

X-ray imaging is widely used as a diagnostic tool in many medical fields. Medical personnel can often reduce their exposure with distance and sufficient radiation protection, as they do not have to be close to the radiation field. Invasive cardiologists cannot take advantage of this. They must work close to the radiation field during multiple sessions throughout their career, exposing themselves to scatter radiation. Radiation shielding and lead clothing is used to reduce their dose. Monte Carlo (MC) simulations are the standard for calculating dose. FLUKA is a general-purpose tool that use the MC method to simulate particle transport and interactions with matter. These features make the program able to simulate and measure, amongst other quantities, absorbed dose and fluence.

The aim of this study is to evaluate the feasibility of using MC simulations through FLUKA to calculate and evaluate the dose given to the interventional cardiologists (operator) for different radiation shielding. An operation room at Haukeland University Hospital (HUS) used for interventional cardiac procedures was recreated in FLUKA and used during the simulations. Data from real procedures at the operation room was attained to recreate a realistic energy spectrum, beam placement, and spread of the radiation source.

The different radiation shielding had a definitive impact on the dose given to the operator according to the simulations. The defining feature of the setups was the inclusion of gaps between the in the different layers of shielding or the floor. Such gaps did result in almost ten times higher dose at some parts in the operator. A significant reduction of the dose was also observed when placing a lead blanket over the patient's body, outside the radiation field.

In conclusion, FLUKA is viable tool in assessing the relative effect of different shielding setups and how they relate to the dose given to the operator. It can recreate energy spectrums and beam geometries based on real data. To reduce the dose given to the operator, the focus should be to avoid gaps between shielding components or to add a lead blanket over the patient.

Contents

ACKNOWLEDGEMENTS.....	III
ABSTRACT.....	V
1. INTRODUCTION AND PROJECT AIM.....	13
2. THEORY.....	15
2.1 INTERVENTIONAL CARDIOLOGY.....	15
2.2 RADIATION PHYSICS.....	17
2.2.1 <i>Photons and energy ranges</i>	17
2.2.2 <i>Photoelectric effect</i>	18
2.2.3 <i>Compton scattering</i>	18
2.2.4 <i>Photon attenuation</i>	19
2.2.5 <i>Hounsfield scale</i>	20
2.2.6 <i>Production of photons for medical application</i>	20
2.3 DOSIMETRY.....	21
2.3.1 <i>Kerma and Absorbed Dose</i>	21
2.3.2 <i>Effective dose</i>	22
2.3.3 <i>Dose Area Product</i>	25
2.4 BIOLOGICAL EFFECTS OF RADIATION.....	25
3. METHODS.....	27
3.1 FLUKA.....	27
3.1.1 <i>FLUKA settings</i>	27
3.1.2 <i>CT</i>	28
3.2 SCORING IN FLUKA.....	28
3.2.1 <i>Regions of interest</i>	28

3.2.2	<i>Scoring H10 & H0.07</i>	32
3.3	RADIATION SOURCE	33
3.3.1	<i>Beam angles</i>	33
3.3.2	<i>Field geometry</i>	34
3.3.3	<i>Cumulative energy spectrum</i>	34
3.4	RADIATION SHIELDING SETUPS	35
3.4.1	<i>Full protection extended to floor - Lead Screen, Blanket, extended to Floor (SBF)</i> .	37
3.4.2	<i>Full protection - Lead Screen, Blanket (SB)</i>	38
3.4.3	<i>Full protection with gap - Lead Screen, Blanket, Gap (SGB)</i>	39
3.4.4	<i>Gap without blanket - Lead Screen, Gap (SG)</i>	40
3.4.5	<i>No protection - Zero protection (Z)</i>	41
3.5	AIR KERMA MEASUREMENTS AT HUS	42
4.	RESULTS	44
4.1	SPECTRUM SCORING	44
4.2	FLUENCE SCORING	44
4.2.1	<i>Fluence in front of the operator</i>	45
4.2.2	<i>Fluence across the operating room</i>	46
4.3	DOSE SCORING	48
4.3.1	<i>Skin dose</i>	49
4.3.2	<i>Dose heat maps</i>	49
4.4	DOSE RATE MEASUREMENTS AT HUS	51
	DISCUSSION	53
5.	FUTURE WORK	59
5.1	POTENTIAL PARAMETERS	59

5.2	INCORPERATE H10 AND H0.07.....	59
5.3	EDIT CT TO INCLUDE SHIELDING RATHER THAN PLACING IT AROUND PROTECTION	60
5.4	HAVING BOTH OPERATOR AND PATIENT AS CT-SCANS.....	60
5.5	LINKING SCORING TO REAL LIFE DOSE.....	61
CONCLUSION		62
REFERENCES.....		64

LIST OF ABBREVIATIONS

DAP	D ose A rea P roduct
DSA	Norwegian Radiation and Nuclear Safety Authority
FLUKA	FL Uktuierende KA skade
FPS	F rames P er S econd
HUS	Haukeland University Hospital
kVp	K ilovolt P eak
LNT	L inear N o T hreshold
mAs	m illi A mpere-seconds
MC	M onte C arlo
RDSR	R adiation D ose S tructure R eport
SNR	S ignal-to- N oise R atio

1. Introduction and project aim

Invasive cardiac interventions use X-ray images as a diagnostic and guiding tool while operating. The images of the patient are essential to get an internal view of the patient as well as to guide their catheters, as the operators have no direct visuals to rely on during procedures. The patient is directly exposed to the radiation field, thus ionizing radiation, during procedures. Operators cannot always leave the patient while imaging. Then they are exposed to radiation through scatter radiation mostly due to Compton scattering [1]. Over 30,000 invasive cardiology procedures were performed in 2019 in Norway [2]. The operators get a low, but cumulative dose over multiple procedures, unlike their patients, who receive a higher dose only a few times.

Two measures can be applied to reduce the dose received by the operators: reducing the imaging dose and shielding. The former option also reduces the image quality, while the latter involves adding lead shielding to themselves, the patient table and/or hanging it from the ceiling. Examples of worn protection are lead vests, skirts, hats, thyroid shields, and glasses. Adding more shielding to the patient table or X-ray equipment is limited by weight and accessibility to the patient. The shielding setup should ideally be easy to use and change during procedures. The shielding worn by the operators is heavy and warm. This results both in reduced dexterity, comfort and strain injuries due to the extra weight. All this creates a trade-off between minimizing dose and strain injuries to the operator while maximizing movability and access to the patient.

Operators working interventional cardiology are required to wear dosimeters that are monitored by Norwegian Radiation and Nuclear Safety Authority. The dosimeters only measure the cumulative effective dose at a small area, but the radiation exposure may vary at different regions of the operator. That leads to single dosimeters and other point

Introduction and project aim

dose measurements cannot give a sufficiently detailed information of the effectiveness of different shielding measures.

The aim of this study was to investigate the feasibility of using Monte Carlo simulations through FLUKA to assess the dose given to the operator for different shielding arrangements. This will be done by examining the scored dose and fluence for each shielding setup. Knowing the effectiveness of different shielding arrangements allows invasive cardiologists to make informed decisions regarding shielding and develop good working routines considering trade-offs between their own protection and accessibility to the patient.

The dose distributions and photon fluence was studied through FLUKA, a software that performs Monte Carlo simulations for particle interactions, which is considered to be the gold standard for calculating dose. Creating a virtual operating room allows constant access, testing and allows for a large scope for manipulating the setup and radiation source without exposing any subjects to excess radiation.

2. Theory

2.1 Interventional cardiology

Interventional cardiology allows medical staff to diagnose and do coronary procedures without having to surgically open the patient's chest. This allows for interventions inside arteries and has a lower associated risk compared to similar surgical procedures like bypasses.

Angiography is an imaging technique used by interventional cardiologist to visualize blood vessels. This is done by adding a contrast agent into the patient's bloodstream, making it highly visible on X-ray images. Operators can inject the contrast agent only in the vessels they want to inspect by inserting a catheter, a narrow, flexible tube, into the patient's arteries and maneuver it to the arteries in question [3]. However, this requires the operators to remain at the patient's side when taking the X-ray images, exposing them to scatter radiation. Another common procedure in interventional cardiology is Percutaneous Coronary Intervention (PCI). PCI involves treating narrowing of coronary arteries due to plaque. Using angiography, operators can diagnose and locate such narrow arteries. Once there, operators can widen the artery by inflating a balloon and/or place a stent keeping the artery in place [4].

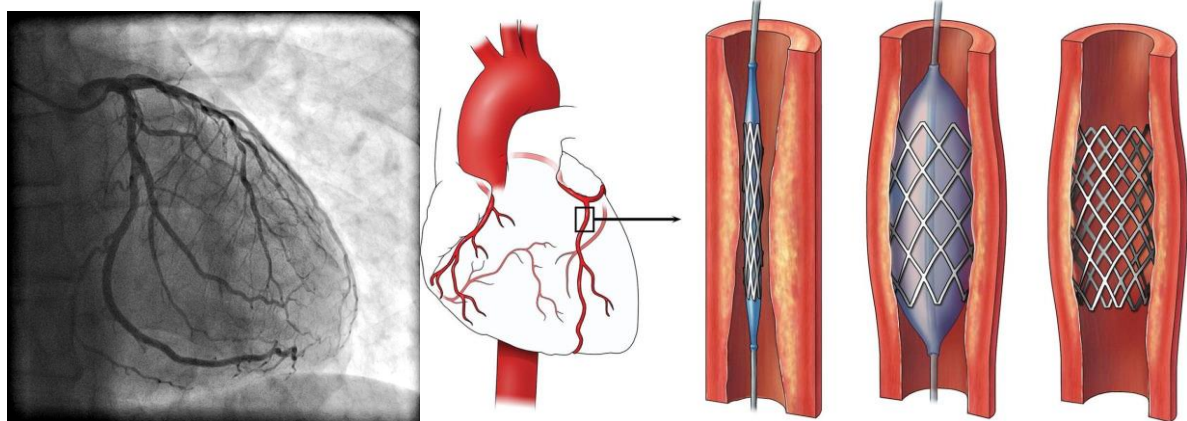


Figure 2.1 - (Left) Picture of a coronary angiogram [5]. (Right) Displays the process of widening blood vessel in a PCI [6].

Theory

The C-arm (depicted below) used in interventional cardiology has a variety of settings, such as field size and FPS. This study focuses mainly on its two different modes, fluoroscopy (fluoro), and stationary acquisition (acquisition). Fluoro mode gives a lower dose rate, with reduced images quality and often reduced framerate. The fluoro mode is used while orienting and positioning during procedures when a low image quality will suffice. Acquisition mode, also called cine, has a better signal-to-noise ratio (SNR) and temporal resolution compared to fluoro mode. Improved image quality in X-ray images normally comes with an increased dosage, to both the operator and the patient. Better detectors, image processing, and other technological improvements can naturally improve the image quality without the associated increase in dose, however that will not be considered in this project. Higher temporal resolution is attained by increasing the frames per second, and image quality is highly dependent on the number of photons reaching the detector. The latter can be achieved by increasing the X-ray tube current and imaging time or increasing the X-ray tube voltage. Increasing the current results in more electrons hitting the anode and is proportionally related to the numbers of photons created. Increasing the voltage makes each electron produce more photons as they interact with the anode and increases the peak energy of photons created [7]. All forms of improving the image quality results in a higher dose given to the patient and the operators. This is something the operators must consider during procedures. The operators can minimize the dose given to the patient and themselves by using fluoro over acquisition mode and a lower FPS when the lower image quality and frame rate will suffice.

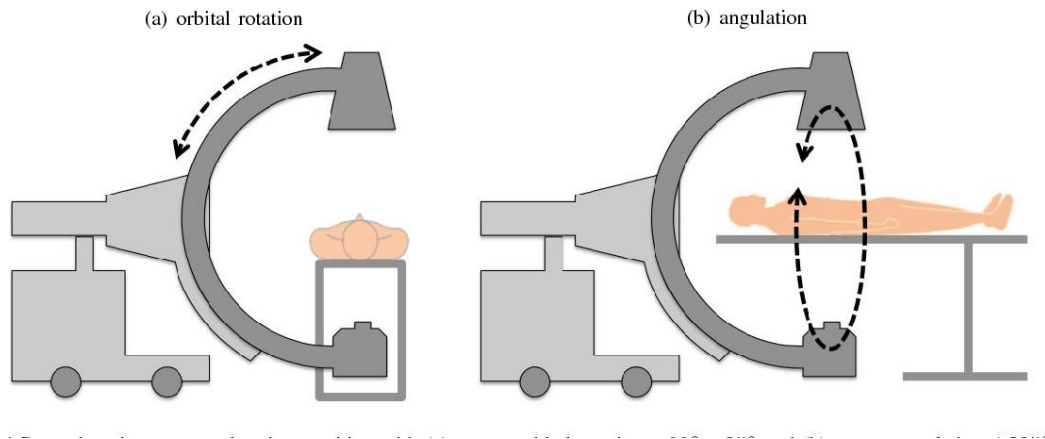


Figure 2.2 - This figure shows a C-arm (dark grey) and a patient lying on an operating table.

2.2 Radiation physics

2.2.1 Photons and energy ranges

Photons interact with matter through four mechanisms: photoelectric effect, coherent (Rayleigh) scattering, incoherent (Compton) scattering and pair production. Pair production requires at least the energy of two times the mass of an electron multiplied with the speed of light squared. That energy, 1.022 MeV, is beyond the range of energies used in this project. Coherent scattering does not contribute to given dose, as it is an elastic interaction between a photon and an electron and does not alter any chemical processes. It does cause scattering, thus introducing some noise to X-ray images. As seen in the figure below, it accounts for roughly 10% to 0.1% of the total mass attenuation coefficient in the 1-100 keV range. The mass attenuation coefficient of water is dominated by photoelectric interactions for the lower energies (up to circa 10 keV in water). Whereas incoherent (Compton) interactions dominate from 50 keV and above in water.

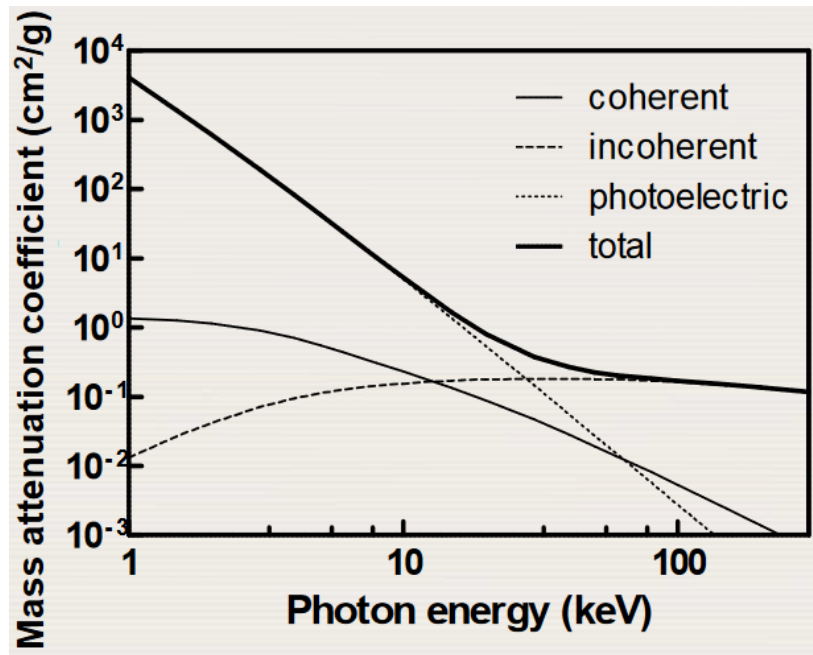


Figure 2.3 - Mass attenuation coefficient for water for photons. [8]

2.2.2 Photoelectric effect

Photoelectric effect is when a photon ejects an electron previously bound to an atom or ion, giving the electron all its energy while consuming the photon. This changes the electrical charge of the atom or ion, altering its chemical properties. The photoelectric effect is highly dependent on the electron density [7]. The probability of a photoelectric effect happening in water decreases with the energy (Figure 2.3).

2.2.3 Compton scattering

Compton scattering occurs when a photon collides with a charged particle. The interaction causes the photon to lose energy and change trajectory due to conservation of momentum and energy. The photon is not consumed during the process. The probability of compton scattering occurring increases with the 1-100 keV energy range. Compton scattering happens mainly with electrons in said energy range, and is therefore also highly dependent on the electron density [7]. The energy of the outgoing photon follows this relation:

Theory

$$E' = \frac{E}{1 + (E/m_e c^2)(1 - \cos \theta)} \quad (2.1)$$

E : Original photon energy, E' : New photon energy, m_e : mass of an electron, θ : change in direction

2.2.4 Photon attenuation

Photons do not have a finite range in matter, unlike charged particles. The intensity of a photon beam is reduced as they traverse matter. A narrow beam of monoenergetic photons follows this relationship [9].

$$dI = -\mu I dx \quad (2.2)$$

I is the intensity, μ is the linear attenuation coefficient and x is the distance traveled through the material. The linear attenuation coefficient can be normalized to mass attenuation coefficient by dividing by the material's density.

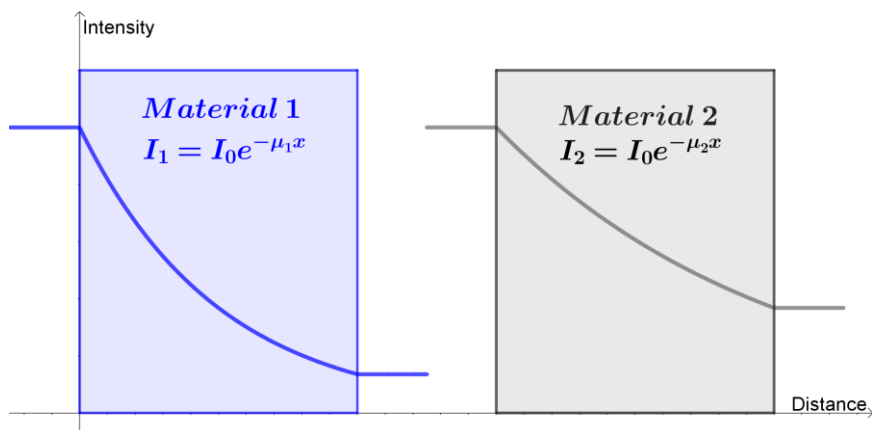


Figure 2.4: Illustration of attenuation of monoenergetic photons through different material where $\mu_1 > \mu_2$

Absorption edge is the increase of absorption rate of electrons at specific energies. It occurs at energy levels just above the binding energy of an electron. The k-edge corresponds to the energy required to eject an electron in the innermost shell, the k-shell. Higher shells also have absorption edges, but their energies are much lower and thus less relevant [7]. Iodine and Barium have k-edges at typical X-ray range (33 & 37 keV [10]) and are thus often used for contrast.

2.2.5 Hounsfield scale

The Hounsfield scale is a scale made to define how well X-rays propagate through different material, also called radiodensity. It is used to interpret and encode CT images. It is defined by setting the HU-value for water (0 HU) and air (-1000 HU) at standard temperature and pressure (0 °C, 1 kPa). The unit is calculated as shown below where μ is the linear attenuation coefficient. [11]

$$HU = 1000 \cdot \frac{\mu - \mu_{water}}{\mu_{water} - \mu_{air}} \quad (2.3)$$

2.2.6 Production of photons for medical application

An X-ray tube is used to generate X-rays. Electrons are heated up by a high voltage through a filament called the cathode. The energy from the heat allows electrons to be released into the vacuum of the tube. The electrons are then accelerated toward a target, anode, by a large voltage difference between the anode and cathode. The anode is typically made from tungsten. The traversing electrons interact with the charged particles in the anode and create photons. At the anode, the electrons are slowed down and deflected, and excite the bound electrons at the anode. The former is called bremsstrahlung and creates a continuous energy spectrum of photons. The traversing electrons get an energy of eV , where e is the electron charge and V is the voltage difference between the anode and cathode. The maximum energy of a created photon is therefore eV , as a traversing electron can at most lose all its energy through one photon. The voltage is often in the kV-range, and the peak voltage is often called kilovolt-peak (kVp). The latter type of photon creation is when the traversing electrons excite the bound electrons. The bound electrons release photons when they go back to a more stable energy level. The photon energies created correspond to the energy levels of the atom and is characteristic to each atom and are therefore called characteristic energy spectrum. These specific photon energy levels correspond to the absorption

Theory

edges discussed in 2.2.4. The X-ray field is then shaped by collimators, made uniform by a flattening filter to achieve desired field geometry [12].

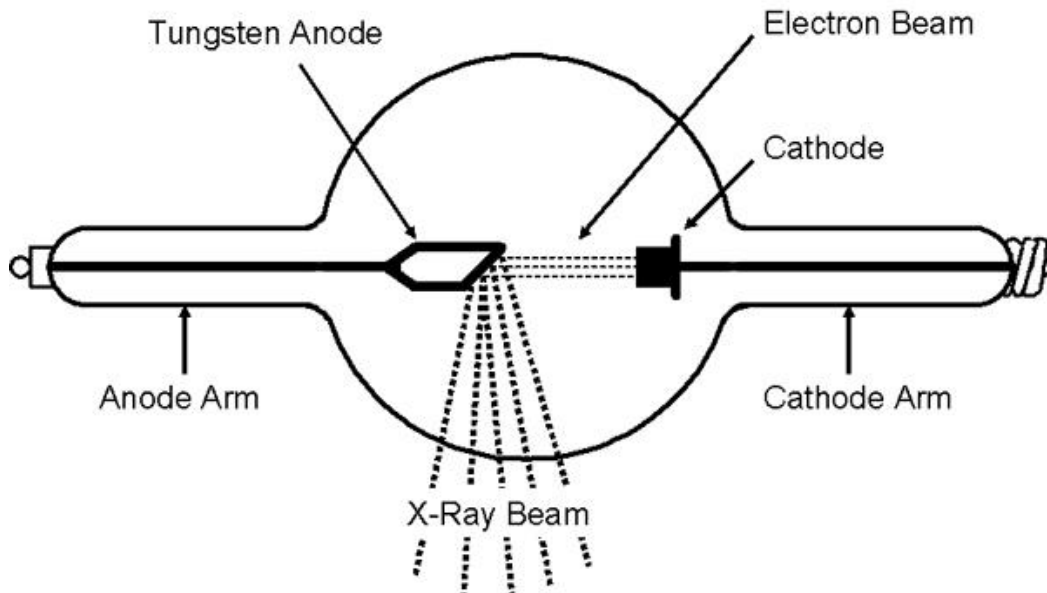


Figure 2.5 - Example of an x-ray tube [13]

2.3 Dosimetry

2.3.1 Kerma and Absorbed Dose

Kerma stand for Kinetic Energy Released per unit MAAss. It is a measure of the combined kinetic energy (dE) of all charged particles freed by uncharged particles per units of mass (dm). Photons are the only uncharged particle that will be considered when using kerma in this study, not neutrons.

$$K = \frac{dE}{dm}$$

The SI units for Kerma is J/kg , where $1 \frac{J}{kg} = 1 Gy$

Theory

Absorbed dose has the same units as kerma, $1 \frac{J}{kg} = 1 Gy$, but they measure different quantities. The absorbed dose, D , is a measure of how much energy is deposited by ionizing radiation (dE) per unit of mass (dm).

$$D = \frac{dE}{dm} \quad (2.4)$$

Absorbed dose does not consider the type of radiation or the radiosensitivity of the absorbing tissue. [8]

2.3.2 Effective dose

Effective dose, E , sums the dose given and weighted by considering the type of ionizing radiation and the tissue's radiation sensitivity:

$$E = \sum_T w_T \sum_R w_R D_{T,R} \quad (2.5)$$

where w_T is the tissue weight, w_R is the radiation weight and $D_{T,R}$ is the absorbed dose given to a specific tissue, T , with radiation R . Effective dose is measured in Sv. $1 \frac{J}{kg} = 1 Sv$. Note that $\sum_T w_T = 1$. [14] A list of tissue and radiation weights can be found below in table 2.1 and 2.2

Table 2.1 - Radiation weighting factors (ICRP 1991b)

Type and energy range	Radiation weighting factor, w_R
Photons, all energies	1
Electrons and muons, all energies	1
Neutrons, energy < 10 keV	5
10-100 keV	10
100 keV - 2 MeV	20
2 MeV - 20 MeV	10
>20 MeV	5
Protons, other than recoil protons, energy > 2 MeV	5
Alpha particles, fission fragments, heavy nuclei	20

Table 2.2 - Tissue weighting factors (ICRP 1991b)

Tissue	Tissue weighting factor, w_T
Bone surfaces	0.01
Bladder	0.05
Breast	0.05
Colon	0.12
Gonads	0.20
Liver	0.05
Lungs	0.12
Esophagus	0.05
Red bone marrow	0.12
Skin	0.01
Stomach	0.12
Thyroid	0.05
Remainder	0.05
TOTAL	1.0

2.3.3 Dose Area Product

The dose area product (DAP) is used to monitor radiographic and fluoroscopy. It is a measure of how much dose the patient receives. It is calculated by multiplying the dose, D , with the beam area, A . Its most common units are $Gy \cdot cm^2$ [15].

2.4 Biological effects of radiation

The biological effect of radiation is divided into two categories, deterministic and stochastic. Deterministic effects cover acute radiation sickness because of high doses over a short period of time. Such acute radiation damage includes skin erythema, cataract, or epilation [16]. Stochastic effects are the increased chance of getting cancer and heritable defects. Doses received during medical imaging does not normally cause any deterministic effects. On the other hand, it is expected that stochastic effects can occur. A direct causal link between ionizing radiation and damage to hereditary material and later development of cancer can in principle be made. However, that is practically impossible due to the small scale, in which these interactions take place and possible long delay between cancer development and exposure. Therefore, a statistical approach is used to evaluate long term effects of ionizing radiation, however there are several factors that makes this approach difficult to apply to low doses. Firstly, people do not want to be given excess dose. Secondly, studies require a large number of subjects to account for other factors due to the low probability of an incident occurring. Thirdly, possibly causing numerous cancer cases, even for scientific purposes, is unethical. Thus, data of higher dose and dose rates from Hiroshima are used to model the increased cancer risk for lower doses as well. The most used model is the Linear No-Threshold Model [17]. This model assumes that the excess chance of developing cancer resulting from exposure to ionizing radiation follows a linear relation to the given dose. [9, 17]. For comparison, an average Norwegian citizen is estimated to receive a total dose of 5.2 mSv per year. [18]

Theory

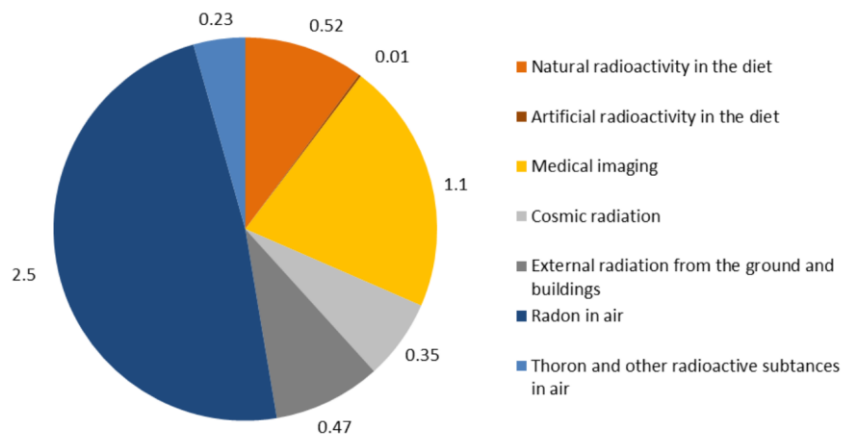


Figure 2.6 - Summary of the average radiation dose (mSv/year) received by the Norwegian population from various sources [18]

3. Methods

3.1 FLUKA

FLUKA version 2011.2x.8 was used for all MC simulations in this study. The simulation parameters are stored in what is called an input file, and the input files are further organized into card. The cards contain information regarding the simulation logic, specific physics settings, geometry, materials, scoring, and the radiation source. Each radiation shielding setup as well as the setup related to the air kerma measurements at HUS has its own input-file, but they share the same physics and radiation field geometry, and most of the geometry. Their differences consist of the inclusion and the placement of lead shielding, and different energy spectrums for the air kerma measurements. Each radiation shielding setup are farther discussed and visualized at chapter 3.4. All input files for the setups can be found at Appendix A Input files for other work in this study and other FLUKA related resources can also be found the appendix and are referenced at their respective chapters.

3.1.1 FLUKA settings

In FLUKA, a so-called default card must be chosen for each simulation to set the best particle transport settings accuracy given the problem. The default card was set to PRECISION. FLUKA stops simulating photons below a certain energy threshold. The PRECISION sets that at 100 keV for photons. Two EMFCUT cards were used to lower the threshold for all materials and regions to 1 keV as the X-ray machine at HUS operates in the 1-120 keV range. A GLOBAL card was also included to increase the default numbers of available regions one can define to 5000. This was done because of the large number of regions that was made when importing an CT-scan as discussed in the next chapter.

Methods

3.1.2 CT

To get an accurate representation for a human, a CT image was imported into FLUKA. The use of real patient imaging data in the form of CT was approved by Regional Committees for Medical and Health research Etheric (REC). The patient of said CT images gave an informed consent to the use of CT-images in this project. Flair has built in tools to view, process and create voxel-maps from DICOM-files of CT scans. The map is made by evaluating the Hounsfield value at each voxel, define regions for each continuous cluster with same HU-value and assign physical properties to each region accordingly. All these voxel-clusters are placed inside a box-formed region called voxel-cage. Due to how FLUKA handles geometry, no other object can be defined inside the VOXEL region. This results in some lead shielding being placed along the VOXEL-cage, rather than along the patient. Ideally both the patient and the operator would be a CT-scan, but FLUKA cannot use two voxel-cards at the same time. That results in only the patient being a CT-scan, favoring a realistic photon attenuation and scattering in the radiation field.

3.2 Scoring in FLUKA

FLUKA can obtain physical quantities, such as dose and fluence, from its simulations. Obtaining this information is called scoring. FLUKA has multiple scoring cards used to determine what, how and where FLUKA will access the wanted quantities. This project used the USRBDX card to score the energy spectrum immediately in front of the beam and USRBIN cards to score all fluence and dose over all regions of interest.

3.2.1 Regions of interest

Two key regions were scored for each setup to evaluate the effect of the radiation shielding setups, the photon fluence across the whole room and the absorbed dose given to a box containing the cylindrical operator. A selected region between the operator and the radiation source was also chosen to evaluate the fluence in front of the operator,

Methods

and the dose scoring was used to assess the operator's skin dose. In addition, the energy spectrum of the beam at the radiation source was scored and used to validate the simulated energy spectrum.

The fluence scored in FLUKA was presented in four plots, three heat maps and one 1D-plot, to see how the photons spread across the operating room. The specific regions for each plot are depicted below.

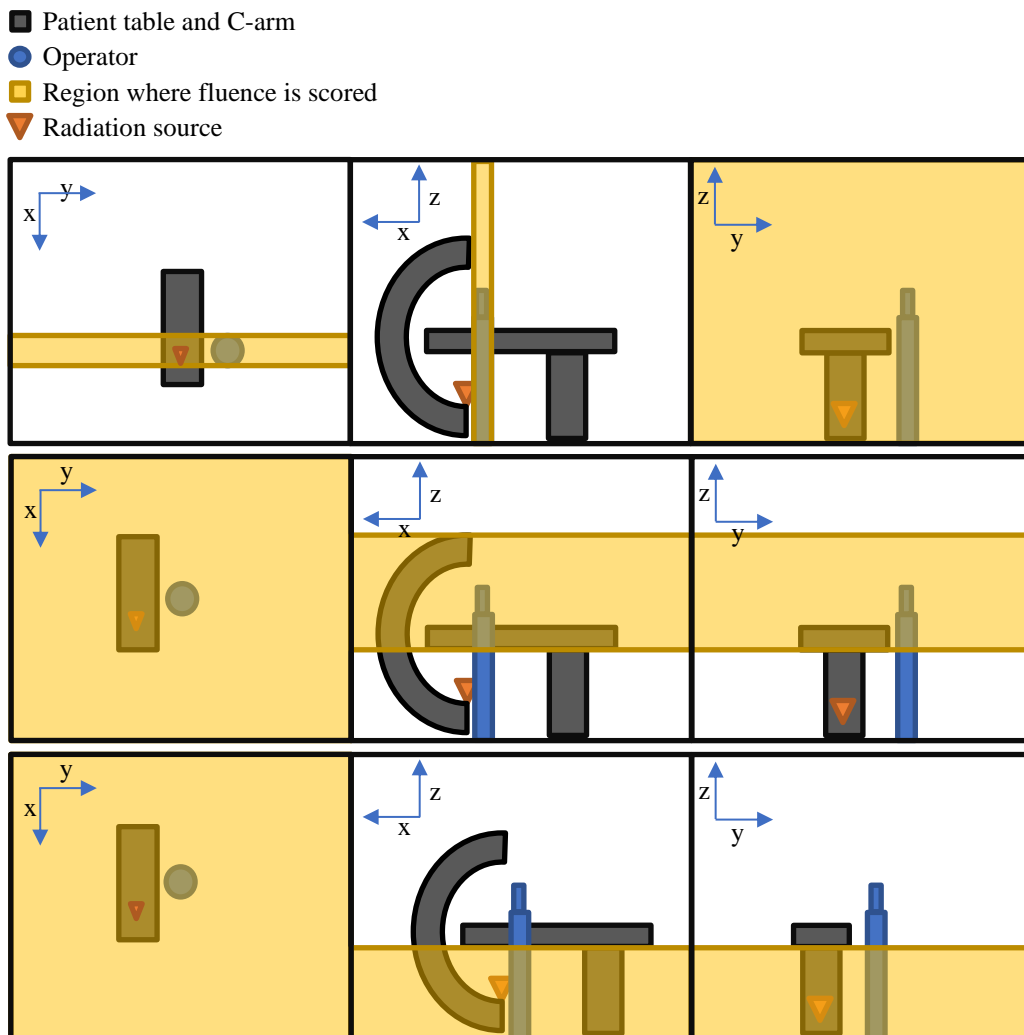


Figure 3.1 - Each row represent a different region used to plot the fluence and contain the same three different viewpoints. The overlaying yellow visualizes what specific region is used to score each plot. The viewpoint completely overlayed in yellow represents the same orientation the corresponding heat map.

Methods

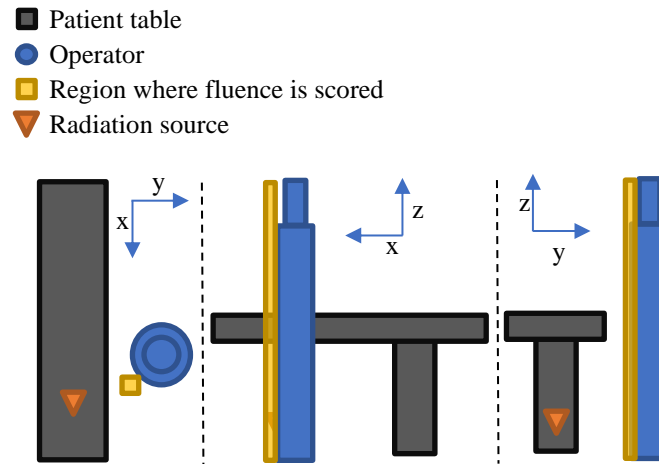


Figure 3.2 - This shows the operator (blue) and the scored area (yellow) in relation to the patient table (grey) from three different angles. The patient would lie the x-direction with the radiation source below the center of their chest.

As with the photon fluence, the dose was presented in heat maps and a 1D-plot. The region used for the 1D-plot is similar to the region for the 1D-fluence plot. However, the upper 30 cm of the scored region (150-180 cm height) is excluded. This upper region would contain both air and waters, while the everything below contains only water. This is because the cylinder representing the operator's head has a smaller radius than the rest of the cylinder-body. In summary, the upper region was omitted when evaluation of the operator's skin dose to avoid misunderstandings, as the dose given to different material combinations are not directly comparable. The dose distribution of said region is included in the 2D-plots.

Methods

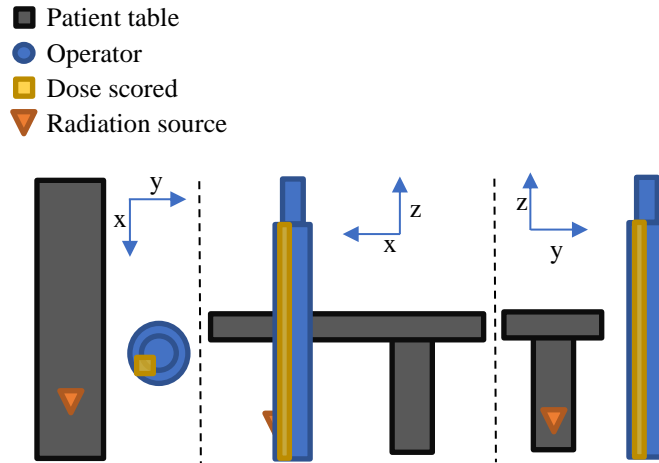


Figure 3.3 - This shows the region used to evaluate the skin dose to the operator in Figure 4.6. The patient would lie the x-direction with the radiation source below the center of their chest.

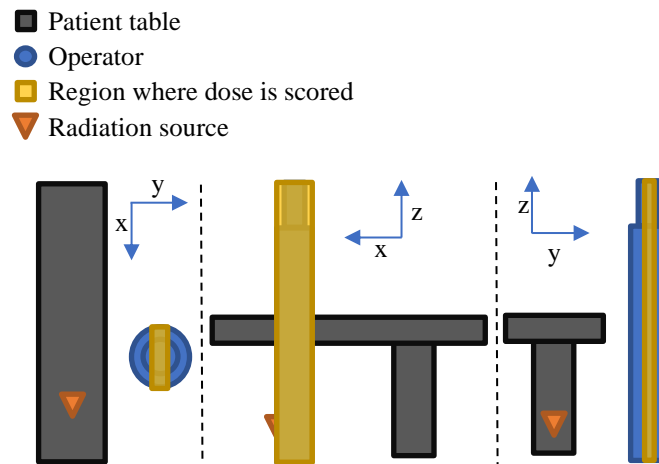


Figure 3.4 - This figures shows the selected region used to plot the coronal dose heat maps, Figure 4.7.

Methods

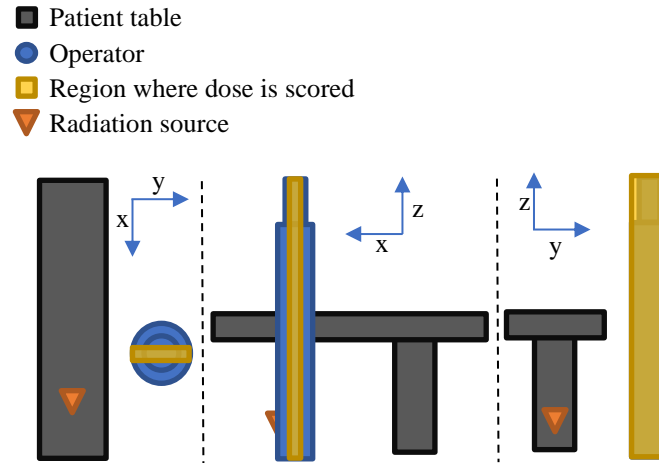


Figure 3.5 - This figure shows the selected region used to plot the sagittal dose heat maps, Figure 4.8.

3.2.2 Scoring H10 & H0.07

The operators in Norway are provided a personal dosimeter by DSA that records equivalent dose at both 10 mm and 0.07 mm soft tissue depth (H10 and H0.07) [16, 19]. That is difficult to score directly in FLUKA as one would need fine division to get those exact depths, thus reducing statistics at those regions. A method to obtain these quantities was therefore developed in this project. Fluence can be obtained from the standard scoring options in FLUKA. This can be converted to air kerma using table A.1 in ICRP 74, and air kerma can be converted to H10 and H0.07 separately with table A.24 and A.25 in ICRP 74 [20]. The energy intervals in the different tables do not overlap. Therefore, the coefficients from table A.24 and A.25 were linearly interpolated to match the energy levels in table A.1. The coefficients were then used to make a single conversion coefficient from fluence to H10 and H0.07 respectively for each energy level.

The FLUSCW-card and the accompanying script, fluscw.f, in Appendix C Fluscw.f is made to generally be able to weight scorings of fluence. The script was further developed to import the coefficients and corresponding energy levels for both H10 and H0.07 conversions. The script only does the conversion, if the scoring bin ID matches the specified ID in the script. This makes it possible to specify if the fluence scored

Methods

will be converted to H10, H0.07 or neither for each scoring card. Testing in FLUKA showed that the conversion would only work correctly for one scoring card per ID. Subsequent scoring cards with the same ID would score 0 dose. This can be circumvented by checking for multiple IDs in the scrip's logic. For instance, the script could do the H10 conversion for bin ID 30 and 32, allowing a single scoring card with ID 30 and another single scoring card with ID 32 to perform the conversion.

3.3 Radiation source

The X-ray tube creates a range of photon energies rather than monoenergetic photons due to how they are made, as discussed in 0. The X-ray machine also changes the kVp and mAs according to the thickness of the patient and mode to ensure image quality as discussed in chapter 2.1. The script `discrete.f` is used in conjunction with FLUKA to create said spectrum and field geometry.

3.3.1 Beam angles

The C-arm at HUS has a range of possible beam angles. This is to allow the operators to find angles that give a clear view of where they are currently working. All X-ray equipment in Helse Vest, including the cat-labs at HUS, is connected to the local radiation database at HUS. The database automatically stores detailed information in the DICOM Radiation Dose Structure Report (RDSR) format. The RDSR stores multiple quantities, where the C-arm angle and mode, DAP, kVp, mAs and beam filtration are relevant for this study. This data was analyzed and processed by C. Davidsen in OpenREM, which is an open source program used to record patient dose. All simulations are based on the Anteroposterior (AP) projection, which is when the beam is placed directly under the isocenter. FLUKA can, by default, specify the position, direction, and spread of the radiation source. These simulations use the external script `discrete.f` in Appendix B to specify the beam spread as discussed in 3.3.2.

Methods

3.3.2 Field geometry

While at HUS, a typical field size was estimated to be a $10.8 \cdot 10.8 \text{ cm}^2$ cross section in the middle of the patient by measuring the image size during a procedure. The C-arm shapes the photon field with collimators (as discussed in 2.2.6). This is emulated by sending the photons with a random direction each primary. The distribution of possible angles is chosen to achieve the desired field size of 10.8 cm width within the patient. The selection of random angle and photon energy is handled by the script discrete.f. The law of large numbers ensures the correct energy spectrum and smooth distribution with enough primaries. The figure below illustrates this further. The input for the energy spectrum can be found in Appendix B and a scoring of the spectrum at chapter 4.1

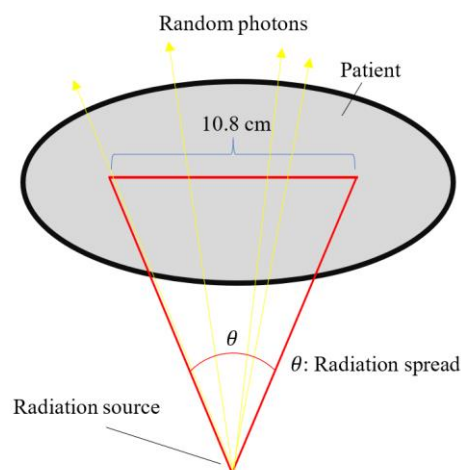


Figure 3.6: The beam direction is set to a random angle within the radiation spread (red) and sends one photon (yellow) with a random energy specified by the spectrum each primary.

3.3.3 Cumulative energy spectrum

The kVp and mAs varies to ensure a sufficient image quality, as mentioned in chapter 2.1. Different kVp results in different energy spectrums. A representative energy spectrum was created to compensate for the different energy spectrums over various procedures. This make it possible to evaluate the average dose given to operators over long-term rather than from one specific procedure and its spectrum. The cumulative

Methods

energy spectrum was made by making an energy spectrum for each kVp with SpekCalc. Each energy spectrum was then weighted by how much DAP was recorded for each respective kVp. Then the spectrums were weighted and added together, creating a cumulative energy spectrum. The kVp, corresponding DAP values and filtration values comes from the RDSR data automatically collected. The SpekCalc settings can be found in Figure 0.1. Each spectrum only varied the kVp. The RDSR database stores beam angle and mode. That makes it possible to create specific cumulative spectrums for each angle and C-arm mode separately. In summary, the cumulative spectrum made and used in this project is weighted by DAP, and only uses data from the beam angle AP and fluoro mode. Figure 3.7 below shows said spectrum.

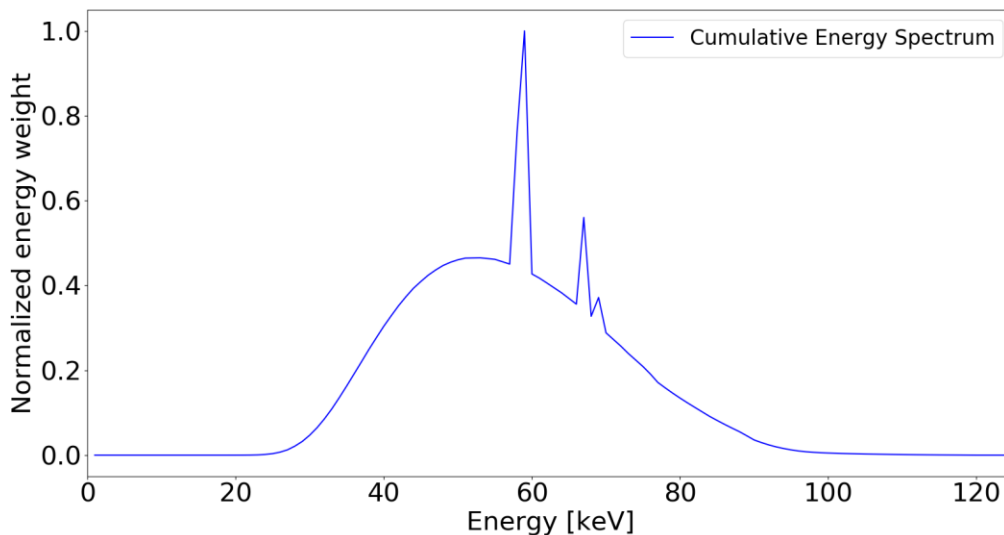


Figure 3.7: Plot of the cumulative spectrum weighted against DAP from the OpenREM data during procedures. Only data during fluoro mode and AP projection is used to create the weights.

3.4 Radiation shielding setups

Various radiation shielding setups were made in FLUKA to evaluate if FLUKA is a viable tool to study the effect of different radiation shielding setups. Measurements of shielding dimensions, C-arm and the X-ray guided operating room at HUS were done

Methods

to recreate it as accurately as possible in FLUKA. The radiation source is placed at the bottom end of the crescent shape. All specific details of the setups can be found in the input files. The walls, ceiling and floor were set to concrete. Concrete is not previously defined in FLUKA, and table 0.1 in the appendix shows the composition of concrete used in the simulations. Each setup ran 3,000,000,000 primaries each.

Table 3.1: Describes all objects shown in Figure 3.8 to Figure 3.12

Object	Description
A	Cylindrical operator made of water
B	CT-scan of patient
C	Various 0.5 mm lead shielding
D	Patient table and table foot made from carbon
E	C-arm made from carbon

3.4.1 Full protection extended to floor - Lead **S**creen, **B**lanket, extended to **F**loor (**SBF**)

Setup SBF is made and an ideal. All lead protection is in contact with each other, creating a continuous layer for lead. This setup has all shielding components, the blanket over the patient, lead screen above the patient and lead screen attached to the side of the bed. The lead screen attached to the bed is extended to stop 1 cm above the floor, unlike all other setups, which have a gap of 15 cm

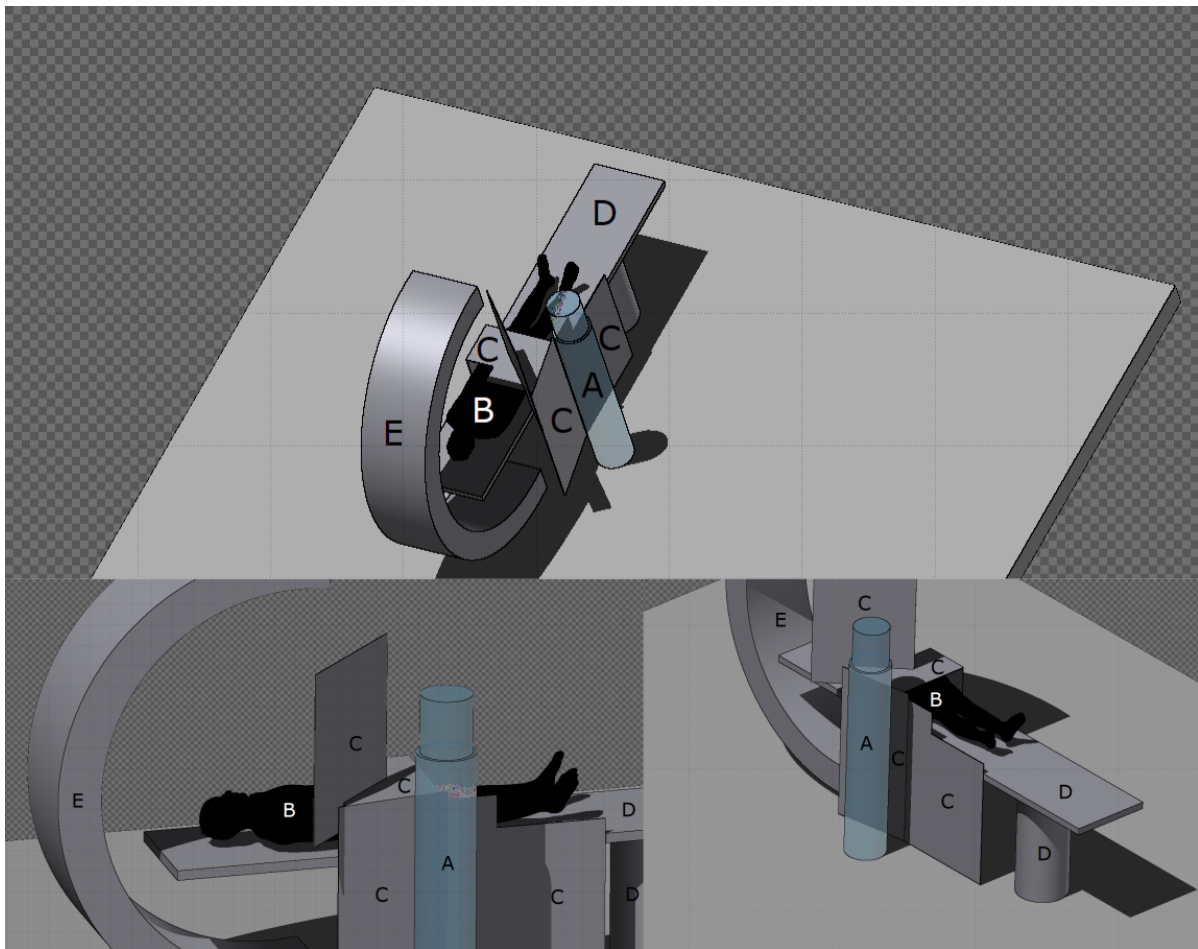


Figure 3.8 - Shows radiation shielding setup SBF from different perspectives. The walls and ceiling have been removed from the picture for a clearer view. Farther details of each region specified by a letter can be found in Table 3.1

Methods

3.4.2 Full protection - Lead **S**creen, **B**lanket (**SB**)

Setup SB is a typical setup for radiation shielding during cardiac intervention. It contains the same components as Setup SBF, the lead blanket over the patient, lead mounted to the table and lead screen, and there are no gaps between the components. The lead attached at the bed leaves a gap of 15 cm above the floor. This distinction from the previous setup can be seen at the bottom right in their respective figures, (Figure 3.8 and Figure 3.9).

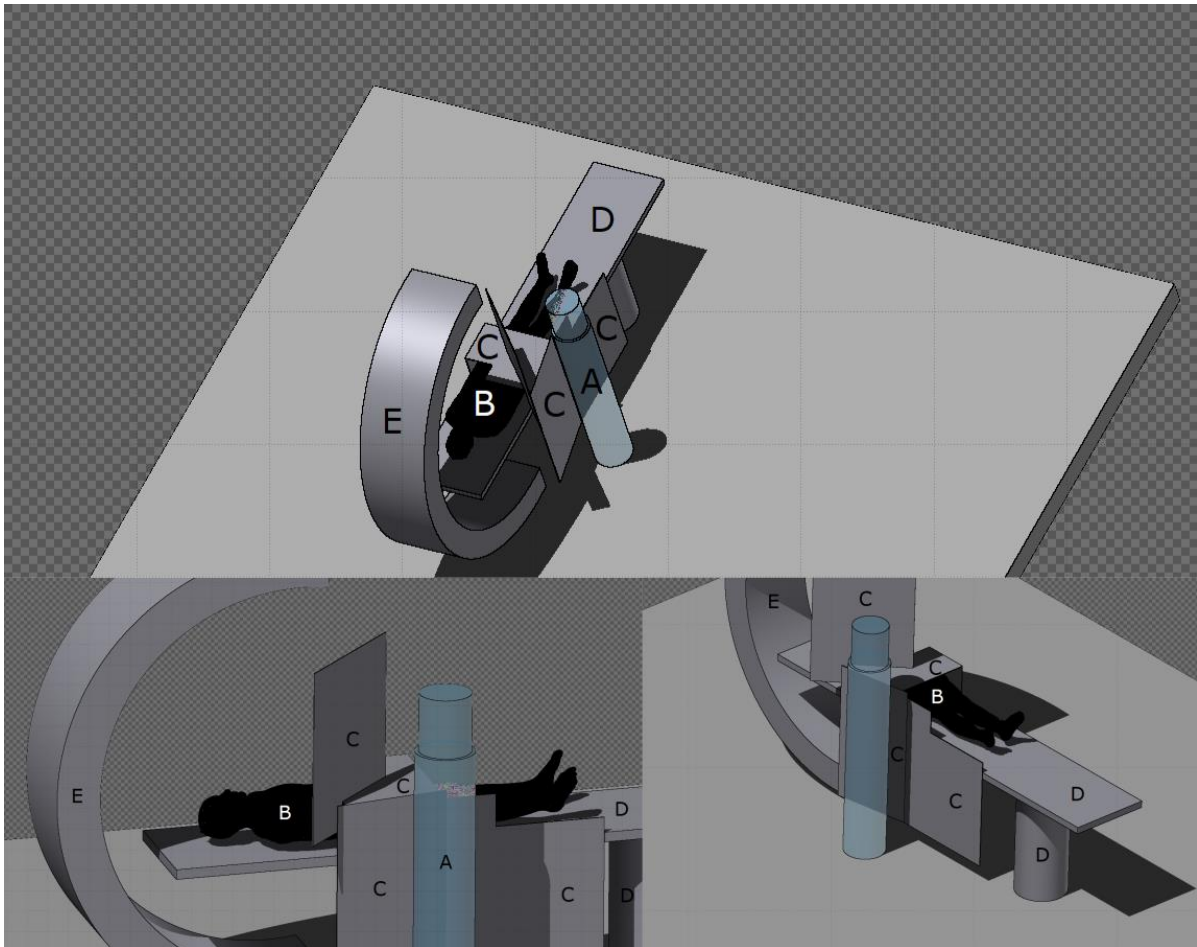


Figure 3.9 - Shows radiation shielding setup SB from different perspectives. The walls and ceiling have been removed from the picture for a clearer view. An explanation of each denoted figure can be found in Table 3.1.

Methods

3.4.3 Full protection with gap - Lead **S**creen, **B**lanket, **G**ap (**SGB**)

This is the first setup that has a gap. Setup SGB still contains all shielding components, but the lead shield over the patient is raised. That creates a gap between the lead blanket and the lead screen. It can be best seen in the lower left perspective in the figure below.

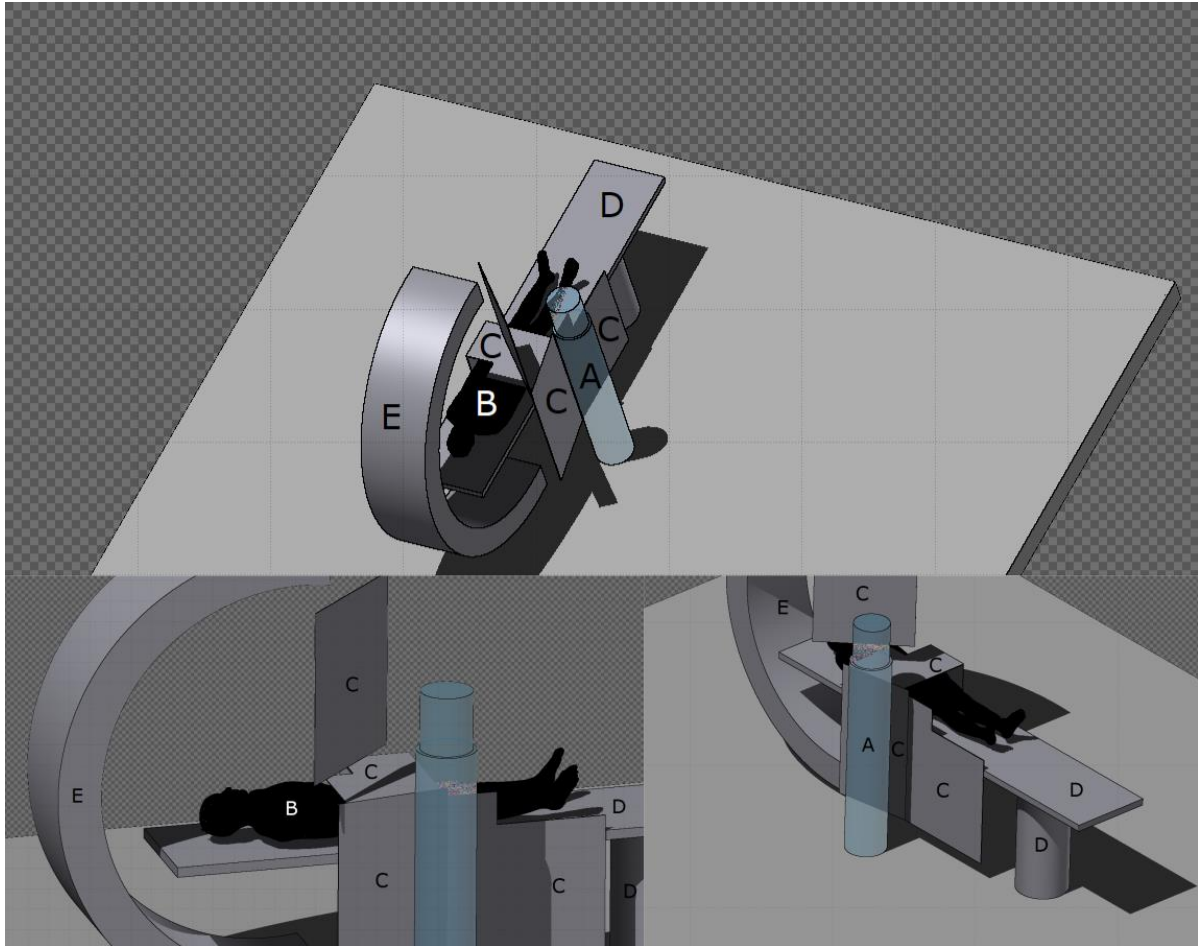


Figure 3.10 - Shows radiation shielding setup SGB from different perspectives. The walls and ceiling have been removed from the picture for a clearer view. An explanation of each denoted figure can be found in Table 3.1.

Methods

3.4.4 Gap without blanket - Lead **Screen**, **Gap (SG)**

The lead screen over the patient is still raised, and the lead blanket over the patient has been removed completely in Setup SG. The lead protection at the side of the bed remains in place.

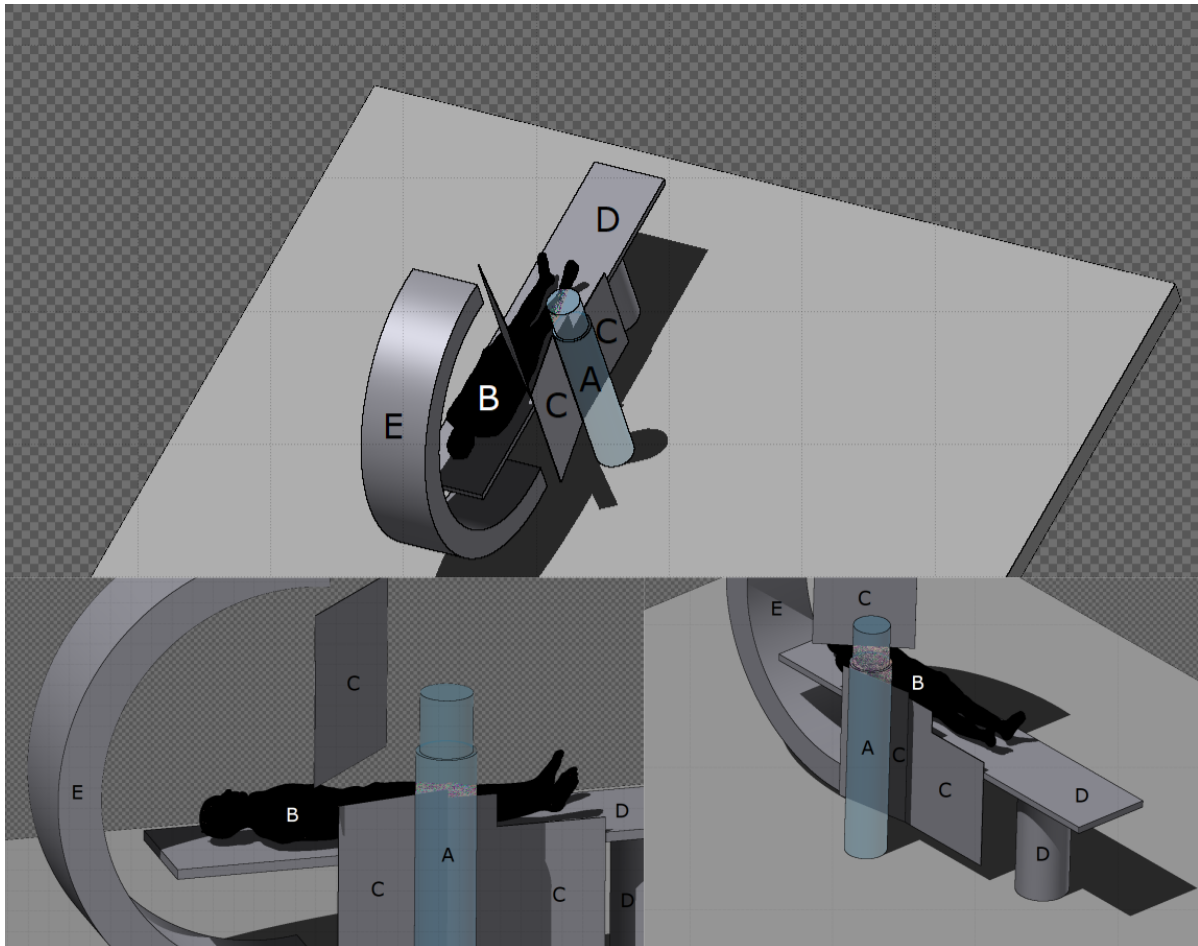


Figure 3.11 - Shows radiation shielding setup SG from different perspectives. The walls and ceiling have been removed from the picture for a clearer view. An explanation of each denoted figure can be found in Table 3.1.

Methods

3.4.5 No protection - **Z** zero protection (Z)

All shielding components between the operator and the radiation source have been removed in Setup Z. The lead attached to the side of the table has been placed farther away from the radiation source.

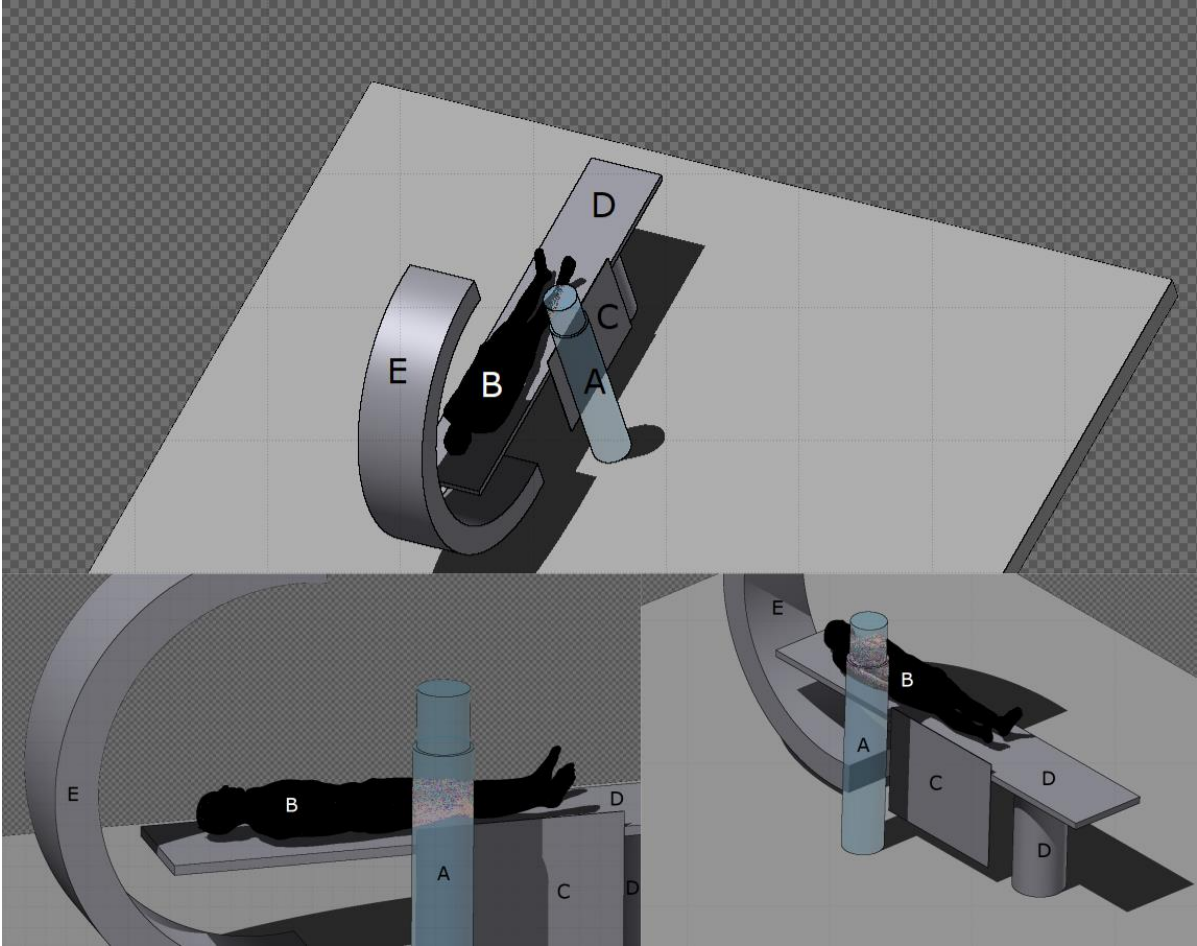


Figure 3.12 - Shows radiation shielding setup Z from different perspectives. The walls and ceiling have been removed from the picture for a clearer view. An explanation of each denoted figure can be found in Table 3.1.

3.5 Air kerma measurements at HUS

Measurements of the dose rate was taken at HUS. This was done to be able to relate the dose scored in FLUKA to dose rates during procedures. The scaling factors can be seen in table 4.1 and 4.2. They were found by calculating the quotient between the dose rate at Haukeland and the dose scored in FLUKA. The air kerma measurements were taken with a RaySafe X2 Survey Sensor. The sensor is on an energy compensated silicon diode array [21]. A cylindrical phantom with a radius of 16 cm and length of 14.5 cm made of PMMA was placed in the radiation field to emulate a person scattering photons into the room. The detector was attached to a microphone stand and placed at three different locations close to where the operators would stand to ensure correct scaling near our regions of interest. The specific locations of the detector in space are shown and further specified in figure 3.13. Measurements for both fluoro and acquisition were taken at each detector placement. The C-arm was turned on a few seconds before the detector started to sample and turned off after it was finished to maintain a steady dose rate while recording. The kVp from each measurement was recorded. The average kVp for each C-arm mode was used to create a specific energy spectrum with. The lab's radiation shielding setup during the measurements and the PMMA phantom was recreated in FLUKA to have a similar dose distribution. The simulations were run with 100,000,000 primaries each and the input files for FLUKA and energy spectrum are included in 0The detector measures air kerma, whereas FLUKA scores absorbed dose. Air kerma and absorbed dose was assumed to be equal, as these energies produced by the C-arm are relatively low (5-120 keV).

Methods

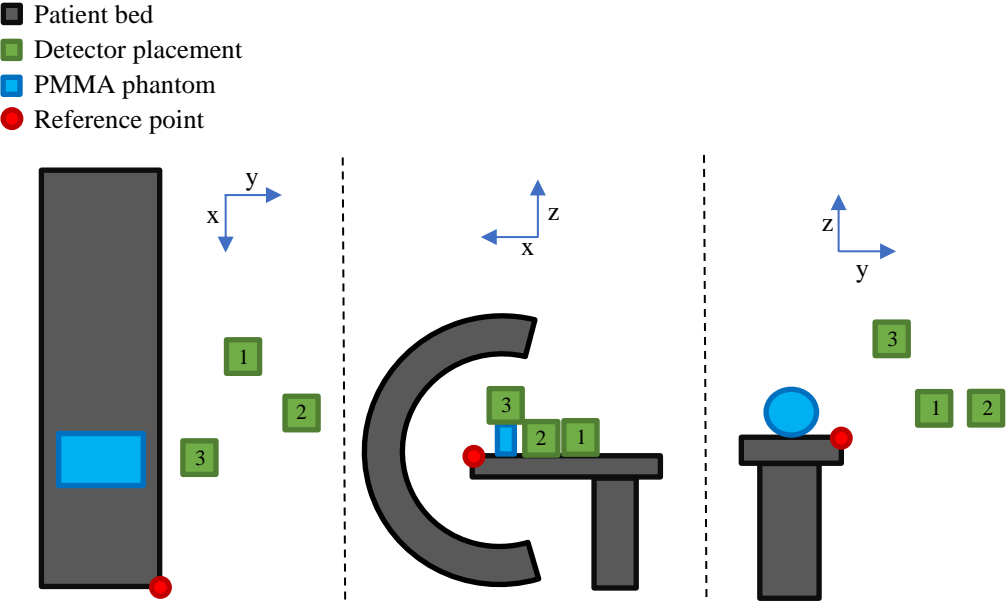


Figure 3.13 - Shows the detector placements relative to the corner of the table from two different points of view. A PMMA was used the measurements and simulations. The positions of the detector relative to the reference point in cm are: 1: (-126, 36, 24) - 2: (-83.5, 63, 24) - 3: (-51, -24, 40)

4. Results

4.1 Spectrum scoring

The energy spectrum was scored directly in front of the radiation source. This makes it possible to compare the scoring to the spectrums input data to validate the simulated simulations, specifically the discrete.f script. Details on how the cumulative spectrum is made is discussed in chapter 3.3.3. The bin size of the input data is 1 keV. The input spectrum was shifted 0.5 keV. This is equivalent to plotting each weight the input spectrum with its average energy. The scored spectrum (red) is aligns directly above the spectrum input data (blue).

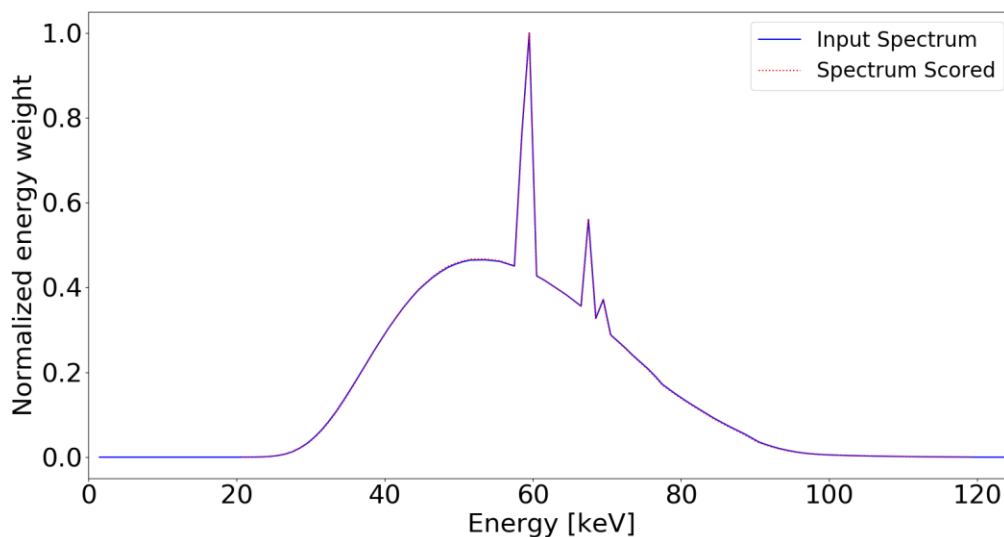


Figure 4.1 - A plot of the spectrum scored (red dots) directly in front of the operator. The input spectrum (blue lines) is added for comparison.

4.2 Fluence scoring

The photon fluence is the measure of particles per area. In this project fluence refers specifically to numbers of photons per square centimeter. The fluence is not necessarily directly correlated to dose, but it strongly correlates to dose and it gives an insight of

Results

where the photons travel. The fluence was scored across the whole room. Certain cross sections across the whole room as well as the fluence in front of operator were used to evaluate the protection setups.

4.2.1 Fluence in front of the operator

A region between the operator and the source with the dimensions of roughly 6·6·180 cm³ was used to evaluate the shielding setups. The fluence in this region is plotted below for each shielding setup. Setup Z has no shielding between the operator and the field and has higher fluence for all heights compare to all other setups. The fluence for Setup Z is 10 to 100 times higher than the fluence to Setup SBF, which is lowest. The fluence increases slightly to a height of 50 cm. The fluence decreases from that height, but has an increase from 80 to 115 cm. This is the height of the patient and patient table. Setup SB, SGB and SG have the same shielding below the patient table, 0.5 mm lead from the table to 15 cm above the floor. These setups also have similar fluence up to the height of 85 cm, where the patient table starts. The fluence for Setup SB continues to decrease to 150 cm. In Setup SGB, the lead screen mounted to the ceiling is raised 15 cm to create a gap in the shielding. The fluence for this setup starts increasing again and peaks at 150 cm. The fluence is almost 10 times higher than for Setup SB at SGB's peak. Setup SG maintains the raised lead screen and removes the blanket. Its fluence also increases to a local maximum at about a height of 150 cm, where it is more than 10 times higher than for Setup SB. The shielding in Setup SBF only differs from Setup SB in having the lead mounted to the patient table reach 1 cm above the floor. Setup SBF has the lowest fluence for all heights up to 175 cm. It has almost identical fluence to Setup SB for the last 15 cm.

Results

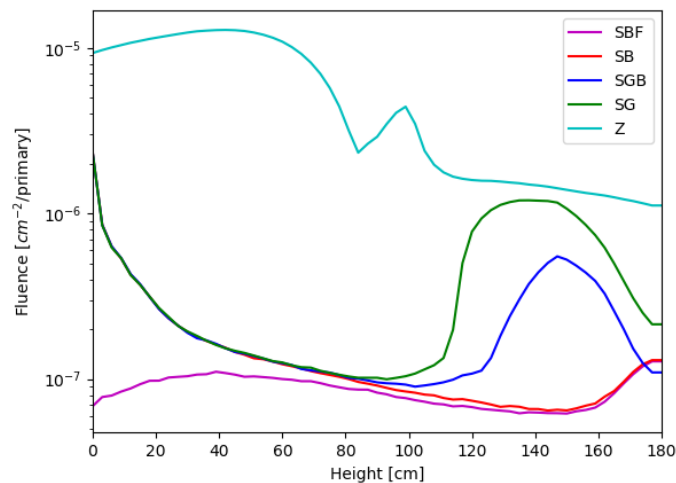


Figure 4.2 - Graph of the fluence in front of the operator at all heights for all radiation shielding setups. The scored region is $276 \leq x < 282$, $-363 \leq y < -357$, $0 \leq z < 180$ (height) which is visualized in Figure 3.2.

4.2.2 Fluence across the operating room

Figure 4.3 show that the highest concentration of the photons is below the patient table. Setup SB to SG have a gap between the lead shielding and the floor. These plots show a large portion of photons escape through the gap close to the floor. The fluence drops two orders of magnitude as they traverse the operator. This suggest they attenuate, possibly delivering a large dose at the operator's feet. Setup SGB and SG both have a gap between the lead shielding above the patient. The fluence there is clearly higher, and the removal of the blanket further adds to the increased fluence, as seen in Setup SGB.

Results

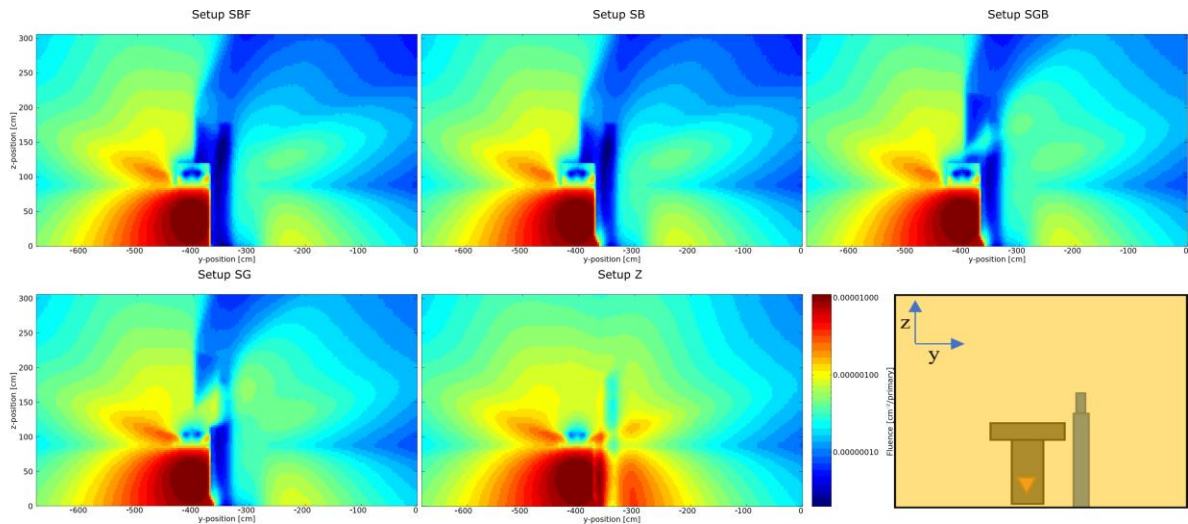


Figure 4.3 - This shows the fluence in the cross section going through the operator measured for each setup and a cross sectional view of the geometry of the plane. The first row in Figure 3.1 specifies the regions further.

There are three parts that block the fluence below the table ($z < 85$ cm), the foot of the patient table (top), the operator and radiation shielding (top right), and the C-arm (bottom). However, the table foot and C-arm does not shield the operator. Setup SB to SG share the same shielding below the table, and their fluence distributions are alike. Setup SBF has the most shielding and lowest fluence in this region.

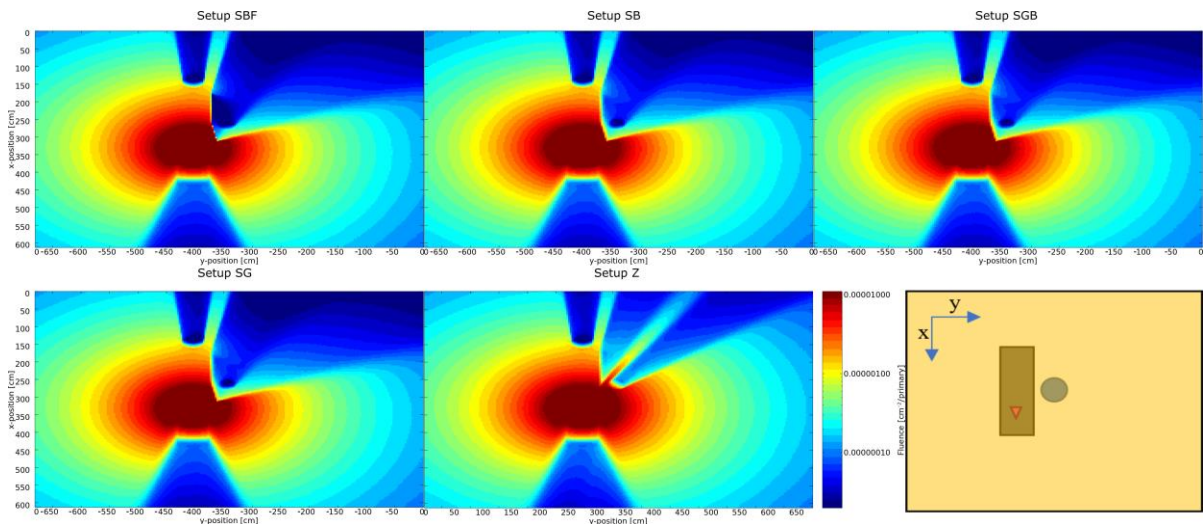


Figure 4.4 - This shows the fluence below the table ($0 \leq z < 84$) for each setup and a cross sectional view of the geometry of the plane. The second row in Figure 3.1 specifies the regions further.

Results

The shielding effect of the C-arm is also apparent above the table ($z > 85$), but is not relevant to the operator in this region either. Both Setup SBF and SB have the lowest fluence at the operator. Introducing the gap in Setup SGB shifts the fluence gradients to the top right, increasing the fluence near the operator. Setup SG increases this trend further, thus increasing the fluence. The fluence near the operator is highest for the setup with least protection, Z.

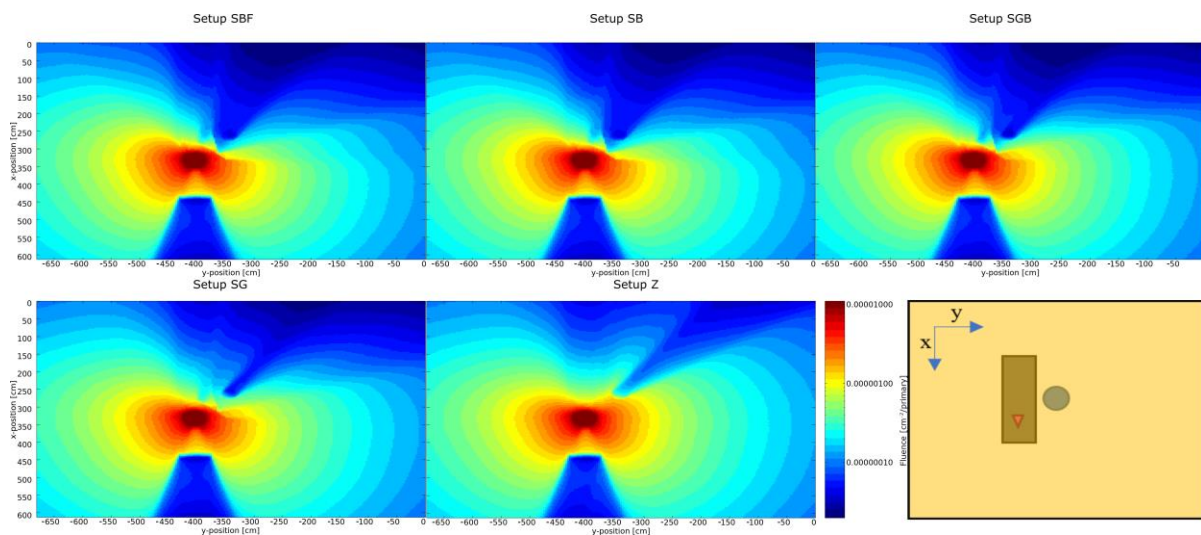


Figure 4.5 - This shows the fluence above the table ($84 \leq z < 252$) for each setup and a cross sectional view of the geometry of the plane. The third row in Figure 3.1 specifies the region used to score further

4.3 Dose scoring

The LNT-model assumes the excess cancer risk is proportional to the dose received. The dose given to the operator is therefore an important part of the simulations in this study. It allows for investigation into if and how the different shielding setups relate to different doses delivered to the operator. The operator's dose has been quantified in two different ways, heat maps of different cross sections of the operator and skin dose over different heights to the operator.

Results

4.3.1 Skin dose

The dose scored varies more from neighboring heights than the fluence in figure 4.2. However, the dose trends are similar to that of the fluence for each setup. No radiation shielding (Setup Z) gives the highest dose for all heights with a local maximum at 100 cm height. Setup SB, SGB and SG all have the same dose at the heights 0-85 cm, where the patient table starts. The dose for Setup SB decreases from 85 cm and above. Both Setup SGB and SG have an increased dose from 110 cm and above, where SG has the highest dose. The dose has a higher relative increase when introducing a gap in the setup, compared to removing the patient blanket.

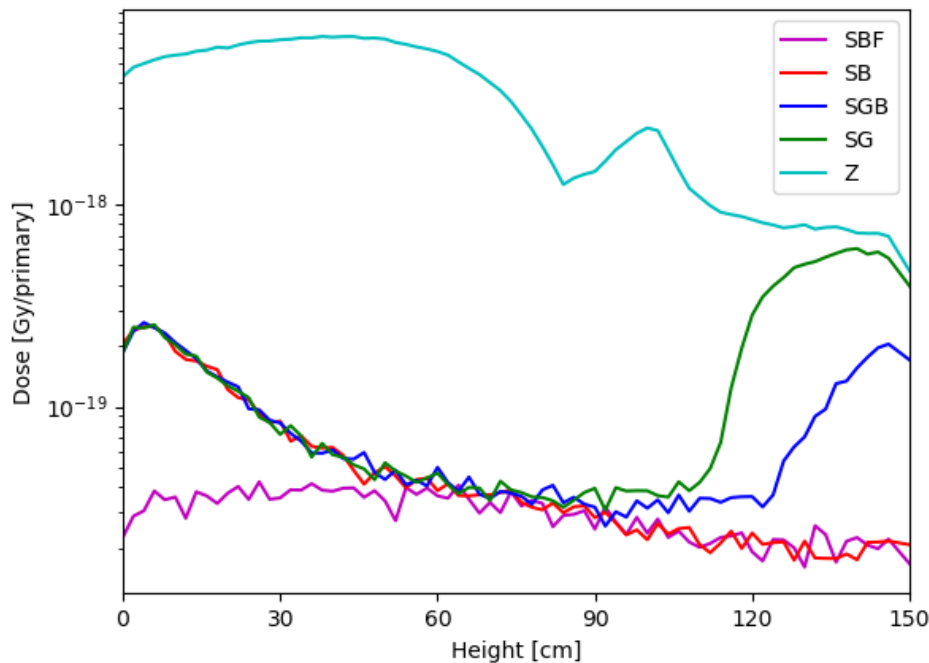


Figure 4.6 - Graph of the skin dose given to the operator at different heights for all radiation shielding setups. The region scored is $272 \leq x < 274$, $-357 \leq y < -355$, $0 \leq z < 150$ (height) which is visualized in figure 3.3. Note that the plot stops at a height of 150 cm unlike the corresponding fluence map, as discussed in chapter 3.2.

4.3.2 Dose heat maps

Results

The dose over this cross section is mainly given to the operator at its left side. There are two regions with higher noise, top left and right, and at the outer left and right edge. These regions are where the dose is scored over both water and air. The operator's dose is scored over a box-shaped region, while the operator is modeled as two water cylinders. The top corners are outside the smaller radius of the water cylinder modeling the head, thus containing air. The outmost edges also contain air and water, as the cylinder gets thinner than the box-region used to score. The dose on the left side below 120 cm are similar for all setups, excluding Setup Z. The operator gets a higher dose at a progressively larger area in the upper chest and neck region, as radiation protection is removed.

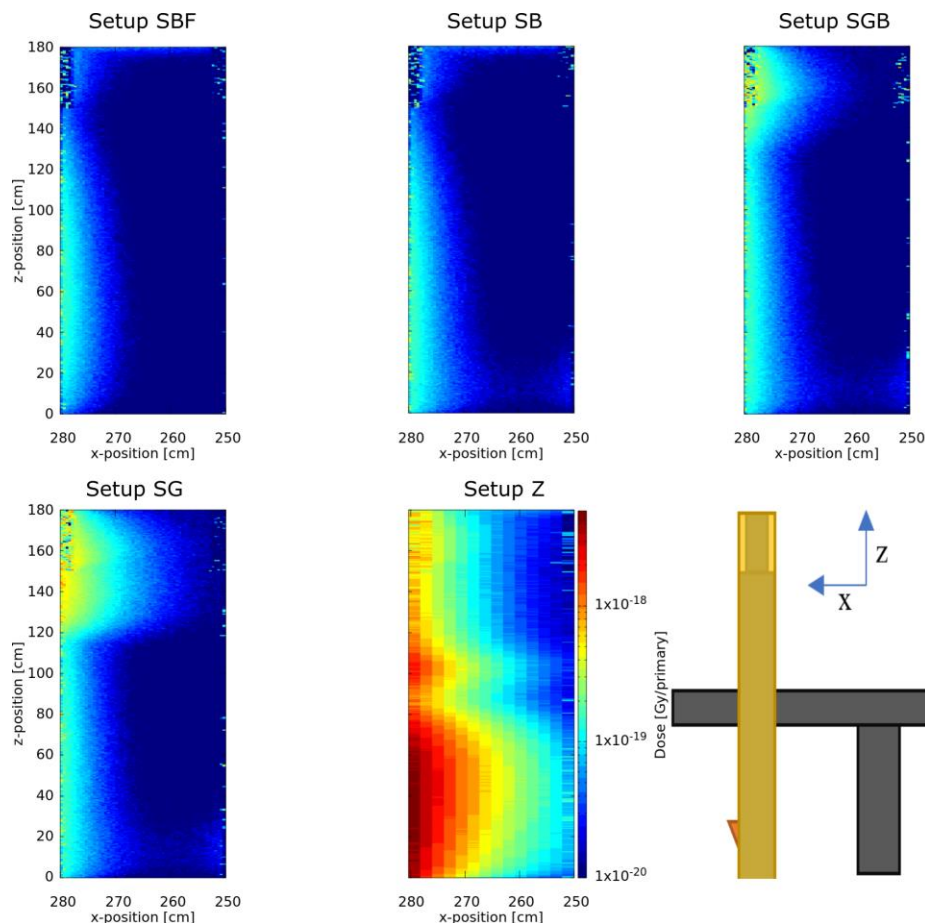


Figure 4.7 - Dose distribution to the operator over the coronal plane for all setups. The z-axis represents the height of the operator. This cumulative cross section was plotted for $-350 \leq y < -340$. Setup Z has less resolution in the x-axis due to an error in the scoring card during its simulations.

Results

The dose plots below contain the same region with increased noise as mentioned in the last paragraph. The operator gets a higher dose closer the radiation source, which is at the left side of plot. This closes to the patient bed and the radiation source. The same tendency of more dose in the upper chest and neck area can be found in the coronal plot of the dose above.

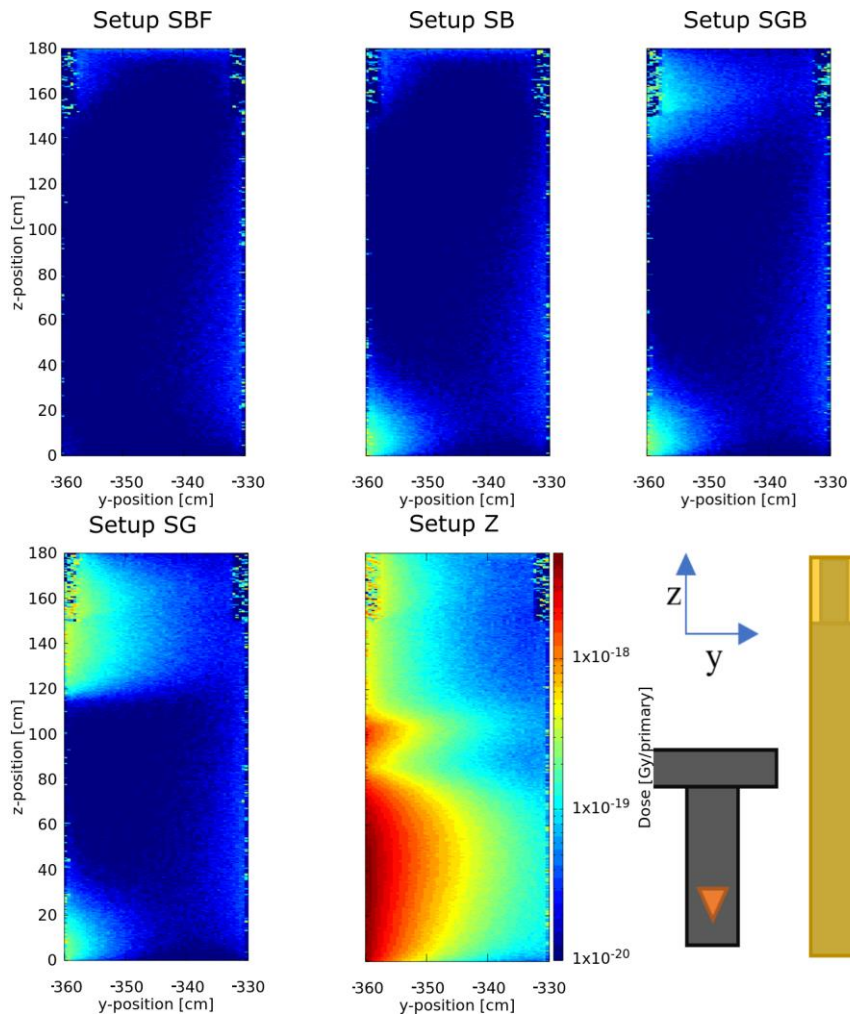


Figure 4.8 - Dose distribution to the operator over the sagittal plane for all setups. The z-axis represents the height of the operator. This cumulative cross section was plotted with $260 \leq x < 270$

4.4 Dose rate measurements at HUS

Air kerma measurements at HUS was done to relate simulated dose per primary photon to real dose rates. That would against allow for estimates of annual dose exposure. All

Results

data gathered at HUS and the specific FLUKA files done to simulate could be found at OA visualization and specific information regarding detector placements can be found in chapter 0. The uncertainty of the dose scored in FLUKA is statistical and is presented in the scoring date after each simulation. The RaySafe X2 Survey Sensor provided four significant digits in its measurements. This means the total error of the scaling factor is dominated by the statistical uncertainty in FLUKA. The smallest and largest scaling factor for each placement was calculated as such:

$$\text{Smallest scaling factor} = \frac{\text{Dose rate at HUS}}{\text{Dose scored in FLUKA} + \text{uncertainty}}$$

$$\text{Largest scaling factor} = \frac{\text{Dose rate at HUS}}{\text{Dose scored in FLUKA} - \text{uncertainty}}$$

Table 4.1: Table comparing dose scored in FLUKA with dose rate measured at Haukeland using the acquisition mode at 15 FPS

Acquisition mode	Dose scored in FLUKA [mGy/primary]	Uncertainty [mGy/primary]	Dose rate at HUS [mGy/s]	Smallest scaling factor [primary/s]	Largest scaling factor [primary/s]
Placement 1	7.2E-16	1E-16	0.00604	7.1E+12	1.0E+13
Placement 2	7.1E-16	9E-17	0.00674	8.5E+12	1.1E+13
Placement 3	2.0E-15	3E-16	0.00856	3.8E+12	5.0E+12

Table 4.2: Table comparing dose scored in FLUKA with dose rate measured at Haukeland using the fluoro mode at 7.5 FPS

Fluoro mode	Dose scored in FLUKA [mGy/primary]	Uncertainty [mGy/primary]	Dose rate at HUS [mGy/s]	Smallest scaling factor [primary/s]	Largest scaling factor [primary/s]
Placement 1	1.7E-15	2E-16	0.000798	4.3E+11	5.4E+11
Placement 2	1.0E-15	2E-16	0.000855	7.2E+11	1.0E+12
Placement 3	3.1E-15	2E-16	0.00112	3.4E+11	4.0E+11

There is no scaling factor that fits between the error for each mode respectively. The air kerma rate measured at Haukeland are more similar than the absorbed dose scored in FLUKA.

Discussion

The cumulative spectrum created based on data from AP orientation and the fluoro mode was created, and the energy spectrum scored in FLUKA is close to the spectrum specified by the input. The different shielding setups have a clear difference in dose given to and fluence near the operator. This supports the use of MC simulations in FLUKA to evaluate different shielding setups. Relating the dose/primary to real dose rates requires further examination into why the dose rates measured at HUS do not follow the dose distribution scored in FLUKA.

Spectrum Scoring

The scored spectrum matches the cumulative energy spectrum created. This is to be expected over this many (3,000,000,000) primaries. The spectrum was scored both ways. That increases the chances of scoring backscattering. This does not appear to have any significant effect in this. Backscattering could be a larger factor if denser matter were close to the radiation source. using different C-arm projections that are closer to the table.

Fluence scoring

Fluence in front of the operator

Fluence is not necessarily directly related to radiation dose. The dose depends on the energy spectrum, but the fluence and dose distribution in figure 4.2 and 4.6 follow the same trends for each setup. The different setups clearly have different fluence in front of the operator, making it possible to compare the setups considering the fluence. The fluence scored in front of the operator varies up to a factor of 100 times at the same position heights for different radiation protection setups. This does compare an unrealistic scenario of no shielding to an improved setup. It does, however, show the value of having shielding.

The largest deviation in fluence in the 1D-fluence plot is below the table. This is where the radiation source is, and the fluence heat map (Figure 4.3) show this is where most

Discussion

of the radiation is. Naturally, Setup Z with least protection sees the highest fluence. The legs also do not contain any vital organs and are less radiosensitive compared to organs in the upper body, according to the tissue weights in Table 2.2. However, operators still want to minimize the dose whenever possible. This lead protection is also not in the operator's main workspace and does not hinder the maneuverability as much as other radiation shielding, and it can be a continuous piece of lead, leaving no gaps. All this makes the shielding below the patient table easy to manage during procedures and less susceptible to improper use. Also, the shielding below appears to not only effect the fluence below the table. The 1D-fluence plot shows that Setup SBF has lower fluence up to a height of 175 cm, suggesting further value of shielding below the table. All this supports the value of making shielding below the table cover a larger area. The patient table's weight limit is the main limiting factor to this area of protection. Shielding thickness is not a parameter in this study, but thinner shielding that reaches the floor, could result in lower doses for the same shielding weight. One could also have a minimum requirement of shielding and add longer or thicker protection if the weight of the patients allows it.

Both setup SGB and SG have a gap between the layers of lead, but SG also lacks the blanket over the patient. The increase in fluence is larger when introducing the gap (Setup SB to SGB) than when the blanket is removed (Setup SGB to SG). This suggests the gap has a larger relative effect on the fluence than the blanket. The lead screen attached to the ceiling at HUS can attach flexible shielding at its lower end. This makes it easier to maintain a continuous layer of protection during procedures.

As with the other shielding discussed, increasing the blankets dimensions would reduce the fluence at the operator. It, too, adds to the total weight on the patient table. The lead blanket over the patient is also in the sterile zone. It is therefore required to be sterile too. This sets higher requirements to cleaning than for instance the shielding under the table. Increasing the size of the blanket could make it more difficult to sterilize and/or keep sterile.

Discussion

Setup SGB has the lowest fluence in the 1D-plot for the tallest 5 cm. Here it is important to emphasize that the lead screen is raised, not cropped, to create the gap. The elevated lead screen provides more protection at top of the operator. The same reduction trend at the top of the operator is seen in Setup SG too, which also have a raised lead screen. A thinner, taller lead screen could be beneficial for the same reasons as discussed for the shielding below the table.

Fluence across the operating room

Fluence is a useful measure to evaluate the spread of radiation through the room. This is because the fluence heat maps essentially show photon tracks. The radiation spread is visible as the fluence gradually decreases on the photon's path through the air or other medium.

Figure 4.3 illustrates that most radiation is below the patient table, and that the photon radiation get through the gap at waist height in SGB, SG and the gap at the floor in all, but SBF. This is to be expected. Interestingly, the difference in fluence at the operator with and without the gap, meaning the difference between Setup SB and SGB, is less apparent in the yx-fluence heat map (Figure 4.5), compared to the other fluence plots and dose plots. This underlines the need to explore and view the shielding setups from multiple angles. The fluence gradient lines in 4.5 show that the fluence quickly rises to the left of the operator (immediately below on the plot), behind the shielding. This increase in fluence is largely independent of the gap and patient blanket. This suggests widening the screen would be the main way to reduce said increase in fluence.

Dose scoring

Skin dose

The operator's skin dose varies more than the fluence in front of the operator, especially where the dose is low. This is because of the low number of incidents, due to the radiation shielding. However, the dose-height trends for each setup is visible. The variance can naturally be improved by running more primaries and possibly by evaluate the skin dose through different means. The method created to convert fluence to H10

Discussion

and H0.07 needs the fluence in front of the operator, which has less statistical error. This conversion does however contribute to more uncertainties between its two conversion steps and interpolation.

The dose plots follow a similar trend as the fluence plots in front of the operator. This means the different shielding setups has the same reduction in the dose given to the operator as discussed considering the fluence in front of the operator. Dose is innately more interesting, when considering protection, as it is directly linked to increases cancer risk according to the LNT-model. This means that preventing the gap at the floor or between the lead shielding is important to reduce the operator dose.

Dose Heat Maps

The heat maps in figure Figure 4.7 shows that the operator receives a dose to their left for all setups. This suggest the radiation scatters around on the outside of the shielding and coincides with the discussion of figure 4.5. Once again, prioritizing the area of the shielding over thickness could be more weight efficient. The main distinction between the setups in these dose distributions is the dose given to the neck when introducing the gap between the blanket and screen. This further support the need for thyroid shields when the gap cannot be avoided. Figure 4.8 illustrates the same effect of the shielding as the skin dose (Figure 4.6). The expose at the operator's feet is mainly depended on the gab above the floor, and the gap and removal of the blanked both increase the given dose at the operator's upper chest and neck.

The outer left and right side and top right and top left side of each dose hate map has more noise. This is because these regions contain air. Photons attenuate less in in air compared to water, resulting in worse statistics. One can also argue that it makes these regions difficult to compare to the rest of the plots. However, the regions are small and localized, making the effects of the shielding visible. Such overlap will always be present, when using cylinder operators and box-shaped scoring regions. A possible future work around is to incorporate the H10 and H0.07 scoring and focus on those.

Calibrations at HUS

There was not possible to find a single conversion coefficient for either fluoro or acquisition mode, also accounting for uncertainties. However, it is hard to find the definitive cause with only three detector locations. The error could be due to a combination of multiple elements. They fall into three main categories: mistakes in the dimensions in FLUKA, the materials used FLUKA and mistakes during measurements. Manufacturers do not want to reveal the exact composition of their products. This makes it difficult to have the correct material for some parts of the simulation. This cannot innately be improved.

More measurements should be taken, in order to find a calibration coefficient for each mode. Mistakes in the simulations dimensions and mistakes during measurements can be improved by more measurements at HUS in the form of additional placement and more per placement. The uncertainties in the simulations can be improved by running more primaries. The detectors' relatively small volume further supports the need for more primaries.

Finding a calibration coefficient is a prerequisite to evaluate shielding setups based on absolute dose. The dose scoring remains a relative quantity without the calibration from dose per primary to dose or dose per second. Evaluations based on a relative quantity is useful but limited. Relative dose comparisons tell you which setup is best, while absolute dose comparisons tell you which setups are good enough. Thus, a calibration is needed to conclude that for instance lead vests are not necessary with certain shielding setups.

Using FLUKA MC simulation to assess dose to operator

An advantage in using FLUKA simulations to assess the dose to the operator is that it is easier to add or make changes to the setup compared to a real setup. This allows for the exploration of many parameters. Some are discussed in chapter 5.1. Exploring more parameters will quickly add to run time, especially if the parameters are independent of each other This motivates a selective approach to parameters. Scoring in FLUKA

Discussion

can also easier evaluate multiple datapoints compared to measurements, giving a more detailed understanding of the dose and fluence distribution.

5. Future Work

5.1 Potential parameters

This study focused on the feasibility of using MC simulations to assess the dose given to operator by looking at different shield geometries. There are more potential shield protection setups that could be investigated, many which have been discussed in this study. However, one of the benefits with recreating the operating room is that it gives unlimited access and freedom to investigate many potential parameters.

The C-arm has two modes, fluoro and acquisition. As discussed, these modes have been developed with different utilization in mind. However, their main difference in the simulations comes from their typically different energy spectrums. It would most likely be more useful to explore their differences after calibrations to assess absolute dose have been done.

The C-arm has a range of different beam angles. Beam angles could impact the exposure of the operator directly by changing the radiation field. The effectiveness of the shielding could also be dependent on the angles. Such knowledge will allow operators to check if the hypothetical better angles give a sufficient view to operate without the need to change any of their radiation shielding. If that were the case, it would be an easy and cost-effective solution compared to changing or editing their existing equipment.

5.2 Incorporate H10 and H0.07

H10 and H0.07 are conventions for evaluate dose at 10 and 0.07 cm soft tissue depths respectively. Future work could go into incorporating said quantities to the simulation's tool for evaluating the operator's skin dose. They have advantages over simply scoring the dose. Operators and other professionals are familiar with these quantities because

Future Work

H10 and H0.07 are established conventions. This makes them more relatable and easier to compare to other scientific works that uses the same quantities.

The H10 and H0.07 conversion methods developed in this study rely on fluence scoring. The fluence in front of the operator had better statistics than the skin dose. This opens the possibility to be able to reduce the number of primaries required to get the desired precision, saving run time. Reducing the run time has two immediate benefits, lowers the entry point to do a study and it leaves room to use the saved time to other work.

5.3 Edit CT to include shielding rather than placing it around protection

A limiting factor in this study was the inability to add materials into the voxel-cage. The geometry of the lead shielding close to the patient had to be approximated to avoid overlapping with the voxel-cage. It is possible to edit the CT-scans. This would allow for the shielding to exist within the voxel-cage as a part of the imported CT-scan itself. This be a step toward a more realistic simulation, and in turn more realistic results from the simulation.

5.4 Having both operator and patient as CT-scans

All simulations of the shielding setups were made with a patient as an imported CT-scan, while the operator was estimated as cylinders. This is because of FLUKA cannot innately run a simulation with two CT-scan at the same time. A possible way around this would be to divide the operating room into two sperate parts. Each part containing the patient or the operator. One would simulate the patient's half first and record the radiation on the border entering the other half. The other half would then be simulated with the recorded radiation. Importing a CT-scan to represent the operator could also be the first step toward a more complete evaluation of effective dose. It would be easier to define different organs and compensate for their radiosensitivity.

5.5 Linking scoring to real life dose

The simulations in FLUKA are limited to relative dose comparisons by itself, which has been used for most parts of this study. There were done calibration measurements in this study to relate dose per primary to dose rate. As mentioned, such calibration would help to validate the simulations, but more work would have to be done to do this comparison. In addition, being able to assess real dose rates would allow conclusion such as if certain shielding setups reduced the dose rate enough to let operators remove some or all their worn protection. Removing worn protection would not only be a quality of life improvement, but also reduce associated strain injuries.

Conclusion

The goal of this study was to explore the feasibility of using FLUKA simulations to evaluate the operator's received radiation dose during interventional cardiology procedures. The effects on operator dose from different radiation shielding setups was investigated through FLUKA simulation. An operating room was recreated in FLUKA and five different radiation shielding setups were implemented for said room. Data from real procedures were used to define the beam characteristics and create an energy spectrum that considers varying defining features. The fluence and dose were scored for each setup to evaluate the dose given to the operator. The scored data from the simulation indicates that avoiding gaps between the shield components and/or the floor is crucial in reducing the dose given to the operator. Having a lead blanket over the patient also has an advantageous shielding effect according to the simulations. The ability to evaluate these results suggests that Monte Carlo simulations through FLUKA is a viable tool to evaluate the relative effectiveness of radiation shielding. This opens for further exploration of parameters and their relation to the operator's dose. The current results also allow for informed decisions when comparing radiation shielding setups. Measurements in the operating room and specific FLUKA simulations were made to relate the scored dose in FLUKA to real dose rates. The measurements and simulations did not yield sufficiently good results to get do a reliable conversion between dose per primary and dose per second. With new and more extensive measurements, such a conversion would make it possible to extend the relative dose and fluence from the simulations done in this study to absolute dose rates received by the operator, including annual and career long estimates of dose exposure. The MC simulations could be used to investigate the potential for reducing the operator's personal protection equipment. Overall, the work performed in this thesis shows that MC simulations has the potential to provide detailed information about shielding effectiveness, far beyond what can be achieved through measurements in the lab alone and can become a useful tool in radioprotection for X-ray guided medicine.

Conclusion

References

1. Beth A. Schueler, P.-T.J.V., RT(R) - Haraldur Bjarnason, MD - Anthony W. Stanson, MD, *An Investigation of Operator Exposure in Interventional Radiology*.
2. Siren Hovland, E.N., Kjetil H. Løland and Svein Rotevatn, *NORSK REGISTER FOR INVASIV KARDIOLOGI (NORIC)*. 2020.
3. Magne Brekke, A.B., *Angiografi*. 2020, Store medisinske leksikon.
4. Steigen, T., *PCI 2018*, Store medisinske leksikon.
5. OneWelbeck, *Angiogram*. 2021.
6. Oro, R., *Percutaneous Coronary Intervention*. 2021.
7. Hammer, M. *X-Ray Physics: X-Ray Interaction with Matter and Attenuation*. 2014; Available from: <http://xrayphysics.com/attenuation.html>.
8. Podgorsak, E.B., *Radiation Oncology Physics: A Handbook for Teachers and Students*. 2005.
9. Herman Cember, T.E.J., *Introduction to Health Physics*. 2009.
10. Merritt, E.A., *X-ray Absorption Edges*. 2012.
11. Greenway, D.D.J.B.a.K., *Hounsfield unit*. 2021.
12. Stuart C. White, M.J.P., *Oral Radiology - Principles and Interpretation*. 2000: A Harcourt Health Sciences Company.
13. Frame, P., *Coolidge X-ray Tubes*. 2009.
14. ICRP, *The 2007 Recommendations of the International Commission on Radiological Protection*, ICRP, Editor. 2007.
15. Dr D. J. Bell, D.Z.V. *Dose area product*. 2021; Available from: <https://radiopaedia.org/articles/dose-area-product-1>.
16. Cedric Davidsen, K.B., Ellisif Nygaard, Kjell Vikenes, Svein Rotevatn, Vegard Tuseth, *Temporal Trends in X-Ray Exposure during Coronary Angiography and Percutaneous Coronary Intervention*. 2020.
17. Allison Campbell, J.J., Jaafer Khani, Maddy Strange, Jason Donev, *Linear no-threshold model*. 2020.
18. Mari Komperød, A.L.R., Eva G Friberg, *Radiation Doses to the Norwegian Population; Summary of radiation doses from planned exposure and the environment*. 2015.
19. Authority, N.R.a.N.S. *Yrkesmessig eksponering for ioniserende stråling - persondosimetri*. 2020 29.07.20 [cited 21 04.03]; Available from: <https://dsa.no/persondosimetri/yrkesmessig-eksponering-for-ioniserende-straling-persondosimetri>.
20. D. Beninson, H.J.D., I. A. Ilyin, W. Jacobi, H. P. Jammet, A. Kaul, D. Li, J. Liniecki, H. Matsidaira, F. Mettler, W. K. Sinclair, B. Lindell, K. Z. Morgan, L. S. Taylor, *Conversion Coefficients for use in Radiological Protection against External Radiation*. 1996.
21. RaySafe. *X2 Survey Sensor*. 2021; Available from: <https://www.raysafe.com/products/x-ray-test-equipment/raysafe-x2-x-ray-test-device/x2-survey-sensor>.

Appendix A FLUKA input files

Atomic composition of concrete used in FLUKA

Table 0.1: Atomic composition of concrete used in FLUKA with a density of 2.05 g/cm^3

Element	Proportion
Carbon	0.23
Oxygen	0.40
Silicon	0.12
Calcium	0.10
Hydrogen	0.10
Magnesium	0.02

Setup SB

* Increases maximum regions

GLOBAL 5000.

TITLE

Lab 2 - Haukeland - Fluoro, AP, Setup SB

* Set the defaults for precision simulations

DEFAULTS

PRECISIO

* Define the beam characteristics

BEAM -8E-05 0.0 0.0 PHOTON

* Define the beam position

BEAMPOS 330. -404. 30. 0.0 0.0

* Needed for the source script

SOURCE

* Sets energy threshold

EMFCUT -1E-06 1E-6 0.0 VACUUM AIR PROD-CUT

* Sets energy threshold

EMFCUT -1E-06 1E-6 BEDSCR VOXE3143

* Needed for fluscw_flu.f

USERWEIG 3. 0.0 0.0

* Fluence over the whole room

USRBIN 10. PHOTON -21. 613. 0.0 306.FluRoom

```

USRBIN      0.0 -681.  0.0  204.  227.  102. &
* Dose over the whole room
USRBIN      10.  DOSE  -21.  613.  0.0  306.DoseR
USRBIN      0.0 -681.  0.0  204.  227.  102. &
* Spectrum in front of the beam
USRBDX      101.          -22. DETFRONT  ROOM  1.ESpet
USRBDX      0.000124 0.000001  124.          &
* Dose given to the patient
USRBIN      10.  DOSE  -23.  372.5 -379.5  118.8DosePat
USRBIN      184. -428.2  90.  377.  98.  58. &
* Dose given to the operator
USRBIN      10.  DOSE  -24.  280.  -330.  150.DoseOp
USRBIN      250. -360.  0.0  60.  60.  360. &
* Hp(10.0) - Check1
USRBIN      10.  DOSE  -29.  266.5 -360.  150.D
USRBIN      263.5 -361.  147.  1.  1.  1. &
* Hp(10.0) - Check2
USRBIN      10. DOSE-EQ -29.  266.5 -360.  150.D-EQ
USRBIN      263.5 -361.  147.  1.  1.  1. &
* Hp(10.0) - Check3
USRBIN      10. PHOTON -29.  266.5 -360.  150.Flu
USRBIN      263.5 -361.  147.  1.  1.  1. &
* Hp(10.0)
* Must be BIN 30
USRBIN      10. PHOTON -30.  266.5 -360.  150.Hp10
USRBIN      263.5 -361.  147.  1.  1.  1. &
* Rotates the lead screen hanging from the ceiling
ROT-DEFI    1.          -135. -480.8326  84.8528  0.0rotScr
* Rotates the lead wall on the floor (Unused)
ROT-DEFI    2.          60.70.0961894421.410162  rotWall
* Rotates the lead skirt mounted to the bed
ROT-DEFI    3.          -100. -412.7720 -187.1664  rotSki
* Rotates the patient
* -x->y (Max)
* -y->z (Max)
* z->x (Min)
ROT-DEFI    104.  90.  90.  379.5 -118.85  184.rotPat
GEOBEGIN
VOXELS      0.0  0.0  0.0  rotPat  Pat
  0  0
SPH blkbody 0.0 0.0 0.0 100000.
* Vacuum around the room
SPH void    0.0 0.0 0.0 10000.
* Outer cylinder creating the C-arm

```

RCC machOut 330.5 -376.5 129. 0.0 -55. 0.0 122.
* Inner cylinder creating the C-arm
RCC machIn 330.5 -376.5 129. 0.0 -55. 0.0 100.
* Stops the C-arm, creating a crescent shape
YZP machStop 315.5
* The main room
RPP room 0.0 613. -681. 0.0 0.0 306.
* Defines the roof
XYP roof 306.
* Defines the floor
XYP floor 0.0
* Adds concrete around the room
RPP fR -4. 617. -685. 4. -20. 326.
* Outer layer of the wall to add lead inside
RPP wallsOut -4. 617. -685. 4. 0.0 306.
* Mid layer of the wall to add lead inside
RPP wallsMid -2.1 615.1 -683.1 2.1 0.0 306.
* Inner layer of the wall to add lead inside
RPP wallsIn -1.9 614.9 -682.9 1.9 0.0 306.
* Region in front of the detector
RPP detFront 325. 335. -409. -399. 30. 30.00001
* Lead skirt mounted to the bed
RPP bedSki 176. 256. -374. -373.5 15. 98.
* Lead skirt mounted to the bed
RPP bedSki2 231. 256. -374. -373.5 89. 115.
\$start_transform rotSki
RPP bedSki3 0.0 0.5 -59. 0.0 15. 119.35
\$end_transform
\$start_transform rotScr
* Lead skirt mounted to the ceiling
RPP leadScr 0.0 0.5 -72. 0.0 105. 194.
\$end_transform
* Lead blanket over the patient
*
RPP leadBla 260. 310. -428.7 -350. 90. 119.35
RPP leadBla1 260. 310. -428.2 -350. 90. 118.85
RPP leadBla2 295. 310. -428.7 -405. 90. 119.35
PLA stopBla 0.176327 -1. 0.0 256. -373.5 90.
* Patient bed
RPP bed 75.5 392.5 -434. -374. 85. 90.
* Foot of the bed
RCC bedFoot 145. -404. 0.0 0.0 0.0 85. 19.
* Operator's body
RCC opBody 265. -345. 0.0 0.0 0.0 150. 15.

```

* Operator's lead vest
RCC opVest 265. -345. 40. 0.0 0.0 110. 15.3
* Operator's head
RCC opHead 265. -345. 150. 0.0 0.0 30. 13.
END
BEDSCR 5 +bedSki3|bedSki|bedSki2 |(leadBla -leadBla1 -leadBla2 -stopBla )
LEADSCR 5 +leadScr -leadBla
* Lead end
WALLSMID 5 +wallsMid -wallsIn
* Carbon start
BED 5 +bed|bedFoot
* Carbon end
MACH 5 +machOut -machStop -machIn
OP 5 +opBody |opHead
* Concrete start
ROOF 5 +fR -roof
WALLSOUT 5 +wallsOut -wallsMid
WALLSIN 5 +wallsIn -room
* Concrete end
FLOOR 5 +fR +floor
* Air start
ROOM 5 +room -VOXEL -(bed|bedFoot) -detFront -(opBody|opVest|opHead) -
(
    +machOut -machStop -machIn ) -((bedSki3|bedSki|bedSki2) |(leadBla -
leadBla1 -leadBla2 -stopBla )) -
    (leadScr
    -leadBla)
OPVEST 5 +opVest -opBody
* Air end
DETFRONT 5 +detFront
VOID 5 +void -fR
BLKBODY 5 +blkbody -void
END
GEOEND
* Create concrete with the compound card below
MATERIAL 2.05 CONCRETE
COMPOUND 23. CARBON 40. OXYGEN 12. SILICONCONCRETE
COMPOUND 12. CALCIUM 10. HYDROGEN 2.
MAGNESIUCONCRETE
ASSIGNMA CARBON BED MACH
ASSIGNMA LEAD BEDSCR WALLSMID
ASSIGNMA WATER OP
ASSIGNMA AIR ROOM DETFRONT
ASSIGNMA AIR VOXEL

```

```

ASSIGNMA CONCRETE ROOF FLOOR
ASSIGNMA VACUUM VOID
ASSIGNMA BLCKHOLE BLKBODY
RANDOMIZ 1.
START 400000000.
STOP

```

Setup SGB

* Increases maximum regions

```
GLOBAL 5000.
```

TITLE

Lab 2 - Haukeland - Fluoro, AP, Setup SGB

* Set the defaults for precision simulations

```
DEFAULTS PRECISIO
```

* Define the beam characteristics

```
BEAM -8E-05 0.0 0.0 PHOTON
```

* Define the beam position

```
BEAMPOS 330. -404. 30. 0.0 0.0
```

* Needed for the source script

SOURCE

* Sets energy threshold

```
EMFCUT -1E-06 1E-6 0.0 VACUUM AIR PROD-CUT
```

* Sets energy threshold

```
EMFCUT -1E-06 1E-6 BEDSCR VOXE3143
```

* Needed for fluscw_flu.f

```
USERWEIG 3. 0.0 0.0
```

* Fluence over the whole room

```
USRBIN 10. PHOTON -21. 613. 0.0 306.FluRoom
```

```
USRBIN 0.0 -681. 0.0 204. 227. 102. &
```

* Dose over the whole room

```
USRBIN 10. DOSE -21. 613. 0.0 306.DoseR
```

```
USRBIN 0.0 -681. 0.0 204. 227. 102. &
```

* Spectrum in front of the beam

```
USRBDX 101. -22. DETFRONT ROOM 1.ESpet
```

```
USRBDX 0.000124 0.000001 124. &
```

* Dose given to the patient

```
USRBIN 10. DOSE -23. 372.5 -379.5 118.8DosePat
```

```
USRBIN 184. -428.2 90. 377. 98. 58. &
```

* Dose given to the operator

```
USRBIN 10. DOSE -24. 280. -330. 150.DoseOp
```

```
USRBIN 250. -360. 0.0 60. 60. 360. &
```

* Hp(10.0) - Check1

```
USRBIN 10. DOSE -29. 266.5 -360. 150.D
```

```
USRBIN 263.5 -361. 147. 1. 1. 1. &
```

```

* Hp(10.0) - Check2
USRBIN      10. DOSE-EQ  -29. 266.5 -360. 150.D-EQ
USRBIN      263.5 -361. 147. 1. 1. 1. &
* Hp(10.0) - Check3
USRBIN      10. PHOTON  -29. 266.5 -360. 150.Flu
USRBIN      263.5 -361. 147. 1. 1. 1. &
* Hp(10.0)
* Must be BIN 30
USRBIN      10. PHOTON  -30. 266.5 -360. 150.Hp10
USRBIN      263.5 -361. 147. 1. 1. 1. &
* Rotates the lead scen hanging from the ceiling
ROT-DEFI    1.      -135. -480.8326 84.8528 0.0rotScr
* Rotates the lead wall on the floor (Unused)
ROT-DEFI    2.      60.70.0961894421.410162 rotWall
* Rotates the lead skirt mounted to the bed
ROT-DEFI    3.      -100. -412.7720 -187.1664 rotSki
* Rotates the patient
* -x->y (Max)
* -y->z (Max)
* z->x (Min)
ROT-DEFI    104. 90. 90. 379.5 -118.85 184.rotPat
GEOBEGIN
VOXELS      0.0 0.0 0.0 rotPat Pat
0 0
SPH blkbody 0.0 0.0 0.0 100000.
* Vacuum around the room
SPH void    0.0 0.0 0.0 10000.
* Outer cylinder creating the C-arm
RCC machOut 330.5 -376.5 129. 0.0 -55. 0.0 122.
* Inner cylinder creating the C-arm
RCC machIn  330.5 -376.5 129. 0.0 -55. 0.0 100.
* Stops the C-arm, creating a crescent shape
YZP machStop 315.5
* The main room
RPP room    0.0 613. -681. 0.0 0.0 306.
* Defines the roof
XYP roof    306.
* Defines the floor
XYP floor   0.0
* Adds concrete around the room
RPP fR      -4. 617. -685. 4. -20. 326.
* Outer layer of the wall to add lead inside
RPP wallsOut -4. 617. -685. 4. 0.0 306.
* Mid layer of the wall to add lead inside

```

```

RPP wallsMid -2.1 615.1 -683.1 2.1 0.0 306.
* Inner layer of the wall to add lead inside
RPP wallsIn -1.9 614.9 -682.9 1.9 0.0 306.
* Region in front of the detector
RPP detFront 325. 335. -409. -399. 30. 30.00001
* Lead skirt mounted to the bed
RPP bedSki 176. 256. -374. -373.5 15. 98.
* Lead skirt mounted to the bed
RPP bedSki2 231. 256. -374. -373.5 89. 115.
$start_transform rotSki
RPP bedSki3 0.0 0.5 -59. 0.0 15. 119.35
$end_transform
$start_transform rotScr
* Lead skirt mounted to the ceiling
RPP leadScr 0.0 0.5 -72. 0.0 135. 224.
$end_transform
* Lead blanket over the patient
RPP leadBla 260. 310. -428.7 -350. 90. 119.35
RPP leadBla1 260. 310. -428.2 -350. 90. 118.85
RPP leadBla2 295. 310. -428.7 -405. 90. 119.35
PLA stopBla 0.176327 -1. 0.0 256. -373.5 90.
* Patient bed
RPP bed 75.5 392.5 -434. -374. 85. 90.
* Foot of the bed
RCC bedFoot 145. -404. 0.0 0.0 0.0 85. 19.
* Operator's body
RCC opBody 265. -345. 0.0 0.0 0.0 150. 15.
* Operator's lead vest
RCC opVest 265. -345. 40. 0.0 0.0 110. 15.3
* Operator's head
RCC opHead 265. -345. 150. 0.0 0.0 30. 13.
END
BEDSCR 5 +bedSki3|bedSki|bedSki2 | (leadBla -leadBla1 -leadBla2 -stopBla )
LEADSCR 5 +leadScr -leadBla
* Lead end
WALLSMID 5 +wallsMid -wallsIn
* Carbon start
BED 5 +bed|bedFoot
* Carbon end
MACH 5 +machOut -machStop -machIn
OP 5 +opBody |opHead
* Concrete start
ROOF 5 +fR -roof
WALLSOUT 5 +wallsOut -wallsMid

```



```

WALLSIN    5 +wallsIn -room
* Concrete end
FLOOR      5 +fR +floor
* Air start
ROOM       5 +room -VOXEL -(bed|bedFoot) -detFront -(opBody|opVest|opHead) -
(
    +machOut -machStop -machIn ) -((bedSki3|bedSki|bedSki2) |(leadBla -
leadBla1 -leadBla2 -stopBla )) -
    (leadScr
    -leadBla)
OPVEST     5 +opVest -opBody
* Air end
DETFRONT   5 +detFront
VOID       5 +void -fR
BLKBODY    5 +blkbody -void
END
GEOEND
* Create concrete with the compound card below
MATERIAL           2.05                CONCRETE
COMPOUND    23. CARBON    40. OXYGEN    12. SILICONCONCRETE
COMPOUND           12.  CALCIUM        10. HYDROGEN        2.
MAGNESIUCONCRETE
ASSIGNMA    CARBON    BED    MACH
ASSIGNMA    LEAD    BEDSCR WALLSMID
ASSIGNMA    WATER    OP
ASSIGNMA    AIR    ROOM DETFRONT
ASSIGNMA    AIR    VOXEL
ASSIGNMA    CONCRETE    ROOF    FLOOR
ASSIGNMA    VACUUM    VOID
ASSIGNMA    BLCKHOLE    BLKBODY
RANDOMIZ     1.
START    400000000.
STOP

```

Setup SG

* Increases maximum regions

```
GLOBAL    5000.
```

```
TITLE
```

```
Lab 2 - Haukeland - Fluoro, AP, Setup SG
```

* Set the defaults for precision simulations

```
DEFAULTS                                PRECISIO
```

* Define the beam characteristics

```
BEAM    -8E-05                0.0    0.0    PHOTON
```

* Define the beam position

```
BEAMPOS    330.    -404.    30.    0.0    0.0
```

* Needed for the source script

SOURCE

* Sets energy threshold

EMFCUT -1E-06 1E-6 0.0 VACUUM AIR PROD-CUT

* Sets energy threshold

EMFCUT -1E-06 1E-6 BEDSCR VOXE3143

* Needed for fluscw_flu.f

USERWEIG 3. 0.0 0.0

* Fluence over the whole room

USRBIN 10. PHOTON -21. 613. 0.0 306.FluRoom

USRBIN 0.0 -681. 0.0 204. 227. 102. &

* Dose over the whole room

USRBIN 10. DOSE -21. 613. 0.0 306.DoseR

USRBIN 0.0 -681. 0.0 204. 227. 102. &

* Spectrum in front of the beam

USRBDX 101. -22. DETFRONT ROOM 1.ESpet

USRBDX 0.000124 0.000001 124. &

* Dose given to the patient

USRBIN 10. DOSE -23. 372.5 -379.5 118.8DosePat

USRBIN 184. -428.2 90. 377. 98. 58. &

* Dose given to the operator

USRBIN 10. DOSE -24. 280. -330. 150.DoseOp

USRBIN 250. -360. 0.0 60. 60. 360. &

* Hp(10.0) - Check1

USRBIN 10. DOSE -29. 266.5 -360. 150.D

USRBIN 263.5 -361. 147. 1. 1. 1. &

* Hp(10.0) - Check2

USRBIN 10. DOSE-EQ -29. 266.5 -360. 150.D-EQ

USRBIN 263.5 -361. 147. 1. 1. 1. &

* Hp(10.0) - Check3

USRBIN 10. PHOTON -29. 266.5 -360. 150.Flu

USRBIN 263.5 -361. 147. 1. 1. 1. &

* Hp(10.0)

* Must be BIN 30

USRBIN 10. PHOTON -30. 266.5 -360. 150.Hp10

USRBIN 263.5 -361. 147. 1. 1. 1. &

* Rotates the lead screen hanging from the ceiling

ROT-DEFI 1. -135. -480.8326 84.8528 0.0rotScr

* Rotates the lead wall on the floor (Unused)

ROT-DEFI 2. 60.70.0961894421.410162 rotWall

* Rotates the lead skirt mounted to the bed

ROT-DEFI 3. -100. -412.7720 -187.1664 rotSki

* Rotates the patient

* -x->y (Max)

```

* -y->z (Max)
* z->x (Min)
ROT-DEFI 104. 90. 90. 379.5 -118.85 184.rotPat
GEOBEGIN COMBNAME
VOXELS 0.0 0.0 0.0 rotPat Pat
0 0
SPH blkbody 0.0 0.0 0.0 100000.
* Vacuum around the room
SPH void 0.0 0.0 0.0 10000.
* Outer cylinder creating the C-arm
RCC machOut 330.5 -376.5 129. 0.0 -55. 0.0 122.
* Inner cylinder creating the C-arm
RCC machIn 330.5 -376.5 129. 0.0 -55. 0.0 100.
* Stops the C-arm, creating a crescent shape
YZP machStop 315.5
* The main room
RPP room 0.0 613. -681. 0.0 0.0 306.
* Defines the roof
XYP roof 306.
* Defines the floor
XYP floor 0.0
* Adds concrete around the room
RPP fR -4. 617. -685. 4. -20. 326.
* Outer layer of the wall to add lead inside
RPP wallsOut -4. 617. -685. 4. 0.0 306.
* Mid layer of the wall to add lead inside
RPP wallsMid -2.1 615.1 -683.1 2.1 0.0 306.
* Inner layer of the wall to add lead inside
RPP wallsIn -1.9 614.9 -682.9 1.9 0.0 306.
* Region in front of the detector
RPP detFront 325. 335. -409. -399. 30. 30.00001
* Lead skirt mounted to the bed
RPP bedSki 176. 256. -374. -373.5 15. 98.
* Lead skirt mounted to the bed
RPP bedSki2 231. 256. -374. -373.5 89. 115.
$start_transform rotSki
RPP bedSki3 0.0 0.5 -59. 0.0 15. 119.35
$end_transform
$start_transform rotScr
* Lead skirt mounted to the ceiling
RPP leadScr 0.0 0.5 -72. 0.0 135. 224.
$end_transform
PLA stopBla 0.176327 -1. 0.0 256. -373.5 90.
* Patient bed

```

```

RPP bed      75.5 392.5 -434. -374. 85. 90.
* Foot of the bed
RCC bedFoot  145. -404. 0.0 0.0 0.0 85. 19.
* Operator's body
RCC opBody   265. -345. 0.0 0.0 0.0 150. 15.
* Operator's lead vest
RCC opVest   265. -345. 40. 0.0 0.0 110. 15.3
* Operator's head
RCC opHead   265. -345. 150. 0.0 0.0 30. 13.
END
* Lead start
BEDSCR       5 +bedSki3|bedSki|bedSki2
LEADSCR      5 +leadScr
* Lead end
WALLSMID     5 +wallsMid -wallsIn
* Carbon start
BED          5 +bed|bedFoot
* Carbon end
MACH         5 +machOut -machStop -machIn
OP           5 +opBody |opHead
* Concrete start
ROOF         5 +fR -roof
WALLSOUT     5 +wallsOut -wallsMid
WALLSIN      5 +wallsIn -room
* Concrete end
FLOOR        5 +fR +floor
* Air start
ROOM         5 +room -VOXEL -(bed|bedFoot) -detFront -(opBody|opVest|opHead) -
(
      +machOut -machStop -machIn ) -(bedSki3|bedSki|bedSki2) -leadScr
OPVEST       5 +opVest -opBody
* Air end
DETFRONT     5 +detFront
VOID         5 +void -fR
BLKBODY      5 +blkbody -void
END
GEOEND
* Create concrete with the compound card below
MATERIAL          2.05                CONCRETE
COMPOUND          23. CARBON          40. OXYGEN          12. SILICONCONCRETE
COMPOUND          12. CALCIUM         10. HYDROGEN          2.
MAGNESIUCONCRETE
ASSIGNMA CARBON  BED  MACH
ASSIGNMA  LEAD  BEDSCR WALLSMID

```

ASSIGNMA WATER OP
 ASSIGNMA AIR ROOM DETFRONT
 ASSIGNMA AIR VOXEL
 ASSIGNMA CONCRETE ROOF FLOOR
 ASSIGNMA VACUUM VOID
 ASSIGNMA BLCKHOLE BLKBODY
 RANDOMIZ 1.
 START 400000000.
 STOP

Setup Z

* Increases maximum regions

GLOBAL 5000.

TITLE

Lab 2 - Haukeland - Fluoro, AP, Setup Z

* Set the defaults for precision simulations

DEFAULTS PRECISIO

* Define the beam characteristics

BEAM -8E-05 0.0 0.0 PHOTON

* Define the beam position

BEAMPOS 330. -404. 30. 0.0 0.0

* Needed for the source script

SOURCE

* Sets energy threshold

EMFCUT -1E-06 1E-6 0.0 VACUUM AIR PROD-CUT

* Sets energy threshold

EMFCUT -1E-06 1E-6 BEDSCR VOXE3143

* Needed for fluscw_flu.f

USERWEIG 3. 0.0 0.0

* Fluence over the whole room

USRBIN 10. PHOTON -21. 613. 0.0 306.FluRoom

USRBIN 0.0 -681. 0.0 204. 227. 102. &

* Dose over the whole room

USRBIN 10. DOSE -21. 613. 0.0 306.DoseR

USRBIN 0.0 -681. 0.0 204. 227. 102. &

* Spectrum in front of the beam

USRBDX 101. -22. DETFRONT ROOM 1.ESpet

USRBDX 0.000124 0.000001 124. &

* Dose given to the patient

USRBIN 10. DOSE -23. 372.5 -379.5 118.8DosePat

USRBIN 184. -428.2 90. 377. 98. 58. &

* Dose given to the operator

USRBIN 10. DOSE -24. 280. -330. 150.DoseOp

USRBIN 250. -360. 0.0 60. 60. 360. &

* Hp(10.0) - Check1

USRBIN 10. DOSE -29. 266.5 -360. 150.D
 USRBIN 263.5 -361. 147. 1. 1. 1. &
 * Hp(10.0) - Check2
 USRBIN 10. DOSE-EQ -29. 266.5 -360. 150.D-EQ
 USRBIN 263.5 -361. 147. 1. 1. 1. &
 * Hp(10.0) - Check3
 USRBIN 10. PHOTON -29. 266.5 -360. 150.Flu
 USRBIN 263.5 -361. 147. 1. 1. 1. &
 * Hp(10.0)
 * Must be BIN 30
 USRBIN 10. PHOTON -30. 266.5 -360. 150.Hp10
 USRBIN 263.5 -361. 147. 1. 1. 1. &
 * Rotates the lead screen hanging from the ceiling
 ROT-DEFI 1. -135. -480.8326 84.8528 0.0rotScr
 * Rotates the lead wall on the floor (Unused)
 ROT-DEFI 2. 60.70.0961894421.410162 rotWall
 * Rotates the lead skirt mounted to the bed
 ROT-DEFI 3. -100. -412.7720 -187.1664 rotSki
 * Rotates the patient
 * -x->y (Max)
 * -y->z (Max)
 * z->x (Min)
 ROT-DEFI 104. 90. 90. 379.5 -118.85 184.rotPat
 GEOBEGIN COMBNAME
 VOXELS 0.0 0.0 0.0 rotPat Pat
 0 0
 SPH blkbody 0.0 0.0 0.0 100000.
 * Vacuum around the room
 SPH void 0.0 0.0 0.0 10000.
 * Outer cylinder creating the C-arm
 RCC machOut 330.5 -376.5 129. 0.0 -55. 0.0 122.
 * Inner cylinder creating the C-arm
 RCC machIn 330.5 -376.5 129. 0.0 -55. 0.0 100.
 * Stops the C-arm, creating a crescent shape
 YZP machStop 315.5
 * The main room
 RPP room 0.0 613. -681. 0.0 0.0 306.
 * Defines the roof
 XYP roof 306.
 * Defines the floor
 XYP floor 0.0
 * Adds concrete around the room
 RPP fR -4. 617. -685. 4. -20. 326.
 * Outer layer of the wall to add lead inside

```

RPP wallsOut -4. 617. -685. 4. 0.0 306.
* Mid layer of the wall to add lead inside
RPP wallsMid -2.1 615.1 -683.1 2.1 0.0 306.
* Inner layer of the wall to add lead inside
RPP wallsIn -1.9 614.9 -682.9 1.9 0.0 306.
* Region in front of the detector
RPP detFront 325. 335. -409. -399. 30. 30.00001
* Lead skirt mounted to the bed
RPP bedSki 165. 270. -374. -373.5 15. 98.
* Patient bed
RPP bed 75.5 392.5 -434. -374. 85. 90.
* Foot of the bed
RCC bedFoot 145. -404. 0.0 0.0 0.0 85. 19.
* Operator's body
RCC opBody 265. -345. 0.0 0.0 0.0 150. 15.
* Operator's lead vest
RCC opVest 265. -345. 40. 0.0 0.0 110. 15.3
* Operator's head
RCC opHead 265. -345. 150. 0.0 0.0 30. 13.
END
BEDSCR 5 +bedSki
* Lead end
WALLSMID 5 +wallsMid -wallsIn
* Carbon start
BED 5 +bed|bedFoot
* Carbon end
MACH 5 +machOut -machStop -machIn
OP 5 +opBody |opHead
* Concrete start
ROOF 5 +fR -roof
WALLSOUT 5 +wallsOut -wallsMid
WALLSIN 5 +wallsIn -room
* Concrete end
FLOOR 5 +fR +floor
* Air start
ROOM 5 +room -VOXEL -(bed|bedFoot) -detFront -(opBody|opVest|opHead) -
(
+machOut -machStop -machIn ) -bedSki
OPVEST 5 +opVest -opBody
* Air end
DETFRONT 5 +detFront
VOID 5 +void -fR
BLKBODY 5 +blkbody -void
END

```

GEOEND

* Create concrete with the compound card below

```
MATERIAL          2.05          CONCRETE
COMPOUND   23. CARBON   40. OXYGEN   12. SILICONCONCRETE
COMPOUND          12.  CALCIUM          10.  HYDROGEN          2.
MAGNESIUCONCRETE
ASSIGNMA   CARBON   BED   MACH
ASSIGNMA   LEAD   BEDSCR WALLSMID
ASSIGNMA   WATER   OP
ASSIGNMA   AIR   ROOM DETFRONT
ASSIGNMA   AIR   VOXEL
ASSIGNMA   CONCRETE   ROOF   FLOOR
ASSIGNMA   VACUUM   VOID
ASSIGNMA   BLCKHOLE   BLKBODY
RANDOMIZ    1.
START    400000000.
STOP
```

Setup SBF

* Increases maximum regions

```
GLOBAL    5000.
```

TITLE

Lab 2 - Haukeland - Fluoro, AP, SBF

* Set the defaults for precision simulations

```
DEFAULTS          PRECISIO
```

* Define the beam characteristics

```
BEAM    -8E-05          0.0   0.0   PHOTON
```

* Define the beam position

```
BEAMPOS    330.  -404.   30.   0.0   0.0
```

* Needed for the source script

SOURCE

* Sets energy threshold

```
EMFCUT    -1E-06   1E-6   0.0   VACUUM   AIR   PROD-CUT
```

* Sets energy threshold

```
EMFCUT    -1E-06   1E-6          BEDSCR VOXE3143
```

* Needed for fluscw_flu.f

```
USERWEIG          3.          0.0
```

* Fluence over the whole room

```
USRBIN    10.  PHOTON   -21.   613.   0.0   306.FluRoom
```

```
USRBIN    0.0  -681.   0.0   204.   227.   102. &
```

* Dose over the whole room

```
USRBIN    10.  DOSE    -21.   613.   0.0   306.DoseR
```

```
USRBIN    0.0  -681.   0.0   204.   227.   102. &
```

* Spectrum in front of the beam

```
USRBDX    101.          -22.  DETFRONT   ROOM   1.ESpet
```



```

USRBDX  0.000124 0.000001 124. &
* Dose given to the patient
USRBIN  10. DOSE -23. 372.5 -379.5 118.8DosePat
USRBIN  184. -428.2 90. 377. 98. 58. &
* Dose given to the operator
USRBIN  10. DOSE -24. 280. -330. 150.DoseOp
USRBIN  250. -360. 0.0 60. 60. 360. &
* Hp(10.0) - Check1
USRBIN  10. DOSE -29. 266.5 -360. 150.D
USRBIN  263.5 -361. 147. 1. 1. 1. &
* Hp(10.0) - Check2
USRBIN  10. DOSE-EQ -29. 266.5 -360. 150.D-EQ
USRBIN  263.5 -361. 147. 1. 1. 1. &
* Hp(10.0) - Check3
USRBIN  10. PHOTON -29. 266.5 -360. 150.Flu
USRBIN  263.5 -361. 147. 1. 1. 1. &
* Hp(10.0)
* Must be BIN 30
USRBIN  10. PHOTON -30. 266.5 -360. 150.Hp10
USRBIN  263.5 -361. 147. 1. 1. 1. &
* Rotates the lead screen hanging from the ceiling
ROT-DEFI  1. -135. -480.8326 84.8528 0.0rotScr
* Rotates the lead wall on the floor (Unused)
ROT-DEFI  2. 60.70.0961894421.410162 rotWall
* Rotates the lead skirt mounted to the bed
ROT-DEFI  3. -100. -412.7720 -187.1664 rotSki
* Rotates the patient
* -x->y (Max)
* -y->z (Max)
* z->x (Min)
ROT-DEFI  104. 90. 90. 379.5 -118.85 184.rotPat
GEOBEGIN COMBNAME
VOXELS  0.0 0.0 0.0 rotPat Pat
  0 0
SPH blkbody 0.0 0.0 0.0 100000.
* Vacuum around the room
SPH void 0.0 0.0 0.0 10000.
* Outer cylinder creating the C-arm
RCC machOut 330.5 -376.5 129. 0.0 -55. 0.0 122.
* Inner cylinder creating the C-arm
RCC machIn 330.5 -376.5 129. 0.0 -55. 0.0 100.
* Stops the C-arm, creating a crescent shape
YZP machStop 315.5
* The main room

```

```

RPP room    0.0 613. -681. 0.0 0.0 306.
* Defines the roof
XYP roof    306.
* Defines the floor
XYP floor   0.0
* Adds concrete around the room
RPP fR      -4. 617. -685. 4. -20. 326.
* Outer layer of the wall to add lead inside
RPP wallsOut -4. 617. -685. 4. 0.0 306.
* Mid layer of the wall to add lead inside
RPP wallsMid -2.1 615.1 -683.1 2.1 0.0 306.
* Inner layer of the wall to add lead inside
RPP wallsIn  -1.9 614.9 -682.9 1.9 0.0 306.
* Region in front of the detector
RPP detFront 325. 335. -409. -399. 30. 30.00001
* Lead skirt mounted to the bed
RPP bedSki   176. 256. -374. -373.5 1. 98.
* Lead skirt mounted to the bed
RPP bedSki2  231. 256. -374. -373.5 89. 115.
$start_transform rotSki
RPP bedSki3  0.0 0.5 -59. 0.0 1. 119.35
$end_transform
$start_transform rotScr
* Lead skirt mounted to the ceiling
RPP leadScr  0.0 0.5 -72. 0.0 105. 194.
$end_transform
* Lead blanket over the patient
RPP leadBla  260. 310. -428.7 -350. 90. 119.35
RPP leadBla1 260. 310. -428.2 -350. 90. 118.85
RPP leadBla2 295. 310. -428.7 -405. 90. 119.35
PLA stopBla  0.176327 -1. 0.0 256. -373.5 90.
* Patient bed
RPP bed      75.5 392.5 -434. -374. 85. 90.
* Foot of the bed
RCC bedFoot  145. -404. 0.0 0.0 0.0 85. 19.
* Operator's body
RCC opBody   265. -345. 0.0 0.0 0.0 150. 15.
* Operator's lead vest
RCC opVest   265. -345. 40. 0.0 0.0 110. 15.3
* Operator's head
RCC opHead   265. -345. 150. 0.0 0.0 30. 13.
END
BEDSCR      5 +bedSki3|bedSki|bedSki2 | (leadBla -leadBla1 -leadBla2 -stopBla )
LEADSCR     5 +leadScr -leadBla

```

```

* Lead end
WALLSMID 5 +wallsMid -wallsIn
* Carbon start
BED 5 +bed|bedFoot
* Carbon end
MACH 5 +machOut -machStop -machIn
OP 5 +opBody |opHead
* Concrete start
ROOF 5 +fR -roof
WALLSOUT 5 +wallsOut -wallsMid
WALLSIN 5 +wallsIn -room
* Concrete end
FLOOR 5 +fR +floor
* Air start
ROOM 5 +room -VOXEL -(bed|bedFoot) -detFront -(opBody|opVest|opHead) -
(
    +machOut -machStop -machIn ) -((bedSki3|bedSki|bedSki2) |(leadBla -
leadBla1 -leadBla2 -stopBla )) -
    (leadScr
    -leadBla)
OPVEST 5 +opVest -opBody
* Air end
DETFRONT 5 +detFront
VOID 5 +void -fR
BLKBODY 5 +blkbody -void
END
GEOEND
* Create concrete with the compound card below
MATERIAL 2.05 CONCRETE
COMPOUND 23. CARBON 40. OXYGEN 12. SILICONCONCRETE
COMPOUND 12. CALCIUM 10. HYDROGEN 2.
MAGNESIUCONCRETE
ASSIGNMA CARBON BED MACH
ASSIGNMA LEAD BEDSCR WALLSMID
ASSIGNMA WATER OP
ASSIGNMA AIR ROOM DETFRONT
ASSIGNMA AIR VOXEL
ASSIGNMA CONCRETE ROOF FLOOR
ASSIGNMA VACUUM VOID
ASSIGNMA BLCKHOLE BLKBODY
RANDOMIZ 1.
START 400000000.
STOP

```

Appendix B discrete.f

```
*$ CREATE SOURCE.FOR
*COPY SOURCE
*
*==== source
=====
*
SUBROUTINE SOURCE ( NOMORE )

INCLUDE '(DBLPRC)'
INCLUDE '(DIMPAR)'
INCLUDE '(IOUNIT)'
*
*-----*
*
* Copyright (C) 1990-2006 by Alfredo Ferrari & Paola Sala *
* All Rights Reserved. *
* *
* *
* New source for FLUKA9x-FLUKA200x: *
* *
* Created on 07 january 1990 by Alfredo Ferrari & Paola Sala *
* Infn - Milan *
* *
* Last change on 03-mar-06 by Alfredo Ferrari *
* *
* This is just an example of a possible user written source routine. *
* note that the beam card still has some meaning - in the scoring the *
* maximum momentum used in deciding the binning is taken from the *
* beam momentum. Other beam card parameters are obsolete. *
* *
*-----*
*
INCLUDE '(BEAMCM)'
INCLUDE '(FHEAVY)'
INCLUDE '(FLKSTK)'
INCLUDE '(IOIOCM)'
INCLUDE '(LTCLCM)'
INCLUDE '(PAPROP)'
INCLUDE '(SOURCM)'
INCLUDE '(SUMCOU)'
*
LOGICAL LFIRST
```

```

*
c  defining and saving spectrum arrays
  DIMENSION
  ENEPOI(0:1000),ENEPRO(0:1000),ENECUM(0:1000),SUMME(0:0)
  SAVE ENEPOI, ENEPRO, ENECUM, SUMME
c  saving spectrum dimension
  SAVE IMAX
*
  SAVE LFIRST
  DATA LFIRST / .TRUE. /
*
=====
=====*
*
*          BASIC VERSION          *
*
*          *
*
*=====
=====*
  NOMORE = 0
* +-----*
* | First call initializations:
* | IF ( LFIRST ) THEN
* | *** The following 3 cards are mandatory ***
* |   TKESUM = ZERZER
* |   LFIRST = .FALSE.
* |   LUSSRC = .TRUE.
* | *** User initialization ***
* |   CALL OAUXFI('spectrum.dat',LUNRDB,'OLD',IERR)
c  reading spectrum
  DO I=0,1000
    READ(LUNRDB,*,END=1972) ENEPOI(I),ENEPRO(I)
    IMAX=I
  ENDDO
  STOP ' spectrum reading uncomplete!'
1972  CONTINUE
c  Breiten feststellen
  SUMME(0)=ZERZER
  DO I=0,IMAX
    SUMME(0)=SUMME(0)+ENEPRO(I)
  ENDDO
  DO I=0,IMAX
    ENEPRO(I)=ENEPRO(I)/SUMME(0)
  ENDDO
c  building cumulative spectrum
  ENECUM(0)=ENEPRO(0)

```

```

DO I=1,IMAX
  ENECUM(I)=ENECUM(I-1)+ENEPRO(I)
ENDDO
  ENECUM(IMAX)=ONEONE
END IF
* |
* +-----*
* Push one source particle to the stack. Note that you could as well
* push many but this way we reserve a maximum amount of space in the
* stack for the secondaries to be generated
* Npflka is the stack counter: of course any time source is called it
* must be =0
  NPFLKA = NPFLKA + 1
* Wt is the weight of the particle
  WTFLK (NPFLKA) = ONEONE
  WEIPRI = WEIPRI + WTFLK (NPFLKA)
* Particle type (1=proton.....). Ijbeam is the type set by the BEAM
* card
* +-----*
* | (Radioactive) isotope:
  IF ( IJBEAM .EQ. -2 .AND. LRDBEA ) THEN
    IARES = IPROA
    IZRES = IPROZ
    IISRES = IPROM
    CALL STISBM ( IARES, IZRES, IISRES )
    IJHION = IPROZ * 1000 + IPROA
    IJHION = IJHION * 100 + KXHEAV
    IONID = IJHION
    CALL DCDION ( IONID )
    CALL SETION ( IONID )
* |
* +-----*
* | Heavy ion:
  ELSE IF ( IJBEAM .EQ. -2 ) THEN
    IJHION = IPROZ * 1000 + IPROA
    IJHION = IJHION * 100 + KXHEAV
    IONID = IJHION
    CALL DCDION ( IONID )
    CALL SETION ( IONID )
    ILOFLK (NPFLKA) = IJHION
* | Flag this is prompt radiation
  LRADDC (NPFLKA) = .FALSE.
* |
* +-----*

```

```

* | Normal hadron:
  ELSE
    IONID = IJBEAM
    ILOFLK (NPFLKA) = IJBEAM
* | Flag this is prompt radiation
    LRADDC (NPFLKA) = .FALSE.
  END IF
* |
* +-----*
* From this point .....
* Particle generation (1 for primaries)
  LOFLK (NPFLKA) = 1
* User dependent flag:
  LOUSE (NPFLKA) = 0
* User dependent spare variables:
  DO 100 ISPR = 1, MKBMX1
    SPAREK (ISPR,NPFLKA) = ZERZER
  100 CONTINUE
* User dependent spare flags:
  DO 200 ISPR = 1, MKBMX2
    ISPARK (ISPR,NPFLKA) = 0
  200 CONTINUE
* Save the track number of the stack particle:
  ISPARK (MKBMX2,NPFLKA) = NPFLKA
  NPARMA = NPARMA + 1
  NUMPAR (NPFLKA) = NPARMA
  NEVENT (NPFLKA) = 0
  DFNEAR (NPFLKA) = +ZERZER
* ... to this point: don't change anything
* Particle age (s)
  AGESTK (NPFLKA) = +ZERZER
  AKNSHR (NPFLKA) = -TWOTWO
* Group number for "low" energy neutrons, set to 0 anyway
  IGROUP (NPFLKA) = 0
c
c sampling from the normalized cumulative spectrum
  XYZ=FLRNDM(XYZ)
  DO I=0,IMAX
    IF(XYZ.LT.ENECUM(I)) THEN
      GOTO 1973
    END IF
  ENDDO
  STOP ' I did a big mistake'
1973 CONTINUE

```

```

c the sampled energy lies in the bin I (between ENEPOI(I-1) and ENEPOI(I))
c now determining the energy inside the bin I according to a linear spectrum
  ESAMPLE=ENEPOI(I)
* Kinetic energy of the particle (GeV)
  CALL FLNRRN (RGAUSS)
  TKEFLK (NPFLKA) = ESAMPLE
* Particle momentum
  PMOFLK (NPFLKA) = SQRT ( TKEFLK (NPFLKA) * ( TKEFLK (NPFLKA)
& + TWOTWO * AM (IONID) ) )
* Cosines (tx,ty,tz)
  CALL FLNRR2 (RGAUS1, RGAUS2)
* TXFLK (NPFLKA) = UBEAM+0.2*RGAUS1
c XLAN = FLRNDM()*1.4-0.7
c YLAN = FLRNDM()*1.4-0.7
  TXFLK (NPFLKA) = UBEAM+FLRNDM()*0.144-0.072
  TYFLK (NPFLKA) = VBEAM+FLRNDM()*0.144-0.072
* TYFLK (NPFLKA) = WBEAM
c TZFLK (NPFLKA) = -SQRT(1-XLAN**2-YLAN**2)
  TZFLK (NPFLKA) = SQRT ( ONEONE - TXFLK (NPFLKA)**2
& - TYFLK (NPFLKA)**2 )
* Polarization cosines:
  TXPOL (NPFLKA) = -TWOTWO
  TYPOL (NPFLKA) = +ZERZER
  TZPOL (NPFLKA) = +ZERZER
* Particle coordinates
  CALL FLNRR2 (RGAUS1, RGAUS2)
  XFLK (NPFLKA) = XBEAM
  YFLK (NPFLKA) = YBEAM
  ZFLK (NPFLKA) = ZBEAM
* Calculate the total kinetic energy of the primaries: don't change
  IF ( ILOFLK (NPFLKA) .EQ. -2 .OR. ILOFLK (NPFLKA) .GT. 100000 )
& THEN
  TKESUM = TKESUM + TKEFLK (NPFLKA) * WTFLK (NPFLKA)
  ELSE IF ( ILOFLK (NPFLKA) .NE. 0 ) THEN
  TKESUM = TKESUM + ( TKEFLK (NPFLKA) + AMDISC
(ILOFLK(NPFLKA)) )
& * WTFLK (NPFLKA)
  ELSE
  TKESUM = TKESUM + TKEFLK (NPFLKA) * WTFLK (NPFLKA)
  END IF
  RADDLY (NPFLKA) = ZERZER
* Here we ask for the region number of the hitting point.
* NREG (NPFLKA) = ...
* The following line makes the starting region search much more

```


* robust if particles are starting very close to a boundary:
 CALL GEOCRS (TXFLK (NPFLKA), TYFLK (NPFLKA), TZFLK (NPFLKA)
)
 CALL GEOREG (XFLK (NPFLKA), YFLK (NPFLKA), ZFLK (NPFLKA),
 & NRGFLK(NPFLKA), IDISC)

* Do not change these cards:
 CALL GEOHSM (NHSPNT (NPFLKA), 1, -11, MLATTC)
 NLATTC (NPFLKA) = MLATTC
 CMPATH (NPFLKA) = ZERZER
 CALL SOEVSV
 RETURN

*===	End	of	subroutine	Source
=====*				
END				

spectrum.dat

0.000001	0
0.000002	0
0.000003	0
0.000004	4.75887E-57
0.000005	1.73953E-29
0.000006	1.76656E-16
0.000007	9.31083E-10
0.000008	6.31952E-06
0.000009	1.50706E-40
0.00001	3.84041E-30
0.000011	2.06889E-22
0.000012	1.25325E-16
0.000013	4.72659E-12
0.000014	1.07456E-08
0.000015	4.35279E-06
0.000016	0.000477811
0.000017	0.018665387
0.000018	0.354860803
0.000019	3.876051053
0.00002	27.37251319
0.000021	135.5420133
0.000022	527.545115
0.000023	1622.8543
0.000024	4256.749721
0.000025	9524.021782
0.000026	19006.89928
0.000027	33752.44435
0.000028	57457.07926
0.000029	87321.20332

0.00003	127273.7733
0.000031	175323.6075
0.000032	232328.3448
0.000033	296244.4347
0.000034	367611.8193
0.000035	442235.4645
0.000036	519780.6896
0.000037	597478.5417
0.000038	676130.9814
0.000039	750571.4949
0.00004	823904.1787
0.000041	890828.8294
0.000042	955518.5932
0.000043	1013409.8
0.000044	1066784.921
0.000045	1110167.982
0.000046	1150802.769
0.000047	1183981.5
0.000048	1212799.13
0.000049	1233484.923
0.00005	1249129.318
0.000051	1259973.124
0.000052	1261000.361
0.000053	1261806.196
0.000054	1257531.968
0.000055	1252278.345
0.000056	1237356.955
0.000057	1222004.812
0.000058	2065370.101
0.000059	2713317.636
0.00006	1158927.836
0.000061	1132468.655
0.000062	1101590.73
0.000063	1070069.512
0.000064	1038500.827
0.000065	1002283.946
0.000066	965910.6545
0.000067	1520247.664
0.000068	888039.227
0.000069	1008368.032
0.00007	782466.0934
0.000071	739893.4879
0.000072	697335.0112
0.000073	650659.7676

0.000074	608587.2089
0.000075	566168.4316
0.000076	518239.0847
0.000077	464832.6256
0.000078	429923.7513
0.000079	396466.931
0.00008	364665.6289
0.000081	334334.3846
0.000082	305149.0507
0.000083	276242.1122
0.000084	247458.8946
0.000085	221856.4822
0.000086	196920.4372
0.000087	173134.4838
0.000088	150187.5313
0.000089	123853.6628
0.00009	96848.45141
0.000091	79979.17266
0.000092	65059.69969
0.000093	52470.07265
0.000094	42161.52007
0.000095	33509.46416
0.000096	26580.001
0.000097	21636.8198
0.000098	18017.03108
0.000099	15437.91274
0.0001	13561.96139
0.000101	11907.96184
0.000102	10464.20218
0.000103	9288.659713
0.000104	8185.335508
0.000105	7178.312113
0.000106	6321.623066
0.000107	5542.086327
0.000108	4821.66338
0.000109	4149.047806
0.00011	3599.345606
0.000111	3088.344385
0.000112	2620.468222
0.000113	2215.105433
0.000114	1814.727766
0.000115	1459.830384
0.000116	1162.6754
0.000117	889.7219591

0.000118 608.7652587
 0.000119 274.0082396
 0.00012 2.150127048
 0.000121 1.859413647
 0.000122 1.57525501
 0.000123 1.144955926
 0.000124 0.564481429

SpekCalc settings

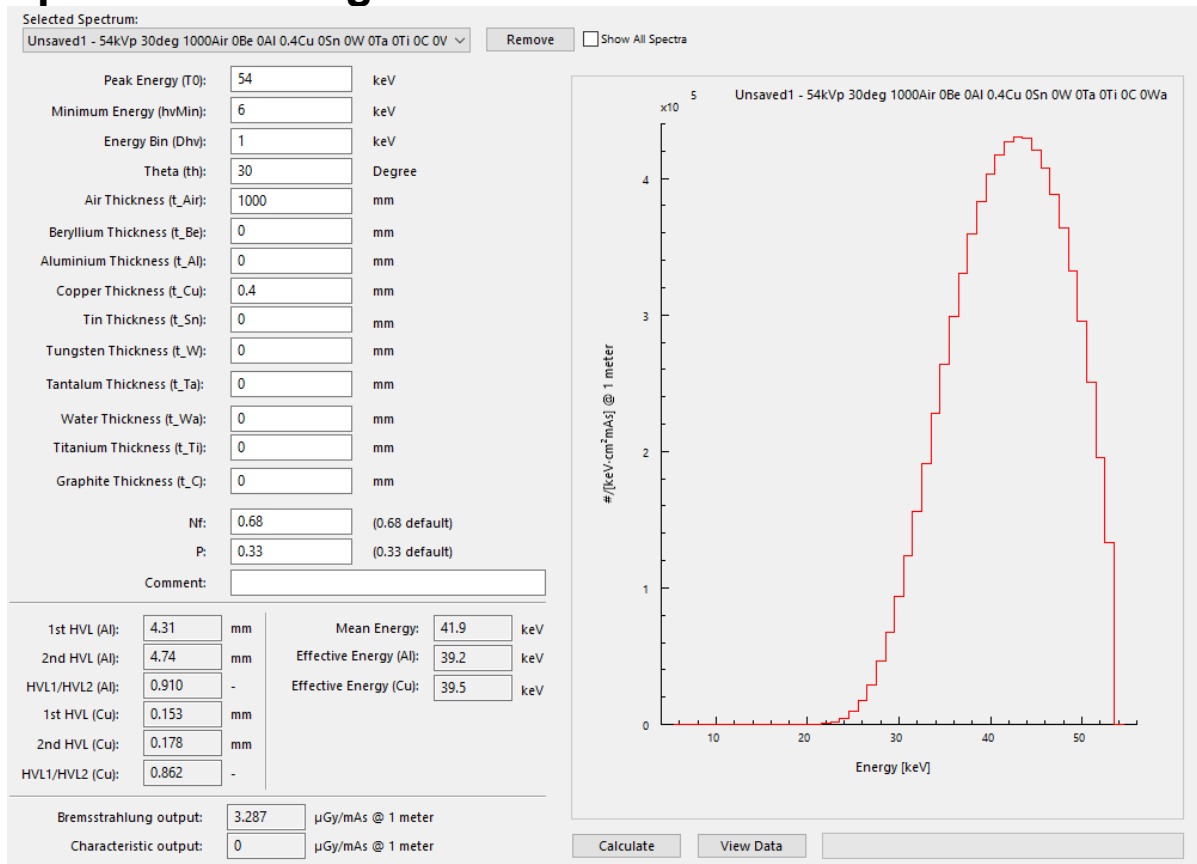


Figure 0.1 - Picture showing the settings used to calculate each energy spectrum later used to weight it by DAP. The only variance was the Peak Energy, which was cycled through for all kVp.

Appendix C fluscw_flu.f

*\$ CREATE FLUSCW.FOR

*COPY FLUSCW

*

*

*====

fluscw

=====*

*

*

DOUBLE PRECISION FUNCTION FLUSCW (IJ , PLA , TXX , TYY ,

```

&          TZZ , WEE , XX , YY ,
&          ZZ , NREG , IOLREG, LLO ,
&          NSURF )

```

```

INCLUDE '(DBLPRC)'
INCLUDE '(DIMPAR)'
INCLUDE '(IUNIT)'

```

```

*
*-----*
*
*
*          *
* Copyright (C) 1989-2005   by   Alfredo Ferrari & Paola Sala *
* All Rights Reserved.
*
*          *
* New version of Fluscw for FLUKA9x-FLUKA200x:
*
*          *
* !!!!!!!!!!!!!!!!!!!!!!!!!!!!!!!!!!!!!!!!!!!!!!!!!!!!!!!!!!!!! *
* !!! This is a completely dummy routine for Fluka9x/200x. !!! *
* !!! The name has been kept the same as for older Fluka !!! *
* !!! versions for back-compatibility, even though Fluscw !!! *
* !!! is applied only to estimators which didn't exist be- !!! *
* !!! fore Fluka89.
*          !!! *
* !!! User developed versions can be used for weighting !!! *
* !!! flux-like quantities at runtime
*          !!! *
* !!!!!!!!!!!!!!!!!!!!!!!!!!!!!!!!!!!!!!!!!!!!!!!!!!!!!!!!!!!!! *
*
*          *
* Input variables:
*
*          *
* Ij = (generalized) particle code (Paprop numbering) *
* Pla = particle laboratory momentum (GeV/c) (if > 0), *
*       or kinetic energy (GeV) (if <0)
*          *
* Txx,yy,zz = particle direction cosines
*          *
* Wee = particle weight
*          *
* Xx,Yy,Zz = position
*          *
* Nreg = (new) region number
*          *
* Iolreg = (old) region number
*          *
* Llo = particle generation
*          *
* Nsurf = transport flag (ignore!)
*          *
*
* Output variables:
*
*          *
* Fluscw = factor the scored amount will be multiplied by *
* Lsczer = logical flag, if true no amount will be scored *
*          regardless of Fluscw
*          *
*
*          *

```

```

* Useful variables (common SCOHLF): *
* *
* Flux like binnings/estimators (Fluscw): *
* ISCRNG = 1 --> Boundary crossing estimator *
* ISCRNG = 2 --> Track length binning *
* ISCRNG = 3 --> Track length estimator *
* ISCRNG = 4 --> Collision density estimator *
* ISCRNG = 5 --> Yield estimator *
* JSCRNG = # of the binning/estimator *
* *
*-----*
*
INCLUDE '(SCOHLF)'
INCLUDE '(USRBIN)' !Access IPUSBN (bin number)
INCLUDE '(TRACKR)' !Access photon energy

DOUBLE PRECISION EMIN(50), EMAX(50), WGT1(50), WGT2(50)
INTEGER NLINE

*-----*

LOGICAL LFIRST
SAVE LFIRST
DATA LFIRST / .TRUE. /

IF ( LFIRST ) THEN
  LFIRST = .FALSE.
  CALL OAUXFI('./tablea1.dat', 95, 'OLD', IERR)
  READ(95, *) !Skip first line
  NLINE = 0
  DO
    NLINE = NLINE + 1
    READ (95, 3, END=10 ) EMIN(NLINE),EMAX(NLINE), WGT1(NLINE),
& WGT2(NLINE)

3    FORMAT(F12.8,F12.8,F12.8,F12.8)
    ENDDO
    CLOSE(UNIT=95)
10   CONTINUE
  ENDIF

FLUSCW = ONEONE
LSCZER = .FALSE.

```

```

IF(IPUSBN(JSCRNG).EQ.-30) THEN ! If bin 30
  DO I=1, NLINE      ! Loop through the table until energy interval is found
    IF (ETRACK .GE. EMIN(I) .AND. ETRACK .LT. EMAX(I)) THEN
      FLUSCW = WGT1(I)
      RETURN
    ENDIF
  ENDDO
ENDIF
IF (IPUSBN(JSCRNG).EQ.-31) THEN
  DO I=1, NLINE      ! Loop through the table until energy interval is found
    IF (ETRACK .GE. EMIN(I) .AND. ETRACK .LT. EMAX(I)) THEN
      FLUSCW = WGT2(I)
      RETURN
    ENDIF
  ENDDO
ENDIF

```

```

RETURN
*====          End          of          function          Fluscw
=====*
```

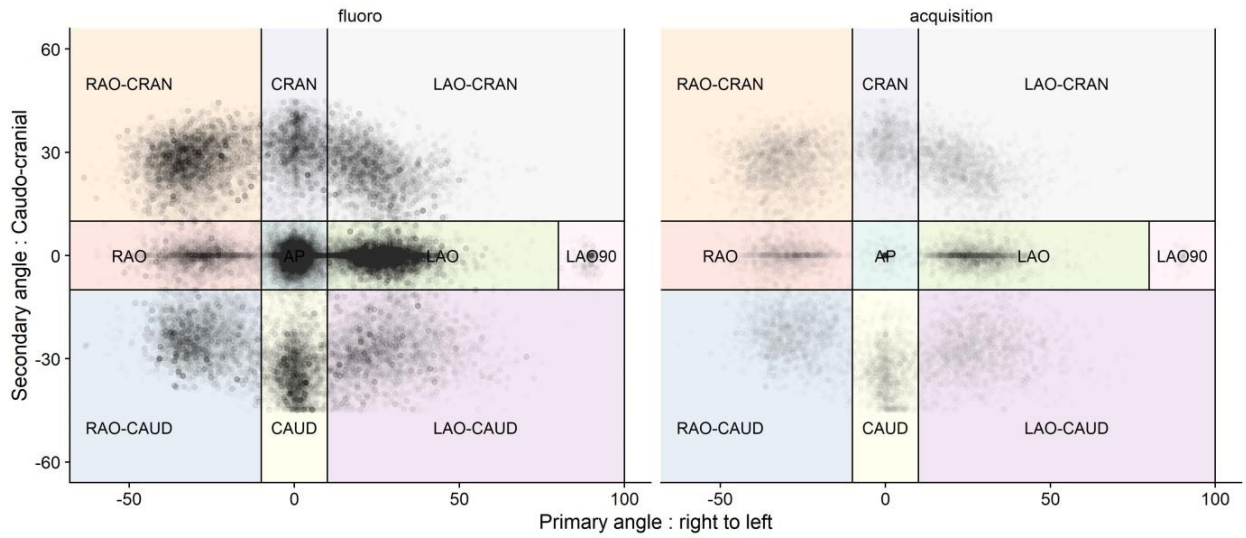
END

tablea2.dat

Emin	Emax	10	007
0	0.0000125	6.68E-14	7.04E-12
0.0000125	0.0000175	8.23E-13	3.06E-12
0.0000175	0.000025	1.02E-12	1.76E-12
0.000025	0.000035	8.01E-13	8.87E-13
0.000035	0.000045	6.39E-13	6.19E-13
0.000045	0.000055	5.70E-13	5.27E-13
0.000055	0.00007	5.46E-13	4.96E-13
0.00007	0.00009	5.84E-13	5.32E-13
0.00009	0.000125	6.71E-13	6.19E-13
0.000125	0.00015	9.62E-13	9.09E-13

Appendix D Beam angles

1e+05 Random samples from a total of 784154 fluoro or acquisitions



Data from OpenREM Haukeland University Hospital in the period 28/02/2017 to 16/04/2020

Figure 0.2 - Chart showing projections of interest and how they are defined. 10^5 random samples plotted were chosen as a compromise between having enough to see a structure and few enough to maintain a greyscale to indicate density.

Table 0.2: List of means, minimums and maximums for both primary and secondary angle for all projections.

Projection	Primary angle			Secondary angle		
	Mean	Min	Max	Mean	Min	Max
AP	0.33	-10.00	10.00	-0.23	-10.00	10.00
CAUD	0.38	-9.96	9.99	-33.04	-45.50	-10.01
CRAN	0.77	-9.99	9.99	30.98	10.01	46.60
LAO	27.03	10.01	80.00	-0.41	-9.99	9.95
LAO-CAUD	27.92	10.00	99.11	-27.47	-46.60	-10.00
LAO-CRAN	23.94	10.00	87.41	24.96	10.00	45.48
LAO90	89.32	80.20	96.60	-1.00	-9.69	7.56
RAO	-28.53	-76.50	-10.01	-0.25	-9.99	9.99
RAO-CAUD	-28.07	-87.20	-10.00	-24.27	-45.00	-10.00
RAO-CRAN	-30.68	-80.28	-10.00	27.30	10.00	46.50

Appendix E H10 & H0.07 conversion coefficients

Table 3 - Table containing the conversion coefficients from photon fluence to H0.07

Photon Energy [MeV]	Conversion coefficient [Sv·cm ²]
0.01	7.04E-12
0.015	3.06E-12
0.02	1.76E-12
0.03	8.87E-13
0.04	6.19E-13
0.05	5.27E-13
0.06	4.96E-13
0.08	5.32E-13
0.1	6.19E-13
0.15	9.09E-13
0.2	1.23E-12
0.3	1.84E-12
0.4	2.42E-12
0.5	2.96E-12
0.6	3.46E-12

0.8	4.13E-12
1	5.24E-12

Table 4 - Table containing the conversion coefficients from photon fluence to H10

Photon Energy **Conversion coefficient**
[MeV] **[Sv·cm²]**

0.01	6.69E-14
0.015	8.24E-13
0.02	1.03E-12
0.03	8.02E-13
0.04	6.39E-13
0.05	5.70E-13
0.06	5.47E-13
0.08	5.84E-13
0.1	6.72E-13
0.15	9.63E-13
0.2	1.28E-12
0.3	1.89E-12
0.4	2.46E-12
0.5	2.99E-12

0.6	3.48E-12
0.8	4.39E-12
1	5.22E-12
1.5	6.99E-12
2	8.54E-12
3	1.11E-11
4	1.35E-11
5	1.57E-11
6	1.79E-11
8	2.23E-11
10	2.67E-11

Appendix F Calibrations at HUS

Measurements

Table 5 - Table of the air kerma measurements made at HUS to calculate the coefficients to convert dose/primary simulated in FLUKA to real dose rates from the C-arm at HUS.

Placement	X-ray FPS	Field size	C-arm mode	Dose rate [mGy/s]	Dose [mGy]	Duration
1	15	20	Ac	0.006037	0.05909	10.56
1	15	20	Ac	0.006037	0.08648	15.45
1	7.5	20	F	0.0007929	0.01165	20.97
1	7.5	20	F	0.0008024	0.01173	21.18
2	15	20	Ac	0.006743	0.09943	15.93
2	15	20	Ac	0.006746	0.1003	16.05
2	7.5	20	F	0.0008547	0.009772	16.38
2	7.5	20	F	0.0008554	0.009698	16.11
3	15	20	Ac	0.008572	0.1267	15.96
3	15	20	Ac	0.008555	0.1236	15.60
3	7.5	20	F	0.001126	0.01245	15.87
3	7.5	20	F	0.001121	0.01271	16.14

Fluoro mode input file

* Increases maximum regions

GLOBAL 5000.

TITLE

Lab 3 - Haukeland

* Set the defaults for precision simulations

DEFAULTS

PRECISIO

* Define the beam characteristics

BEAM -8E-05 0.0 0.0 PHOTON

* Define the beam position

BEAMPOS 330.5 404. 30. 0.0 0.0

* Needed for the source script

SOURCE

* Sets energy threshold

EMFCUT -1E-06 1E-6 0.0 BLCKHOLE AIR PROD-CUT

* Sets energy threshold

*EMFCUT -1E-06 1E-6 OPBODY VOXE3143

* Sets energy threshold

EMFCUT -1E-06 1E-6 PHANTOM BLKBODY

* Fluence over the whole room

USRBIN 10. PHOTON -21. 613. 681. 306.FluRoom

```

USRBIN      0.0  0.0  0.0  200.  200.  200. &
* Detector 1
USRBIN      10.  DOSE  -25.  268.9  341.  117.4Det1
USRBIN     264.1  335.  110.6   2.   2.   2. &
* Detector 2
USRBIN      10.  DOSE  -26.  311.4  314.  117.4Det2
USRBIN     306.6  308.  106.6   2.   2.   2. &
* Detector 3
USRBIN      10.  DOSE  -27.  3443.9  353.  133.4Det3
USRBIN     339.1  347.  126.6   2.   2.   2. &
* Dose given to the patient
*USRBIN      10.  DOSE  -23.  372.  428.  124.DosePat
*USRBIN     184.  379.  95.  200.  200.  200. &
* Dose given to the operator
*USRBIN      10.  DOSE  -24.  310.  360.  180.DoseOp
*USRBIN     280.  330.  0.0  200.  200.  200. &
* Spectrum in front of the beam
USRBDX     101.          -22. DETFRONT  ROOM  1.ESpet
USRBDX     0.000115  1.05E-05  200.          &
* Rotates the lead seen hanging from the ceiling
*ROT-DEFI    1.          95.-395.43646234.427509  0.0rotScr
* Rotates the lead wall on the floor
*ROT-DEFI    2.          60.70.0961894421.410162  rotWall
* Rotates the lead skirt mounted to the bed
ROT-DEFI     3.          95.-396.10887 236.37632  rotSki
* Rotates the patient
* -x->y (Max)
* -y->z (Max)
* z->x (Min)
ROT-DEFI     104.  90.  90.  -428.  -118.85  184.rotPat
GEOBEGIN
COMBNAME
#if 0
VOXELS      0.0  0.0  0.0  rotPat  Pat
#endif
0 0
* Phantom for calibrations
RCC phantom  334. 404. 106. 15. 0.0 0.0 16.
SPH blkbody  0.0 0.0 0.0 100000.
* Vacuum around the room
SPH void     0.0 0.0 0.0 10000.
* Outer cylinder creating the C-arm
RCC machOut  330.5 376.5 110. 0.0 55. 0.0 122.
* Inner cylinder creating the C-arm
RCC machIn   330.5 376.5 110. 0.0 55. 0.0 100.

```

```

* Stops the C-arm, creating a crescent shape
YZP machStop 315.5
* The main room
RPP room 0.0 613. 0.0 681. 0.0 306.
* Defines the roof
XYP roof 306.
* Defines the floor
XYP floor 0.0
* Adds concrete around the room
RPP fR -4. 617. -4. 685. -20. 326.
* Outer layer of the wall to add lead inside
RPP wallsOut -4. 617. -4. 685. 0.0 306.
* Mid layer of the wall to add lead inside
RPP wallsMid -2.1 615.1 -2.1 683.1 0.0 306.
* Inner layer of the wall to add lead inside
RPP wallsIn -1.9 614.9 -1.9 682.9 0.0 306.
* Region in front of the detector
RPP detFront 325.5 335.5 399. 409. 30. 30.00001
$start_transform rotScr
#if 0
RPP leadScr 0.0 0.5 0.0 78. 125. 214.
#endif
$end_transform
$start_transform rotWall
#if 0
RPP leadWall 0.0 0.5 0.0 70. 0.0 181.
#endif
$end_transform
RPP bedSki 197. 270. 373.5 374. 18. 93.
$start_transform rotSki
RPP bedSki3 0.0 0.5 0.0 62. 18. 130.
$end_transform
* Lead skirt mounted to the bed
RPP bedFlap 344.5 361. 266. 266.5 28. 93.
* Patient bed
RPP bed 75.5 392.5 374. 434. 85. 90.
* Foot of the bed
RCC bedFoot 145. 404. 0.0 0.0 0.0 85. 19.
#if 0
* Operator's main body
RCC opBody 295. 345. 0.0 0.0 0.0 150. 15.
#endif
#if 0
* Operator's lead vest

```

```

RCC opVest  295. 345. 40. 0.0 0.0 110. 15.5
#endif
#if 0
* Operator's head
RCC opHead  295. 345. 149. 0.0 0.0 31. 13.
#endif
END
PHANTOM    5 +phantom
#if 0
* Water start/stop
OPBODY     5 +opBody|opHead
#endif
#if 0
* Lead start
OPVEST     5 +opVest -opBody
#endif
#if 0
* Lead starts (temp)
LEADWALL   5 +leadWall
#endif
#if 0
LEADSCR    5 +leadScr
#endif
#if 0
* Air start
ROOM1      5 +room -leadScr -leadWall -(bed|bedFoot) -(opVest|opHead|opBody) -
detFront -(
    +machOut -machStop -machIn -floor ) -(bedSki3|bedSki) -VOXEL
#endif
BEDSCR     5 +bedSki3|bedSki
* Lead end
WALLSMID   5 +wallsMid -wallsIn
* Carbon start
BED        5 +bed|bedFoot
* Carbon end
MACH       5 +machOut -machStop -machIn -floor
* Concrete start
ROOF       5 +fR -roof
WALLSOUT   5 +wallsOut -wallsMid
WALLSIN    5 +wallsIn -room
* Concrete end
FLOOR      5 +fR +floor
* Air start
ROOM       5 +room -(bed|bedFoot ) -detFront -(

```


+machOut -machStop -machIn -floor) -(bedSki3|bedSki) -phantom

* Air end

DETFRONT 5 +detFront

VOID 5 +void -fR

BLKBODY 5 +blkbody -void

END

GEOEND

* Create concrete with the compound card below

MATERIAL 2.05 CONCRETE

COMPOUND 23. CARBON 40. OXYGEN 12. SILICONCONCRETE

COMPOUND 12. CALCIUM 10. HYDROGEN 2.

MAGNESIUCONCRETE

*ASSIGNMA WATER OPBODY OPBODY

ASSIGNMA CARBON BED MACH

ASSIGNMA LEAD BEDSCR WALLSMID

ASSIGNMA AIR ROOM DETFRONT

ASSIGNMA CONCRETE ROOF FLOOR

ASSIGNMA VACUUM VOID

ASSIGNMA BLCKHOLE BLKBODY

*ASSIGNMA AIR VOXEL

ASSIGNMA PMMA PHANTOM

RANDOMIZ 1.

START 1200000.

STOP

Fluoro mode spectrum data

9.5e-06	9.913105e-7
1.05e-05	0.0009248
1.15e-05	0.1156633
1.25e-05	4.829324
1.35e-05	86.09481
1.45e-05	768.7713
1.55e-05	4186.787
1.65e-05	15621.89
1.75e-05	43789.82
1.85e-05	99621.02
1.95e-05	193216.7
2.05e-05	329727.1
2.15e-05	510867.1
2.25e-05	732375.7
2.35e-05	985657.3
2.45e-05	1.258756e+6
2.55e-05	1.540388e+6
2.65e-05	1.819585e+6
2.75e-05	2.094226e+6

2.85e-05	2.351831e+6
2.95e-05	2.579779e+6
3.05e-05	2.785932e+6
3.15e-05	2.964487e+6
3.25e-05	3.119201e+6
3.35e-05	3.247397e+6
3.45e-05	3.352264e+6
3.55e-05	3.430098e+6
3.65e-05	3.487725e+6
3.75e-05	3.525565e+6
3.85e-05	3.546379e+6
3.95e-05	3.550468e+6
4.05e-05	3.542181e+6
4.15e-05	3.521132e+6
4.25e-05	3.490991e+6
4.35e-05	3.451697e+6
4.45e-05	3.404039e+6
4.55e-05	3.349652e+6
4.65e-05	3.290815e+6
4.75e-05	3.226703e+6
4.85e-05	3.160199e+6
4.95e-05	3.090723e+6
5.05e-05	3.017280e+6
5.15e-05	2.942414e+6
5.25e-05	2.864891e+6
5.35e-05	2.789249e+6
5.45e-05	2.712517e+6
5.55e-05	2.635520e+6
5.65e-05	2.556855e+6
5.75e-05	2.480980e+6
5.85e-05	5.045035e+6
5.95e-05	6.949762e+6
6.05e-05	2.252781e+6
6.15e-05	2.177760e+6
6.25e-05	2.103410e+6
6.35e-05	2.030886e+6
6.45e-05	1.958995e+6
6.55e-05	1.887664e+6
6.65e-05	1.817887e+6
6.75e-05	3.316567e+6
6.85e-05	1.682156e+6
6.95e-05	2.025861e+6
7.05e-05	1.492416e+6
7.15e-05	1.431909e+6

7.25e-05 1.373753e+6
 7.35e-05 1.315226e+6
 7.45e-05 1.258014e+6
 7.55e-05 1.200686e+6
 7.65e-05 1.144341e+6
 7.75e-05 1.088388e+6
 7.85e-05 1.033063e+6
 7.95e-05 977979.5
 8.05e-05 923229
 8.15e-05 869179.6
 8.25e-05 814946.6
 8.35e-05 761354.5
 8.45e-05 706897.3
 8.55e-05 653197
 8.65e-05 598930.4
 8.75e-05 545640.2
 8.85e-05 489732.2
 8.95e-05 434571.2
 9.05e-05 373849.1
 9.15e-05 315143.9
 9.25e-05 256451.3
 9.35e-05 174901.2
 9.45e-05 57185.93

Acquisition mode input file

* Increases maximum regions

GLOBAL 5000.

TITLE

Lab 2 - Haukeland - Kalibrering

* Set the defaults for precision simulations

DEFAULTS PRECISIO

* Define the beam characteristics

BEAM -8E-05 0.0 0.0 PHOTON

* Define the beam position

BEAMPOS 342. 404. 30. 0.0 0.0

* Needed for the source script

SOURCE

* Sets energy threshold

EMFCUT -1E-06 1E-6 0.0 VACUUM AIR PROD-CUT

* Sets energy threshold

EMFCUT -1E-06 1E-6 PHANTOM BLKBODY

* Fluence over the whole room

USRBIN 10. PHOTON -21. 613. 681. 306.FluRoom

USRBIN 0.0 0.0 0.0 204. 227. 102. &

* Dose given to the patient

```

*USRBIN      10.  DOSE  -23.  372.  423.  124.DosePat
*USRBIN      184.  374.  95.  376.  98.  58. &
* Dose given to the operator
*USRBIN      10.  DOSE  -24.  310.  360.  180.DoseOp
*USRBIN      280.  330.  0.0  60.  60.  360. &
* Spectrum in front of the beam
USRBDX      101.          -22. DETFRONT  ROOM  1.ESpet
USRBDX      0.000115  1.05E-05  200.          &
* Calibration dose
USRBIN      10.  DOSE  -25.  268.9  341.  117.4Det1
USRBIN      264.1  335.  110.6  1.  1.  1. &
* Calibration dose
USRBIN      10.  DOSE  -25.  311.4  314.  117.4Det2
USRBIN      306.6  308.  110.6  1.  1.  1. &
* Calibration dose
USRBIN      10.  DOSE  -25.  343.9  353.  133.4Det3
USRBIN      339.1  347.  126.6  1.  1.  1. &
* Rotates the lead seen hanging from the ceiling
ROT-DEFI     1.          95.-395.43646234.427509  0.0rotScr
* Rotates the lead wall on the floor
ROT-DEFI     2.          60.70.0961894421.410162  rotWall
* Rotates the lead skirt mounted to the bed
ROT-DEFI     3.          95.-396.10887236.376321  rotSki
* Rotates the patient
* -x->y (Max)
* -y->z (Max)
* z->x (Min)
ROT-DEFI     104.  90.  90.  -428.  -118.85  184.rotPat
GEOBEGIN
  0  0
* Phantom for calibrations
RCC phantom  334. 404. 106. 15. 0.0 0.0 16.
SPH blkbody  0.0 0.0 0.0 100000.
* Vacuum around the room
SPH void     0.0 0.0 0.0 10000.
* Outer cylinder creating the C-arm
RCC machOut  330.5 376.5 110. 0.0 55. 0.0 122.
* Inner cylinder creating the C-arm
RCC machIn   330.5 376.5 110. 0.0 55. 0.0 100.
* Stops the C-arm, creating a crescent shape
YZP machStop 315.5
* The main room
RPP room     0.0 613. 0.0 681. 0.0 306.
* Defines the roof

```

```

XYP roof    306.
* Defines the floor
XYP floor   0.0
* Adds concrete around the room
RPP fR      -4. 617. -4. 685. -20. 326.
* Outer layer of the wall to add lead inside
RPP wallsOut -4. 617. -4. 685. 0.0 306.
* Mid layer of the wall to add lead inside
RPP wallsMid -2.1 615.1 -2.1 683.1 0.0 306.
* Inner layer of the wall to add lead inside
RPP wallsIn  -1.9 614.9 -1.9 682.9 0.0 306.
* Region in front of the detector
RPP detFront 325.5 335.5 399. 409. 30. 30.00001
RPP bedSki   197. 270. 373.5 374. 23. 98.
$start_transform rotSki
RPP bedSki3  0.0 0.5 0.0 62. 23. 98.
#if 0
RPP bedSki4  0.0 0.5 0.0 62. 23. 135.
#endif
$end_transform
* Lead skirt mounted to the bed
RPP bedFlap  344.5 361. 266. 266.5 28. 95.
* Patient bed
RPP bed      75.5 392.5 374. 434. 85. 90.
* Foot of the bed
RCC bedFoot  145. 404. 0.0 0.0 0.0 85. 19.
END
PHANTOM     5 +phantom
BEDSCR      5 +bedSki3|bedSki
* Lead end
WALLSMID    5 +wallsMid -wallsIn
* Carbon start
BED         5 +bed|bedFoot
* Carbon end
MACH        5 +machOut -machStop -machIn -floor
* Concrete start
ROOF        5 +fR -roof
WALLSOUT    5 +wallsOut -wallsMid
WALLSIN     5 +wallsIn -room
* Concrete end
FLOOR       5 +fR +floor
* Air start
ROOM        5 +room -phantom -(bed|bedFoot) -detFront -(
            +machOut -machStop -machIn -floor ) -(bedSki3|bedSki)

```

```

* Air end
DETFRONT 5 +detFront
VOID 5 +void -fR
BLKBODY 5 +blkbody -void
END
GEOEND
* Create concrete with the compound card below
MATERIAL 2.05 CONCRETE
COMPOUND 23. CARBON 40. OXYGEN 12. SILICONCONCRETE
COMPOUND 12. CALCIUM 10. HYDROGEN 2.
MAGNESIUCONCRETE
ASSIGNMA PMMA PHANTOM
ASSIGNMA CARBON BED MACH
ASSIGNMA LEAD BEDSCR WALLSMID
ASSIGNMA AIR ROOM DETFRONT
ASSIGNMA CONCRETE ROOF FLOOR
ASSIGNMA VACUUM VOID
ASSIGNMA BLCKHOLE BLKBODY
RANDOMIZ 1.
START 10000000.
STOP

```

Acquisition mode spectrum data

```

1.12e-05 2.872436e-21
1.22e-05 9.969762e-16
1.3199999999999999e-05 2.179257e-11
1.42e-05 3.618909e-8
1.5199999999999998e-05 0.0000116
1.62e-05 0.0010676
1.7199999999999998e-05 0.037039
1.82e-05 0.6455703
1.92e-05 6.600818
2.02e-05 44.31073
2.12e-05 212.8196
2.22e-05 803.3241
2.3199999999999998e-05 2430.293
2.42e-05 6259.192
2.52e-05 13864.73
2.62e-05 27347.78
2.72e-05 48697.59
2.8199999999999998e-05 81847.62
2.9199999999999998e-05 124606.7
3.02e-05 181183.4
3.12e-05 249841.9
3.2200000000000003e-05 331331

```

3.32e-05 423621.5
3.4200000000000005e-05 526743.6
3.52e-05 635537.2
3.6200000000000006e-05 749429
3.72e-05 865047.9
3.82e-05 982838.7
3.9200000000000004e-05 1.096421e+6
4.02e-05 1.208780e+6
4.1200000000000005e-05 1.314763e+6
4.22e-05 1.417617e+6
4.32e-05 1.512928e+6
4.4200000000000004e-05 1.600998e+6
4.52e-05 1.678304e+6
4.6200000000000005e-05 1.750870e+6
4.72e-05 1.815114e+6
4.8200000000000006e-05 1.872095e+6
4.92e-05 1.919194e+6
5.02e-05 1.959802e+6
5.1200000000000004e-05 1.992356e+6
5.22e-05 2.013844e+6
5.3200000000000006e-05 2.033928e+6
5.42e-05 2.048746e+6
5.52e-05 2.059548e+6
5.6200000000000004e-05 2.059158e+6
5.72e-05 2.057906e+6
5.8200000000000005e-05 5.814431e+6
5.92e-05 8.745380e+6
6.02e-05 2.030030e+6
6.12e-05 2.012740e+6
6.2200000000000001e-05 1.989639e+6
6.32e-05 1.967035e+6
6.42e-05 1.942793e+6
6.52e-05 1.913398e+6
6.62e-05 1.883903e+6
6.7200000000000001e-05 4.441243e+6
6.82e-05 1.819123e+6
6.92e-05 2.483640e+6
7.02e-05 1.657651e+6
7.1200000000000001e-05 1.623859e+6
7.22e-05 1.594044e+6
7.32e-05 1.561985e+6
7.42e-05 1.529314e+6
7.52e-05 1.495348e+6
7.6200000000000001e-05 1.461182e+6

7.72e-05 1.425434e+6
 7.82e-05 1.390196e+6
 7.92e-05 1.354177e+6
 8.02e-05 1.317963e+6
 8.1200000000000001e-05 1.281657e+6
 8.22e-05 1.244822e+6
 8.32e-05 1.208345e+6
 8.42e-05 1.170569e+6
 8.52e-05 1.134071e+6
 8.6200000000000001e-05 1.096474e+6
 8.72e-05 1.059504e+6
 8.82e-05 1.022115e+6
 8.92e-05 984971.1
 9.02e-05 947939.8
 9.1200000000000001e-05 910563.1
 9.22e-05 873923.2
 9.32e-05 836261.4
 9.42e-05 799788
 9.52e-05 762050.2
 9.6200000000000001e-05 725037.2
 9.72e-05 687407.7
 9.82e-05 650273.2
 9.92e-05 612879
 0.0001002 575225.6
 0.00010120000000000001 537538
 0.0001022 498950.4
 0.0001032 461258.9
 0.0001042 421619.1
 0.00010520000000000001 382964.4
 0.0001062 339960.7
 0.0001072 297243.9
 0.0001082 254910.2
 0.0001092 212955.8
 0.00011020000000000001 152309.3
 0.0001112 66684.51

Appendix G HUS_eclipse_materials.inp

*
 * \$Id: material.inp 2852 2013-11-15 13:48:55Z bnv \$
 *
 *
 * Schneider parametrisation of HU to materials

* This file should be used together with the dicom/material.inp

*

* Based on the work of Andrea Mairani

*

MATERIAL	16.	32.066	2.0			SULFUR
MATERIAL	15.	30.973761	2.2			PHOSPHO
MATERIAL	17.	35.4527	0.0029947			CHLORINE
MATERIAL	19.	39.0983	0.862			POTASSIU
* MIXTURE : HU<-1020						
MATERIAL			0.001			0.HU<-1020
COMPOUND	-0.755	NITROGEN	-0.232	OXYGEN	-0.013	ARGONHU<-1020
STERNHEI	10.5961	1.7418	4.2759	0.10914	3.3994	HU<-1020
MAT-PROP			85.7			HU<-1020
* MIXTURE : HU=-1017.5						
MATERIAL			0.001			0.HU<-1015
COMPOUND	-0.755	NITROGEN	-0.232	OXYGEN	-0.013	ARGONHU<-1015
* MIXTURE : HU=-1012.5						
MATERIAL			0.001			0.HU<-1010
COMPOUND	-0.755	NITROGEN	-0.232	OXYGEN	-0.013	ARGONHU<-1010
* MIXTURE : HU=-1005						
MATERIAL			0.001			0.HU<-1000
COMPOUND	-0.755	NITROGEN	-0.232	OXYGEN	-0.013	ARGONHU<-1000
* MIXTURE : HU=-997.5						
MATERIAL			0.001			0.HU<-995
COMPOUND	-0.755	NITROGEN	-0.232	OXYGEN	-0.013	ARGONHU<-995
* MIXTURE : HU=-991.5						
MATERIAL			0.001			0.HU<-988
COMPOUND	-0.755	NITROGEN	-0.232	OXYGEN	-0.013	ARGONHU<-988
* MIXTURE : HU=-981.5						
MATERIAL			0.001			0.HU<-975
COMPOUND	-0.755	NITROGEN	-0.232	OXYGEN	-0.013	ARGONHU<-975
* MIXTURE : HU=-974						
MATERIAL			.003012097			0.HU<-972
COMPOUND	-0.755	NITROGEN	-0.232	OXYGEN	-0.013	ARGONHU<-972
* MIXTURE : HU=-970						
MATERIAL			.00703629			0.HU<-967

COMPOUND -0.755 NITROGEN -0.232 OXYGEN -0.013 ARGONHU<-
 967
 * MIXTURE : HU=-965
 MATERIAL 0.0120665 0.HU<-962
 COMPOUND -0.755 NITROGEN -0.232 OXYGEN -0.013 ARGONHU<-
 962
 * MIXTURE : HU=-956
 MATERIAL 0.021121 0.HU<-950
 COMPOUND -0.755 NITROGEN -0.232 OXYGEN -0.013 ARGONHU<-
 950
 * MIXTURE : HU=-944.5
 MATERIAL .032690524 0.HU<-938
 COMPOUND -0.103 HYDROGEN -0.105 CARBON -0.031
 NITROGENHU<-938
 COMPOUND -0.749 OXYGEN -0.002 SODIUM -0.002 PHOSPHOHU<-
 938
 COMPOUND -0.003 SULFUR -0.003 CHLORINE -0.002 POTASSIUHU<-
 938
 * MIXTURE : HU=-932
 MATERIAL .045266129 0.HU<-925
 COMPOUND -0.103 HYDROGEN -0.105 CARBON -0.031
 NITROGENHU<-925
 COMPOUND -0.749 OXYGEN -0.002 SODIUM -0.002 PHOSPHOHU<-
 925
 COMPOUND -0.003 SULFUR -0.003 CHLORINE -0.002 POTASSIUHU<-
 925
 * MIXTURE : HU=-923
 MATERIAL .054320565 0.HU<-920
 COMPOUND -0.103 HYDROGEN -0.105 CARBON -0.031
 NITROGENHU<-920
 COMPOUND -0.749 OXYGEN -0.002 SODIUM -0.002 PHOSPHOHU<-
 920
 COMPOUND -0.003 SULFUR -0.003 CHLORINE -0.002 POTASSIUHU<-
 920
 * MIXTURE : HU=-917
 MATERIAL .060356855 0.HU<-913
 COMPOUND -0.103 HYDROGEN -0.105 CARBON -0.031
 NITROGENHU<-913
 COMPOUND -0.749 OXYGEN -0.002 SODIUM -0.002 PHOSPHOHU<-
 913
 COMPOUND -0.003 SULFUR -0.003 CHLORINE -0.002 POTASSIUHU<-
 913
 * MIXTURE : HU=-907
 MATERIAL .070417339 0.HU<-900

COMPOUND -0.103 HYDROGEN -0.105 CARBON -0.031
 NITROGENHU<-900
 COMPOUND -0.749 OXYGEN -0.002 SODIUM -0.002 PHOSPHOHU<-
 900
 COMPOUND -0.003 SULFUR -0.003 CHLORINE -0.002 POTASSIUHU<-
 900
 * MIXTURE : HU=-883
 MATERIAL 0.0945625 0.HU<-865
 COMPOUND -0.103 HYDROGEN -0.105 CARBON -0.031
 NITROGENHU<-865
 COMPOUND -0.749 OXYGEN -0.002 SODIUM -0.002 PHOSPHOHU<-
 865
 COMPOUND -0.003 SULFUR -0.003 CHLORINE -0.002 POTASSIUHU<-
 865
 * MIXTURE : HU=-848
 MATERIAL .130277218 0.HU<-830
 COMPOUND -0.103 HYDROGEN -0.105 CARBON -0.031
 NITROGENHU<-830
 COMPOUND -0.749 OXYGEN -0.002 SODIUM -0.002 PHOSPHOHU<-
 830
 COMPOUND -0.003 SULFUR -0.003 CHLORINE -0.002 POTASSIUHU<-
 830
 * MIXTURE : HU=-765
 MATERIAL 0.213276 0.HU<-700
 COMPOUND -0.103 HYDROGEN -0.105 CARBON -0.031
 NITROGENHU<-700
 COMPOUND -0.749 OXYGEN -0.002 SODIUM -0.002 PHOSPHOHU<-
 700
 COMPOUND -0.003 SULFUR -0.003 CHLORINE -0.002 POTASSIUHU<-
 700
 * MIXTURE : HU=-600
 MATERIAL 0.379274 0.HU<-500
 COMPOUND -0.103 HYDROGEN -0.105 CARBON -0.031
 NITROGENHU<-500
 COMPOUND -0.749 OXYGEN -0.002 SODIUM -0.002 PHOSPHOHU<-
 500
 COMPOUND -0.003 SULFUR -0.003 CHLORINE -0.002 POTASSIUHU<-
 500
 * MIXTURE : HU=-310
 MATERIAL 0.699219 0.HU<-120
 COMPOUND -0.103 HYDROGEN -0.105 CARBON -0.031
 NITROGENHU<-120
 COMPOUND -0.749 OXYGEN -0.002 SODIUM -0.002 PHOSPHOHU<-
 120

COMPOUND -0.003 SULFUR -0.003 CHLORINE -0.002 POTASSIUHU<-
 120
 * MIXTURE : HU=-101.5
 MATERIAL 0.943555 0.HU<-83
 COMPOUND -0.116 HYDROGEN -0.681 CARBON -0.002
 NITROGENHU<-83
 COMPOUND -0.198 OXYGEN -0.001 SODIUM -0.001 SULFURHU<-
 83
 COMPOUND -0.001 CHLORINE HU<-83
 * MIXTURE : HU=-68
 MATERIAL 0.964583 0.HU<-53
 COMPOUND -0.113 HYDROGEN -0.567 CARBON -0.009
 NITROGENHU<-53
 COMPOUND -0.308 OXYGEN -0.001 SODIUM -0.001 SULFURHU<-
 53
 COMPOUND -0.001 CHLORINE HU<-53
 * MIXTURE : HU=-38
 MATERIAL 0.980208 0.HU<-23
 COMPOUND -0.110 HYDROGEN -0.458 CARBON -0.015
 NITROGENHU<-23
 COMPOUND -0.411 OXYGEN -0.001 SODIUM -0.002 SULFURHU<-
 23
 COMPOUND -0.001 CHLORINE -0.001 PHOSPHO HU<-23
 * MIXTURE : HU=-8
 MATERIAL 0.995833 0.HU<7
 COMPOUND -0.108 HYDROGEN -0.356 CARBON -0.022
 NITROGENHU<7
 COMPOUND -0.509 OXYGEN -0.001 PHOSPHO -0.002 SULFURHU<7
 COMPOUND -0.002 CHLORINE HU<7
 * MIXTURE : HU=13.5
 MATERIAL 1.014063 0.HU<18
 COMPOUND -0.106 HYDROGEN -0.284 CARBON -0.026
 NITROGENHU<18
 COMPOUND -0.578 OXYGEN -0.001 PHOSPHO -0.002 SULFURHU<18
 COMPOUND -0.002 CHLORINE -0.001 POTASSIU HU<18
 * MIXTURE : HU=49
 MATERIAL 1.050625 0.HU<80
 COMPOUND -0.103 HYDROGEN -0.134 CARBON -0.030
 NITROGENHU<80
 COMPOUND -0.723 OXYGEN -0.002 SODIUM -0.002 PHOSPHOHU<80
 COMPOUND -0.002 SULFUR -0.002 CHLORINE -0.002 POTASSIUHU<80
 * MIXTURE : HU=100
 MATERIAL 1.082500 0.HU<120

COMPOUND -0.094 HYDROGEN -0.207 CARBON -0.062
 NITROGENHU<120
 COMPOUND -0.622 OXYGEN -0.006 SODIUM -0.006 SULFURHU<120
 COMPOUND -0.003 CHLORINE HU<120
 * MIXTURE : HU=160
 MATERIAL 1.118720 0.HU<200
 COMPOUND -0.095 HYDROGEN -0.455 CARBON -0.025
 NITROGENHU<200
 COMPOUND -0.355 OXYGEN -0.001 SODIUM -0.021 PHOSPHOHU<200
 COMPOUND -0.001 SULFUR -0.001 CHLORINE -0.001
 POTASSIUHU<200
 COMPOUND -0.045 CALCIUM HU<200
 * MIXTURE : HU=250
 MATERIAL 1.171370 0.HU<300
 COMPOUND -0.089 HYDROGEN -0.423 CARBON -0.027
 NITROGENHU<300
 COMPOUND -0.363 OXYGEN -0.001 SODIUM -0.030 PHOSPHOHU<300
 COMPOUND -0.001 SULFUR -0.001 CHLORINE -0.001
 POTASSIUHU<300
 COMPOUND -0.064 CALCIUM HU<300
 * MIXTURE : HU=350
 MATERIAL 1.229870 0.HU<400
 COMPOUND -0.082 HYDROGEN -0.391 CARBON -0.029
 NITROGENHU<400
 COMPOUND -0.372 OXYGEN -0.001 SODIUM -0.039 PHOSPHOHU<400
 COMPOUND -0.001 SULFUR -0.001 CHLORINE -0.001
 POTASSIUHU<400
 COMPOUND -0.083 CALCIUM HU<400
 * MIXTURE : HU=450
 MATERIAL 1.288370 0.HU<500
 COMPOUND -0.076 HYDROGEN -0.361 CARBON -0.030
 NITROGENHU<500
 COMPOUND -0.380 OXYGEN -0.001 SODIUM -0.047 PHOSPHOHU<500
 COMPOUND -0.002 SULFUR -0.001 CHLORINE -0.001
 MAGNESIUHU<500
 COMPOUND -0.101 CALCIUM HU<500
 * MIXTURE : HU=550
 MATERIAL 1.347210 0.HU<600
 COMPOUND -0.071 HYDROGEN -0.335 CARBON -0.032
 NITROGENHU<600
 COMPOUND -0.387 OXYGEN -0.001 SODIUM -0.054 PHOSPHOHU<600
 COMPOUND -0.002 SULFUR -0.001 MAGNESIU -0.117
 CALCIUMHU<600
 * MIXTURE : HU=650

MATERIAL	1.407254		0.HU<700		
COMPOUND	-0.066	HYDROGEN	-0.310	CARBON	-0.033
NITROGENHU<700					
COMPOUND	-0.394	OXYGEN	-0.001	SODIUM	-0.061
COMPOUND	-0.002	SULFUR	-0.001	MAGNESIU	-0.132
CALCIUMHU<700					
* MIXTURE : HU=750					
MATERIAL	1.467299		0.HU<800		
COMPOUND	-0.061	HYDROGEN	-0.287	CARBON	-0.035
NITROGENHU<800					
COMPOUND	-0.400	OXYGEN	-0.001	SODIUM	-0.067
COMPOUND	-0.002	SULFUR	-0.001	MAGNESIU	-0.146
CALCIUMHU<800					
* MIXTURE : HU=850					
MATERIAL	1.527344		0.HU<900		
COMPOUND	-0.056	HYDROGEN	-0.265	CARBON	-0.036
NITROGENHU<900					
COMPOUND	-0.405	OXYGEN	-0.001	SODIUM	-0.073
COMPOUND	-0.003	SULFUR	-0.002	MAGNESIU	-0.159
CALCIUMHU<900					
* MIXTURE : HU=950					
MATERIAL	1.587388		0.HU<1000		
COMPOUND	-0.052	HYDROGEN	-0.246	CARBON	-0.037
NITROGENHU<1000					
COMPOUND	-0.411	OXYGEN	-0.001	SODIUM	-0.078
PHOSPHOHU<1000					
COMPOUND	-0.003	SULFUR	-0.002	MAGNESIU	-0.170
CALCIUMHU<1000					
* MIXTURE : HU=1050					
MATERIAL	1.638699		0.HU<1100		
COMPOUND	-0.049	HYDROGEN	-0.227	CARBON	-0.038
NITROGENHU<1100					
COMPOUND	-0.416	OXYGEN	-0.001	SODIUM	-0.083
PHOSPHOHU<1100					
COMPOUND	-0.003	SULFUR	-0.002	MAGNESIU	-0.181
CALCIUMHU<1100					
* MIXTURE : HU=1150					
MATERIAL	1.686941		0.HU<1200		
COMPOUND	-0.045	HYDROGEN	-0.210	CARBON	-0.039
NITROGENHU<1200					
COMPOUND	-0.420	OXYGEN	-0.001	SODIUM	-0.088
PHOSPHOHU<1200					
COMPOUND	-0.003	SULFUR	-0.002	MAGNESIU	-0.192
CALCIUMHU<1200					

* MIXTURE : HU=1250

MATERIAL	1.735184		0.HU<1300		
COMPOUND	-0.042	HYDROGEN	-0.194	CARBON	-0.040
NITROGENHU<1300					
COMPOUND	-0.425	OXYGEN	-0.001	SODIUM	-0.092
PHOSPHOHU<1300					
COMPOUND	-0.003	SULFUR	-0.002	MAGNESIU	-0.201
CALCIUMHU<1300					

* MIXTURE : HU=1350

MATERIAL	1.783426		0.HU<1400		
COMPOUND	-0.039	HYDROGEN	-0.179	CARBON	-0.041
NITROGENHU<1400					
COMPOUND	-0.429	OXYGEN	-0.001	SODIUM	-0.096
PHOSPHOHU<1400					
COMPOUND	-0.003	SULFUR	-0.002	MAGNESIU	-0.210
CALCIUMHU<1400					

* MIXTURE : HU=1450

MATERIAL	1.831668		0.HU<1500		
COMPOUND	-0.036	HYDROGEN	-0.165	CARBON	-0.042
NITROGENHU<1500					
COMPOUND	-0.432	OXYGEN	-0.001	SODIUM	-0.100
PHOSPHOHU<1500					
COMPOUND	-0.003	SULFUR	-0.002	MAGNESIU	-0.219
CALCIUMHU<1500					

* MIXTURE : HU=1550

MATERIAL	1.896131		0.HU<1600		
COMPOUND	-0.034	HYDROGEN	-0.155	CARBON	-0.042
NITROGENHU<1600					
COMPOUND	-0.435	OXYGEN	-0.001	SODIUM	-0.103
PHOSPHOHU<1600					
COMPOUND	-0.003	SULFUR	-0.002	MAGNESIU	-0.225
CALCIUMHU<1600					

* MIXTURE : HU=1800

MATERIAL	2.082143		0.HU<2000		
COMPOUND	-0.034	HYDROGEN	-0.155	CARBON	-0.042
NITROGENHU<2000					
COMPOUND	-0.435	OXYGEN	-0.001	SODIUM	-0.103
PHOSPHOHU<2000					
COMPOUND	-0.003	SULFUR	-0.002	MAGNESIU	-0.225
CALCIUMHU<2000					

* MIXTURE : HU=2535

MATERIAL	2.624279		0.HU<3072		
COMPOUND	-0.034	HYDROGEN	-0.155	CARBON	-0.042
NITROGENHU<3072					

COMPOUND	-0.435	OXYGEN	-0.001	SODIUM	-0.103
PHOSPHOHU<3072					
COMPOUND	-0.003	SULFUR	-0.002	MAGNESIU	-0.225
CALCIUMHU<3072					

Appendix H HUS_eclipse_calibrationcurve.mat

```

-1020 VACUUM 1 1 1 1
-1015 HU<-1015 1 1 1 1
-1010 HU<-1010 1 1 1 1
-1000 HU<-1000 1 1 1 1
-995 HU<-995 1 1 1 1
-988 HU<-988 1 1 1 1
-975 HU<-975 1 1 1 1
-972 HU<-972 0.6666666667 1.334002677 1 1
-967 HU<-967 0.7140401146 1.285959885 1 1
-962 HU<-962 0.8332497911 1.166750209 1 1
-950 HU<-950 0.7142038946 1.238163421 1 1
-938 HU<-938 0.8307379198 1.16926208 1 1
-925 HU<-925 0.8666488509 1.133351149 1 1
-920 HU<-920 0.962958839 1.037041161 -1.4067306 -1.48213224
-913 HU<-913 0.949999499 1.050005011 -1.12123613 -1.45129177
-900 HU<-900 0.914278352 1.085721648 -1.25952096 -1.43241912
-865 HU<-865 0.8191373686 1.180862631 -1.07784302 -1.4434567
-830 HU<-830 0.8682109123 1.139541387 -1.056055 -1.32116188
-700 HU<-700 0.6933875313 1.301895354 -0.81228558 -1.42479258
-500 HU<-500 0.7347437806 1.262603657 -0.80506275 -1.33820665
-120 HU<-120 0.6863074428 1.316759777 -0.72811735 -1.31604366
-83 HU<-83 0.9770233906 1.013454771 -0.9460518 -0.98678178
-53 HU<-53 0.9919006479 1.007559395 -0.97299013 -0.99179308
-23 HU<-23 0.9920297556 1.007438895 -0.98350471 -1.00070415
7 HU<7 0.9921548117 1.010460251 -0.99122357 -1.00690157
18 HU<18 0.9933230611 1.003595275 -0.99325307 -0.99935454
80 HU<80 0.9696609161 1.01784652 -0.97298839 -1.0181043
120 HU<120 0.9884526559 1.010969977 -0.99654442 -1.01014633
200 HU<200 0.9787971968 1.020393843 -0.97336099 -1.00622576
300 HU<300 0.9750292393 1.024471346 -0.97129914 -1.01379475
400 HU<400 0.9762169985 1.023307341 -0.97643768 -1.01781602
500 HU<500 0.9772968945 1.022249043 -0.98139019 -1.02121277
600 HU<600 0.978036219 1.021839118 -0.98480086 -1.02245918
700 HU<700 0.9786660322 1.020907288 -0.98819826 -1.02395399
800 HU<800 0.9795390583 1.020051723 -0.990191 -1.02589902
900 HU<900 0.9803434417 1.019263427 -0.99548346 -1.02939273
1000 HU<1000 0.9810869718 1.016824685 -0.99696374 -1.0302012
1100 HU<1100 0.985280341 1.014425266 -1.00427306 -1.03538414

```


1200 HU<1200	0.9857012854	1.01401274	-1.01239319	-1.04468687
1300 HU<1300	0.9860988233	1.013623153	-1.02226569	-1.05241658
1400 HU<1400	0.9864748542	1.013254643	-1.02964762	-1.0603038
1500 HU<1500	0.9868310774	1.014476726	-1.03805739	-1.06831809
1600 HU<1600	0.9803798462	1.019227751	-1.03511222	-1.06435659
2000 HU<2000	0.9285305889	1.07161235	-0.96931765	-1.07418197
3072 HU<3072	0.8505193735	1.139539251	-0.85327867	-1.07792742